UNIVERSITÄT ZU LÜBECK

From the Institute of Experimental Endocrinology

of the University of Lübeck

Director: Prof. Dr. rer. nat. Jens Mittag

„*Aparecium*: Revealing the Role of the Zona Incerta in Central Thyroid Hormone Action“

Dissertation for Fulfilment of Requirements

for the Doctoral Degree

of the University of Lübeck

from the Department of Natural Sciences

Submitted by

Julia Maier

from Albstadt, Germany

Lübeck, 2024

First referee:	Prof. Dr. Jens Mittag
Second referee:	Prof. Dr. Nico Bunzeck
Date of oral examination:	March 25, 2025
Approved for printing:	March 26, 2025

LIST OF PUBLICATIONS

Portions of this thesis were previously submitted to or published in peer-reviewed journals to address priority considerations:

- **Maier, J.**, Dore, R., Oelkrug, R., Glatzel, A., Cremer, A. L., Binder, S., Schwaninger, M., Oster, H., Backes, H., & Mittag, J. (2024). Inhibition of Thyroid Hormone Signaling in the Zona Incerta Alters Basal Metabolic Rate, Behavior and Serum Glucocorticoids in Male Mice. *Thyroid : official journal of the American Thyroid Association*. In press.

Publications that are not part of this thesis:

- Sreenivasan, V. K. A., Dore, R., Resch, J., **Maier, J.**, Dietrich, C., Henck, J., Balachandran, S., Mittag, J., & Spielmann, M. (2023). Single-cell RNA-based phenotyping reveals a pivotal role of thyroid hormone receptor alpha for hypothalamic development. *Development (Cambridge, England)*, *150*(3), dev201228. https://doi.org/10.1242/dev.201228

Contents

List of Publications ..... **I**
List of Figures ..... **IV**
List of Tables ..... **VI**
List of Abbreviations ..... **VII**
Abstract ..... **X**
Zusammenfassung ..... **XI**

1. Introduction ..... **- 1 -**
1.1 Stress and Anxiety ..... - 1 -
1.1.1 Stress and the Hypothalamus-Pituitary-Adrenal (HPA) Axis ..... - 2 -
1.1.2 Behavioural Anxiety Tests in Rodents ..... - 3 -
1.2. Thyroid Hormones ..... - 4 -
1.2.1 The Hypothalamus-Pituitary-Thyroid (HPT) Axis ..... - 4 -
1.2.2 Thyroid Hormone Associated Diseases ..... - 5 -
1.2.3 Thyroid Hormone Receptors ..... - 6 -
1.3. Aims of this Study ..... - 8 -
2. Materials and Methods ..... **- 10 -**
2.1 Materials ..... - 10 -
2.1.1 Chemicals, drugs, and reagents ..... - 10 -
2.1.2 Consumables and devices ..... - 12 -
2.1.3 Commercially available kits ..... - 15 -
2.1.4 Buffers ..... - 15 -
2.1.5 Software ..... - 16 -
2.2 Methods ..... - 16 -
2.2.1 *In vivo* methods ..... - 18 -
2.2.2 Molecular methods ..... - 21 -
2.3 Statistics and software ..... - 29 -
3. Results ..... **- 30 -**
3.1 Thyroid Hormone actions in the brain ..... - 30 -
3.1.1 Activation of the Zona Incerta by treatment with thyroid hormones ..... - 30 -
3.1.2 What are the effects of central TRα1 signalling in the Zona Incerta? ..... - 32 -
3.2 The role of dopaminergic neurons in the Zona Incerta ..... - 46 -
3.2.1 The effect of T3 on Zona Incerta dopaminergic neurons ..... - 47 -
3.2.2 What are the effects of TRα1 signalling in dopaminergic neurons of the Zona Incerta? ..... - 48 -

4. Discussion ..... - 56 -
4.1 Effects of Thyroid Hormones on the brain ..... - 56 -
4.2 Effects of TRα1 signalling in the Zona Incerta on body weight and thermoregulation ..... - 58 -
4.3 Effects of TRα1 signalling in the Zona Incerta on energy expenditure ..... - 60 -
4.4 Effects of TRα1 signalling in the Zona Incerta on anxiety and stress ..... - 63 -
5. Conclusion and Outlook ..... - 66 -
6. References ..... - 68 -

Appendix XII
Statistical analysis XII
Acknowledgements XIX

LIST OF FIGURES

Figure 1: Hypothalamus-pituitary-adrenal axis. ..... - 3 -
Figure 2: Hypothalamus-pituitary-thyroid axis. ..... - 5 -
Figure 3: Thyroid hormone-mediated gene expression via thyroid hormone receptors. ..... - 7 -
Figure 4: Study aims.. ..... - 9 -
Figure 5: Neuronal activation of the Zona Incerta by treatment with T3 (0.5 mg/L). ..... - 31 -
Figure 6: Experimental in vivo design to explore the effects of central TRα1 signalling in the Zona Incerta.. ..... - 32 -
Figure 7: Validation of virus expression and successful TRα1 signalling inhibition..... - 34 -
Figure 8: Cell-type specific infection of injected AAV. ..... - 35 -
Figure 9: Body weight and food and water intake of mice with inhibited thyroid hormone signalling in the Zona Incerta. ..... - 35 -
Figure 10: Circulating thyroid hormone levels of mice expressing a dominant-negative TRα1 compared to control mice ..... - 36 -
Figure 11: Effects of Zona Incerta thyroid hormone signalling inhibition on core body temperature and locomotion ..... - 37 -
Figure 12: iBAT activity and tail heat loss in mice expressing a mutant TRα1 or control GFP. . - 38 -
Figure 13: Effect of Zona Incerta thyroid hormone signalling inhibition on energy expenditure at different ambient temperatures. ..... - 40 -
Figure 14: qPCR analysis of muscle and liver and glycogen content in mice expressing a dominant-negative TRα1 or control GFP. ..... - 41 -
Figure 15: Effects of Zona Incerta thyroid hormone signalling inhibition on anxiety behaviour. ..... - 43 -
Figure 16: Serum glucocorticoid levels and qPCR analysis of liver and muscle in mice expressing a mutant TRα1 or control GFP. ..... - 44 -
Figure 17: Effects of Zona Incerta thyroid hormone signalling inhibition on the HPA axis. ..... - 45 -
Figure 18: Electrocardiogram data for mice expressing either a dominant-negative TRα1 or control GFP. ..... - 46 -
Figure 19: Dopaminergic neurons in the Zona Incerta. ..... - 47 -
Figure 20: Experimental design to investigate the role of dopaminergic neuron thyroid hormone signalling in the Zona Incerta. ..... - 48 -
Figure 21: Virus injection site confirmation. ..... - 49 -

Figure 22: Effects of thyroid hormone signalling inhibition in the dopaminergic neurons of the Zona Incerta on body weight and food and water intake. ..... - 50 -
Figure 23: Body temperature and locomotion activity at different ambient temperatures in mice lacking thyroid hormone signalling in Zona Incerta dopaminergic neurons or control mice. . - 51 -
Figure 24: Infrared thermography of iBAT and tail in mice expressing either a mutant TRα1 or control mCherry in the dopaminergic neurons of the Zona Incerta. ..... - 52 -
Figure 25: Effects of thyroid hormone signalling inhibition in the dopaminergic neurons of the Zona Incerta on energy expenditure at 22°C under fasting conditions. ..... - 53 -
Figure 26: Anxiety behaviour and glucocorticoids in mice lacking thyroid hormone signalling in Zona Incerta dopaminergic neurons or control mice. ..... - 54 -
Figure 27: Effects of thyroid hormone signalling inhibition in the dopaminergic neurons of the Zona Incerta on electrocardiogram data..... - 55 -
Figure 28: Efferent connections of the Zona Incerta. ..... - 57 -
Figure 29: Effects of thyroid hormone signalling inhibition in the Zona Incerta on the organism. ..... - 66 -

LIST OF TABLES

Table 1: Chemicals, drugs, and reagents ..... - 10 -
Table 2: Consumables and devices ..... - 12 -
Table 3: Commercially available kits ..... - 15 -
Table 4: Buffers ..... - 15 -
Table 5: Software ..... - 16 -
Table 6: Primary antibodies ..... - 22 -
Table 7: Secondary antibodies ..... - 22 -
Table 8: PCR method ..... - 24 -
Table 9: Housekeeping genes ..... - 25 -
Table 10: Genes used for qPCR with respective primer sequences ..... - 25 -
Table 11: Glucose uptake of different brain regions upon T3 treatment. ..... - 31 -
Supplementary Table 1: Statistical tests used in this study and their results XII

LIST OF ABBREVIATIONS

AAV	Adeno-associated virus
Acetyl-CoA	Acetyl coenzyme A
ACTH	Adrenocorticotropic hormone
ARC	Arcuate nucleus
Atp2a1	ATPase sarcoplasmic/endoplasmic reticulum Ca^{2+} transporting 1 (gene)
Atp2a2	ATPase sarcoplasmic/endoplasmic reticulum Ca^{2+} transporting 2 (gene)
Atp2a3	ATPase sarcoplasmic/endoplasmic reticulum Ca^{2+} transporting 3 (gene)
BAT	Brown adipose tissue
BMR	Basal metabolic rate
cAMP	Cyclic adenosine monophosphate
Cidea	Cell death inducing DFFA like effector A (gene)
CPS	Cryo protection solution
CRH	Corticotropin-releasing hormone
Crh	Corticotropin-releasing hormone (gene)
Crhr	Corticotropin-releasing hormone receptor (gene)
CT	Computed tomography
Cyp11b1	Cytochrome P450, family 11, subfamily b, polypeptide 1 (gene)
Cyp11b2	Cytochrome P450, family 11, subfamily b, polypeptide 2 (gene)
DAB	3,3'-diaminobenzidine
DBD	DNA binding domain
DSM	Diagnostic and statistical manual of mental disorders
ECG	Electrocardiogram
EGFP	Green fluorescent protein
FADH2	Flavin adenine dinucleotide
FDG	Fluorodeoxyglucose
FFA	Free fatty acids
GABA	Gamma-aminobutyric acid
GAD	Glutamate dcarboxylase
GC	Genome copies
GFP	Green fluorescent protein

GR	Glucocorticoid receptor
Gr	Glucocorticoid receptor (gene)
GTH	Gemeinsame Tierhaltung
HPA	Hypothalamus-pituitary-adrenal
HPT	Hypothalamus-pituitary-thyroid
Hr	Hairless (gene)
HRP	Horseradish peroxidase
iBAT	Interscapular brown adipose tissue
Klf9	Krüppel-like factor 9 (gene)
LBD	Ligand binding domain
LH	Lateral hypothalamus
MC2R	Melanocortin type 2 receptor
MC4R	Melanocortin type 4 receptor
MCT8	Monocarboxylate transporter 8
ME	Median eminence
NADH	Nicotinamide adenine dinucleotide
OXPHOS	Oxidative phosphorylation
PD	Parkinson's disease
Pde10a	Phosphodiesterase 10A (gene)
PET	Positron emission tomography
PFA	Paraformaldehyde
PGC1	PPAR gamma coactivator-1
PKA	Protein kinase A
PLN	Phospholamban
POMC	Proopiomelanocortin
Pomc	Proopiomelanocortin (gene)
PVN	Paraventricular nucleus
qPCR	Quantitative polymerase chain reaction
RQ	Respiratory quotient
RTHα	Resistance to thyroid hormones due to a mutation in thyroid hormone receptor α
RTHβ	Resistance to thyroid hormones due to a mutation in thyroid hormone receptor β
RXR	Retinoid X receptor

Scd1	Stearoyl-CoA denaturase (gene)
SERCA	Sarco endoplasmic reticulum calcium ATPase
SLN	Sarcolipin
Sln	Sarcolipin (gene)
SNRI	Serotonin norepinephrine reuptake inhibitor
SNS	Sympathetic nervous system
SR	Sarcoendoplasmic reticulum
SSRI	Selective serotonin reuptake inhibitor
T3	3,3',5-triiodothyronine
T4	Thyroxine
TAG	Triglycerides
Tbx19	T-box 19 (gene)
TCA	Tricarboxylic acid
TH	Thyroid hormone
TR	Thyroid hormone receptor
Tra1	Thyroid hormone receptor α1 (gene)
Trb1	Thyroid hormone receptor β1 (gene)
Trb2	Thyroid hormone receptor β2 (gene)
TRE	Thyroid hormone response element
TRH	Thyrotropin-releasing hormone
Trhr	Thyrotropin-releasing hormone receptor (gene)
TRα	Thyroid hormone receptor α
TRβ	Thyroid hormone receptor β
TSH	Thyroid stimulating hormone
Tshb	Thyroid stimulating hormone, subunit β (gene)
UCP1	Uncoupling protein 1
ZI	Zona Incerta

ABSTRACT

The importance of thyroid hormones (THs) for regulation of body temperature and energy metabolism as well as brain functions such as mood is well established. This is most evident in hypo- or hyperthyroidism, which have severe consequences on these parameters. THs exert their effects via thyroid hormone receptors α (TRα) and β (TRβ). Similar to altered ligand availability, mutations in these receptors lead to several deficits, such as defaults in neuronal development and regulation of body temperature, as well as psychomotor alterations. However, it often remains unknown whether defects are caused by TH actions directly on tissue level or centrally in the brain, and in the latter case, which brain regions mediate the central effects of THs.

To address this question, PET/CT scans of mice undergoing treatment with T3 were conducted and showed activation of the Zona Incerta (ZI), a region of the subthalamus, indicating its role in mediating effects of THs. To further investigate the effect of THs in the ZI, TH signalling was inhibited by introducing a dominant-negative TRα1 via adeno-associated virus (AAV) injection into the ZI. In a separate set up, inhibition was specific to dopaminergic neurons by injecting the AAVs into tyrosine hydroxylase-Cre mice.

Analysing these mice revealed that inhibited TH signalling in the ZI caused an increase in basal metabolic rate (BMR) with increased fasting weight loss without affecting body temperature. In addition, it resulted in a chronic stress-like state, in which serum corticosterone was elevated, and a partial anxiety phenotype was present, as habituation to stressful situations was impaired. However, none of these effects were observed in the conditional model, demonstrating that they were not mediated by dopaminergic neurons.

Taken together, the study identifies a new brain region for central actions of THs, the ZI, and implicate it as a key brain region in TH-meditated control of behaviour and energy metabolism.

ZUSAMMENFASSUNG

Die Bedeutung der Schilddrüsenhormone für die Regulierung der Körpertemperatur und des Energiestoffwechsels sowie für Gehirnfunktionen wie die Stimmungslage, ist allgemein bekannt. Am deutlichsten wird dies bei Hypo- oder Hyperthyreose, welche schwerwiegende Folgen für diese Parameter haben. Schilddrüsenhormone üben ihre Wirkung über die Schilddrüsenhormonrezeptoren α und β aus. Ähnlich wie eine veränderte Ligandenverfügbarkeit führen Mutationen in diesen Rezeptoren zu verschiedenen Defiziten, wie Störungen der neuronalen Entwicklung und der Körpertemperaturregulierung sowie psychomotorische Veränderungen. Es ist jedoch oft nicht bekannt, ob die Defekte durch Schilddrüsenhormon-Wirkungen direkt auf Gewebeebene oder zentral im Gehirn verursacht werden und, im letzteren Fall, welche Gehirnregionen die zentralen Wirkungen der Schilddrüsenhormone vermitteln.

Um diese Frage zu klären, wurden PET/CT-Scans von Mäusen durchgeführt, die mit T3 behandelt wurden. Diese zeigten eine Aktivierung der Zona Incerta (ZI), einer Region des Subthalamus, was auf deren Rolle bei der Vermittlung der Wirkungen von Schilddrüsenhormonen hinweist. Um die Wirkung von Schilddrüsenhormonen in der ZI weiter zu untersuchen, wurde die Schilddrüsenhormon-Signalübertragung gehemmt, indem ein adeno-assoziiertes Virus (AAV), welches einen dominant-negativen TRα1 exprimiert, in die ZI injiziert wurde. In einer separaten Versuchsanordnung wurde die Hemmung spezifisch für dopaminerge Neuronen durchgeführt, indem die AAVs in tyrosin hydroxylase-Cre-Mäuse injiziert wurden.

Die Analyse dieser Mäuse ergab, dass die Hemmung der Schilddrüsenhormon-Signalübertragung in der ZI zu einem Anstieg des Grundumsatzes mit erhöhtem Nüchterngewichtsverlust führte, ohne die Körpertemperatur zu beeinflussen. Darüber hinaus führte dies zu einem chronisch stressähnlichen Zustand, bei dem das Serumcorticosteron erhöht war und zu einem partiellen Angstphänotyp, da die Gewöhnung an Stresssituationen beeinträchtigt war. Keine dieser Wirkungen wurde jedoch im konditionalen Modell beobachtet, was beweist, dass sie nicht durch dopaminerge Neuronen vermittelt werden.

Insgesamt identifiziert die Studie eine neue Gehirnregion für zentrale Wirkungen von Schilddrüsenhormonen, die ZI, und deutet darauf hin, dass es sich dabei um eine Schlüsselregion des Gehirns für die Schilddrüsenhormon-vermittelte Kontrolle von Verhalten und Energiestoffwechsel handelt.

1. INTRODUCTION

Mental health disorders pose a great risk, as it has been shown that patients suffering from mental disorders have a median life expectancy decrease of 10 years, and an estimated 14.3% of worldwide deaths can be attributed to mental disorders (Walker et al., 2015). A meta-analysis from 2001 - 2020 showed that global lifetime prevalence of mood disorders is at almost 30% in both males and females, indicating that one in 5 people will at some point in their life suffer from a common mental disorder, including major depressive disorder, bipolar disorder, anxiety disorders and substance use disorders (McGrath et al., 2023). Especially in younger people, incidences of depressive disorders and related deaths, as well as anxiety disorders, have increased over the last decade in the United States (Goodwin et al., 2020; Twenge et al., 2019).

1.1 STRESS AND ANXIETY

There are several different mental disorders, each with their own implications and treatment options. They have been categorised in the Diagnostic and Statistical Manual of Mental Disorders (DSM) (American Psychiatric Association, 2013), that is regularly updated and adapted (Stein et al., 2021).

The most common type of mental disorders are anxiety disorders, which comprise several sub-categories, such as separation anxiety, social anxiety disorder or generalised anxiety disorder (Penninx et al., 2021). Generalised anxiety disorder is characterised as uncontrollable fear or worry for everyday events. It presents with physical symptoms, such as irritability and restlessness, but also fatigue and sleep disturbances (American Psychiatric Association, 2013). However, it is often difficult to distinguish between normative anxiety and anxiety disorders (Penninx et al., 2021).

Current treatments for anxiety disorders include selective serotonin reuptake inhibitors (SSRIs), serotonin norepinephrine reuptake inhibitors (SNRIs), benzodiazepines, tricyclic antidepressants, monoamine oxidase inhibitors and antihistamines with common adverse effects like nausea, diarrhea, headaches, hypertension, cognitive problems and many more (Murrough et al., 2015). Not all patients suffering from anxiety disorders respond to current treatments (Flynn & Chen, 2003; Murrough et al., 2015), which gives rise to the necessity of further treatment options.

While the words stress and anxiety are often used interchangeably when talking about

mental disorders, there are profound differences. Anxiety, as a normal emotion, is a feeling of fear or the anticipation of a threat (American Psychiatric Association, 2013; Crocq, 2015). Excess of anxiety is classified as a mental disorder (Crocq, 2015). Stress itself describes stimuli, both extrinsic and intrinsic, that cause the body to have a biological response. These stimuli can be physical or psychological, and the respective stress response can vary in form and magnitude (Yaribeygi et al., 2017). However, chronic stress can lead to repetitive thoughts and worry, which in turn leads to an increased risk of developing mental disorders like depression or anxiety disorders (Nolen-Hoeksema et al., 1999; Watkins, 2008).

1.1.1 Stress and the Hypothalamus-Pituitary-Adrenal (HPA) Axis

Stress can have severe effects on the body and immune system. While acute stress will usually improve resistance to infections by promoting migration of immune cells to infection sites, chronic stress can lead to a decrease in immune system response. Chronic stress can induce the release of glucocorticoids via the HPA axis, which are known to suppress the immune response (Dragoş & Tănăsescu, 2010).

Upon stimulation by stress, hypophysiotropic neurons of the paraventricular nucleus (PVN) synthesise corticotropin-releasing hormone (CRH), which is released into the anterior pituitary via portal vessels, where it interacts with CRH receptors to release adrenocorticotropic hormone (ACTH) into the bloodstream. ACTH then acts on the adrenal glands at the melanocortin type 2 receptor (MC2R) and stimulates the synthesis and release of glucocorticoids. A negative feedback loop ensures inhibition of excessive activation of the HPA axis (S. M. Smith & Vale, 2006) (Fig. 1). Glucocorticoids can act on CRH neurons, as well as corticotroph cells in the anterior pituitary via the glucocorticoid receptor (GR). The GR belongs to the nuclear receptor family and is classified as a steroid hormone receptor, indicating its binding to steroid hormones. As a nuclear receptor, GR consists of three main domains: an N-terminal domain with a ligand-independent activation function domain 1, a DNA-binding domain (DBD) and a ligand-binding domain (LBD) containing a ligand-dependent activation function domain 2 (Lightman et al., 2020). Through interaction with the GR, glucocorticoids can alter transcription of CRH at CRH neurons (Jeanneteau et al., 2012) and inactivate corticotroph cells of the anterior pituitary to reduce release of ACTH (Lightman et al., 2020).

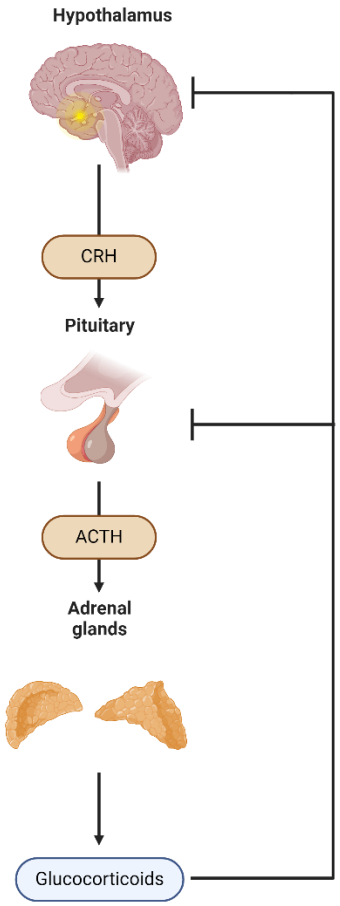

Figure 1: Hypothalamus-pituitary-adrenal axis. *CRH released by the hypothalamus stimulates the anterior pituitary, which in turn releases ACTH into the bloodstream. Through circulation, ACTH reaches the adrenal glands and stimulates the production and release of glucocorticoids. Glucocorticoids can then inhibit the release of CRH and ACTH at the hypothalamus and the anterior pituitary respectively. CRH: Corticotropin-releasing hormone; ACTH: Adrenocorticotropic hormone. Figure was created using Biorender.com.*

1.1.2 Behavioural Anxiety Tests in Rodents

In order to better understand the mechanisms behind stress and anxiety, it is necessary to use animal models, as they allow for more in depth experiments. Rodents, such as mice, show similar regulations of stress and anxiety as humans, and their endocrine effects within the HPA axis are comparable (Kolber et al., 2008; Lightman et al., 2020), which makes them a good candidate to study stress and anxiety. The most common experiments to assess anxiety behaviour in mice are the open field test and the elevated plus maze. In the open field test, mice are left to roam freely in an open field which is divided into centre and outer zones. This is used to analyse how much

time they are spending in the centre zone, as this would make them more visible and vulnerable to predator attacks. Therefore, one can deduce how anxious an individual is (Seibenhener & Wooten, 2015; Walsh & Cummins, 1976). In the elevated plus maze, mice are put on a plus-shaped maze, where two arms are closed off by walls on either side and the other two arms are open. Similar to the open field, mice will venture onto the open arms with the risk of being discovered by predators, while the closed arms hide them and give them more security. Additionally, the elevated plus maze can give more insight into exploratory behaviour, as it can show how often animals move to the open arms (Komada et al., 2008; Lister, 1987; Rodgers & Dalvi, 1997).

1.2. Thyroid Hormones

The thyroid is important for many regulatory pathways in the body and disruptions in the organ and its hormone signalling pathways can lead to many complications. THs, namely 3,3',5-triiodothyronine (T3) and thyroxine (T4), are released by the thyroid via the hypothalamus-pituitary-thyroid (HPT) axis (Duntas, 2016).

1.2.1 The Hypothalamus-Pituitary-Thyroid (HPT) Axis

Upon stimulation by different factors, the hypothalamus releases thyrotropin-releasing hormone (TRH) via TRH neurons originating in the PVN that project to the median eminence (ME) (Ishikawa et al., 1988; Segerson et al., 1987). Therefore, TRH can reach the anterior pituitary, where it stimulates the release of thyroid stimulating hormone (TSH) (Harris et al., 1978). As the name suggests, TSH acts in the thyroid gland to stimulate the release of THs. In healthy patients, a negative feedback loop ensures correct concentrations of circulating TH, as T3 and T4 can act on the hypothalamus to exert transcriptional regulation of TRH and on the pituitary to regulate transcription of TSH (X. Cheng et al., 2023; Ortiga-Carvalho et al., 2016) (Fig. 2).

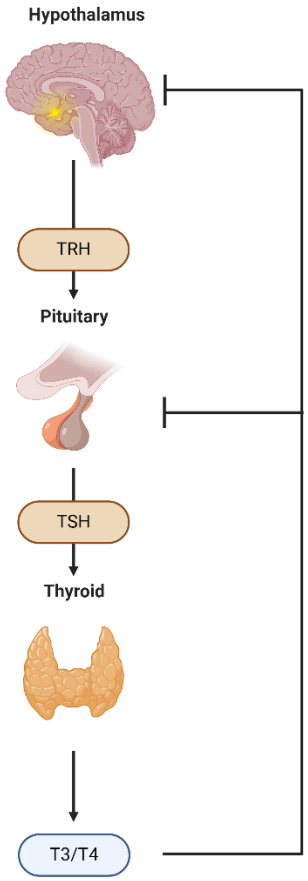

Figure 2: Hypothalamus-pituitary-thyroid axis. *TRH produced by the hypothalamus is released and stimulates the production and release of TSH by the pituitary gland. Through the bloodstream, TSH reaches the thyroid gland, which then releases THs. THs act in a negative feedback loop to exert transcriptional regulation of TRH and TSH at the hypothalamus and pituitary respectively. TRH: Thyrotropin-releasing hormone; TSH: Thyroid stimulating hormone; T3: 3,3',5-triiodothyronine; T4: Thyroxine. Figure created with Biorender.com.*

1.2.2 Thyroid Hormone Associated Diseases

Alterations in the HPT axis, as well as disruptions of the thyroid gland itself, can lead to a myriad of symptoms. Most commonly, patients can suffer from either elevated TH concentrations, known as hyperthyroidism (De Leo et al., 2016; Lee & Pearce, 2023), or decreased TH concentrations, known as hypothyroidism (Chaker et al., 2017). These conditions can have different causes, such as autoimmune diseases, inflammation or even carcinomas of the thyroid, as well as medication and genetic factors.

The most common cause for hyperthyroidism is Graves' disease, an autoimmune disorder in which the thyroid produces too much TH (Lee & Pearce, 2023). Patients suffering from

hyperthyroidism often present with increased body temperature, heat intolerance and weight loss, as well as hypertension and tachycardia, irritability and anxiety (De Leo et al., 2016). THs play an important role in the regulation of metabolism and energy homeostasis. They affect development of many tissues and the metabolic rate (Mullur et al., 2014). Common treatments for hyperthyroidism include antithyroid medications, thyroid gland ablation or surgical removal of the thyroid (Kravets, 2016).

Hypothyroidism in contrast is most often caused by an autoimmune disease called Hashimoto's disease, which leads to the inflammation of the thyroid gland and destruction of thyrocytes (Weetman, 2021). An additional cause can be so called congenital hypothyroidism, where hypothyroidism is already present at birth and can lead to severe neurological development disruptions, if not treated immediately (Wassner, 2018). It presents with growth delay, as well as reduced physical activity and feeding difficulty, among others (Guerri et al., 2019). Typical symptoms of acute hypothyroidism are weight gain, lethargy and cold intolerance (Chaker et al., 2017), but also changes in mood, like depression (Nuguru et al., 2022) or anxiety (Bathla et al., 2016). Hypothyroidism is most commonly treated with levothyroxine to replace missing TH (Chaker et al., 2017).

1.2.3 Thyroid Hormone Receptors

THs act on their target tissues via thyroid hormone receptors (TRs). TRs are nuclear receptors with an amino-terminal domain (A-B domain) necessary for localisation to the nucleus (Andersson & Vennström, 1997), as well as a DBD and an LBD. Nuclear receptors function as transcription factors, they can bind to DNA and can activate or repress the expression of their target genes in a ligand-binding dependant manner (Evans & Mangelsdorf, 2014). TRs bind to DNA at so called thyroid hormone response elements (TREs) as a heterodimer with the retinoid X receptor (RXR) (Brent, 2012) (Fig. 3).

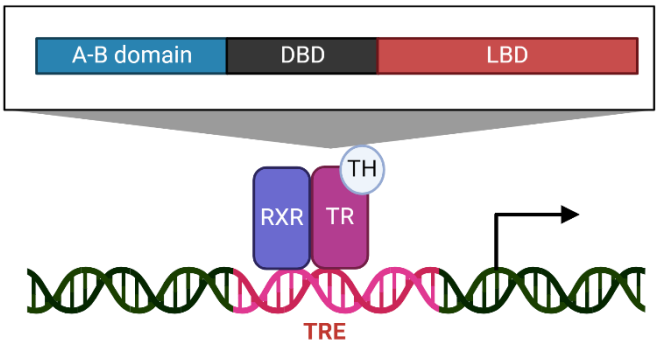

***Figure 3: Thyroid hormone-mediated gene expression via thyroid hormone receptors**. TRs consist of an A-B domain, a DBD and an LBD. Upon binding of THs, TRs form heterodimers with RXRs and bind to DNA at TREs. Via recruitment of co-activators or co-repressors (not shown), this induces gene expression of TH target genes. A-B domain: Amino-terminal domain; DBD: DNA-binding domain; LBD: Ligand-binding domain; RXR: Retinoid X receptor; TH: Thyroid hormone; TR: Thyroid hormone receptor; TRE: Thyroid hormone response element. Figure created with Biorender.com*

There are two main types of TRs, thyroid hormone receptor α (TRα) and thyroid hormone receptor β (TRβ), with isoforms TRα1, TRα2 and TRβ1-2 resulting from different splicing (Ortiga-Carvalho et al., 2014). The isoforms are differentially expressed and regulated throughout the body. While TRα1 and TRα2 are predominantly found in the brain (Williams, 2000), TRβ can be found highly expressed in liver, kidneys and HPT axis (S.-Y. Cheng et al., 2010). The differential expression of TRα and TRβ isoforms allows for tissue specific responses to THs, ensuring regulation of development and metabolic homeostasis.

TRα1, TRβ1 and TRβ2 are the primary functional receptors, whereas TRα2 is not capable of binding THs and acts as a dominant-negative inhibitor, as it blocks off TREs to TH-binding TRs (Katz & Lazar, 1993). This allows for adaptation to hormonal responses in different tissues as a regulatory mechanism.

1.2.3.1 Thyroid Hormone Receptor Knockouts and Mutations

To study the role of TRs more closely, knockout mice for either TRα or TRβ have been generated. TRα knockout mice present with bradycardia, as shown in prolonged QRS- and QT-times, as well as a decrease in body temperature and mild hypothyroidism (Wikström et al., 1998). Additionally, a homozygous knockout leads to growth retardation and a short lifespan, as TRα knockout mice die within 5 weeks (Fraichard et al., 1997).

In contrast, TRβ knockout mice show dysfunction of the HPT axis and elevated TSH levels,

as well as resistance to thyroid hormones (O'Shea & Williams, 2002), which highlights the role of TRβ in the TH mediated negative feedback loop control of the HPT axis (Lezoualc'h et al., 1992). In humans, resistance to THs due to a mutation in TRβ (RTHβ) has been known for a long time, ever since it was first described in 1967 (Refetoff et al., 1967). Patients suffering from RTHβ present with increased levels of THs but normal TSH levels (Pappa & Refetoff, 2021). However, resistance to THs due to a mutation in TRα (RTHα) is a disorder that has only been described recently (Bochukova et al., 2012). RTHα patients show growth retardation, intellectual deficits, dysmorphic facies, dyspraxia and skeletal dysplasia (Moran & Chatterjee, 2015). Due to the relatively new discovery, a mouse model for RTHα with a mutation in TRα1, TRα1R384C, was generated to define the phenotype. This mutation causes a 10-fold decreased binding affinity to T3, which results in a dominant-negative effect, since the receptor still binds to TREs but does not have any effect on the transcription of TR target genes. Due to its decreased binding affinity to T3, the receptor is not completely unfunctional and can be reactivated by treatment with T3 (Tinnikov et al., 2002). These mice have normal levels of THs but present with increased metabolism, which is due to overactivation of the brown adipose tissue (BAT) (Sjögren et al., 2007). However, they also have decreased body temperature, which can be attributed to increased tail heat loss (Warner et al., 2013). Additionally, the mice show increased anxiety and locomotor deficiencies (Venero et al., 2005), indicating central effects on the brain. However, the exact locations for these actions remain unknown.

1.3. Aims of this Study

THs have strong effects on brain function, as evidenced by their ability to regulate body temperature (Johann et al., 2019; Sentis et al., 2021) and mood (Fischer & Ehlert, 2018; Lekurwale et al., 2023), as well as neurodevelopmental defects and anxiety observed in TRα1 mutant mice (Venero et al., 2005), but locations are not defined, as TRα1 mutants show a full body mutation and further research is needed to identify the role of specific brain regions. Additionally, TRα1 mutant phenotype might be caused by an overlap of developmental and acute effects. Since many locations of central TH actions still remain unknown, this thesis aims to investigate the precise location where THs act to modulate behaviour and metabolism (Fig. 4). Previous studies show the involvement of the hypothalamus in the control of body temperature (Johann et al., 2019; Sentis et al., 2024), but other central effects of THs are not as precisely understood. Mutations in the TRα1 causing inhibited binding of T3 leads to deficiencies in locomotion activity,

as well as anxious behaviour and hypermetabolism (Mittag, Wallis, et al., 2010). The exact mechanism of how TH signalling can exert these effects is still only partially understood.

In order to better understand the mechanisms behind central TH actions, it is necessary to identify which brain regions are responsible for the effects observed in TRα mutant mice or patients suffering from thyroid associated diseases.

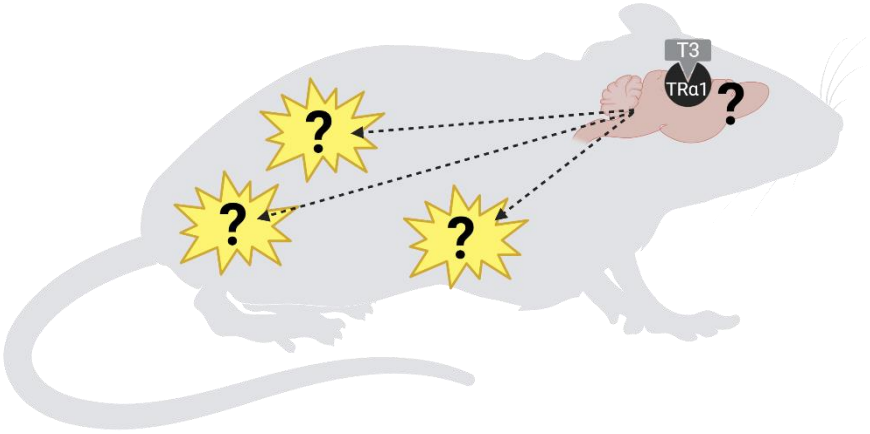

Figure 4: Study aims. *The aim of this study is to identify brain regions that are activated by T3 and that are the neuroanatomical location of central T3 effects. Figure created with Biorender.com.*

The main questions posed are:

1. Which brain regions show neuronal activation with systemic T3 treatment?
2. What are the effects of inhibition of TH signalling in these regions on behaviour and metabolism?
3. Which neuronal populations mediate the observed effects?

2. Materials and Methods

2.1 Materials

2.1.1 Chemicals, drugs, and reagents

Table 1 contains a list of all chemicals, drugs, and reagents used in this study.

Table 1: Chemicals, drugs, and reagents

Item	Catalog no.	Origin
3,3'-Diaminobenzidine	D5637-5G	Sigma Aldrich Chemie GmbH, Germany
Acetic acid	3738.4	Carl Roth GmbH + Co. KG, Germany
Anti-Fade Fluorescence Mounting Medium	Ab104135	Abcam, UK
Avidin/Biotin Blocking Kit	SP-2001	BIOZOL Diagnostics, Germany
Bepanthen eye ointment	01578675	Bayer, Germany
β-mercaptoethanol	M6250	Sigma Aldrich Chemie GmbH, Germany
Carprofen (Rimadyl®)	Vnr462986	Pfizer Inc., USA
Chloroform	C2432	Sigma Aldrich Chemie GmbH, Germany
D(+)-Saccharose ($C_{12}H_{22}O_{11}$)	9097.1	Carl Roth GmbH + Co. KG, Germany
di-Sodium hydrogen phosphate dihydrate ($Na_2HPO_4*2H_2O$)	1.0658	Supelco, Inc., USA
di-Sodium phosphate (Na_2HPO_4)	T876.2	Carl Roth GmbH + Co. KG, Germany
Eosin G-solution 0.5% water	X883.2	Carl Roth GmbH + Co. KG, Germany
Ethanol ≥ 70%	T913.2	Carl Roth GmbH + Co. KG, Germany
Ethanol ≥ 99,8%	K928.4	Carl Roth GmbH + Co. KG, Germany
Ethylene glycol	6881.1	Carl Roth GmbH + Co. KG, Germany
Glycerol	6967.1	Sigma Aldrich Chemie GmbH, Germany
Hydrochloric acid (HCl; 37 %)	9277.1	Carl Roth GmbH + Co. KG, Germany
Hydrogen peroxide (30%)	216763	Sigma Aldrich Chemie GmbH, Germany
Isoflurane	TU061219	Zoetis Inc., USA
Mayer's hemalum solution	1.09249.1000	Sigma Aldrich Chemie GmbH, Germany
Micromount Mounting Medium	3801731	Leica Biosystems Richmond, Inc., USA

Monosodium phosphate (NaH_2PO_4)	K300.1	Carl Roth GmbH + Co. KG, Germany
Normal donkey serum	END9010-10	BIOZOL Diagnostics, Germany
Normal goat serum	ENG9010-10	BIOZOL Diagnostics, Germany
Nuclease-free water	P119E	Promega GmbH, Germany
Paraformaldehyde solution (32 %)	15714	VWR International, Germany
Potassium chloride (KCl)	P017.1	Carl Roth GmbH + Co. KG, Germany
Potassium dihydrogen phosphate (KH_2PO_4)	P018.2	Carl Roth GmbH + Co. KG, Germany
ProLong Diamond Antifade Mountant with DAPI	P36971	LifeTechnologies, USA
QIAzol	79306	QIAGEN GmbH, Germany
RNaseZAP™	AM9780	Th. Geyer GmbH, Germany
Sodium chloride (NaCl)	9265.2	Carl Roth GmbH + Co. KG, Germany
Sodium chloride (NaCl; 0.9 % sterile)	6605514	Fresenius Kabi Deutschland GmbH, Germany
Sodium citrate ($C_6H_5Na_3O_7$)	4088.3	Carl Roth GmbH + Co. KG, Germany
Sodium hydroxide (NaOH)	1310-73-2	Carl Roth GmbH + Co. KG, Germany
Standard chow diet	1314	Altromin, Germany
Tissue-Tek® O.C.T.™ Compound	4583	Sakura Finetek USA, Inc. USA
Triton™X-100	X100	Sigma Aldrich Chemie GmbH, Germany
Vaseline	771055	Balea; dm-Drogeriemarkt GmbH + Co.KG, Germany
VECTASTAIN® Elite® ABC-HRP Kit, Peroxidase (Standard)	PK-6100	BIOZOL Diagnostics, Germany
Xylocaine (10 mg/mL)	XYL1050	AstraZeneca, UK

2.1.2 Consumables and devices

Table 2 lists all consumables and devices that were used in this thesis.

Table 2: Consumables and devices

Item	Origin
23U-Series Color Industrial Camera	The Imaging Source Europe GmbH, Germany
96-PCR plate	Sarstedt AG & Co., Germany
Absorbable suture (V396H Coated Vicryl)	Ethicon, Germany
Acculab ATL-224-I Atilon Analytical Balance 220g x 0.0001	Sartorius Stedim Biotech GmbH, Germany
Adhesive clear PCR seal sheets	BiozymScientific GmbH, Germany
Alcohol pads	B. Braun SE, Germany
Anaesthesia Unit 410	High Precision Instruments, Univentor, Malta
BD MicrolanceTM 3, 26G x ½" (0,45x13mm)	Becton Dickinson GmbH, Germany
Benchtop centrifuge MC6	Sarstedt AG & Co., Germany
Biosphere® Plus (20 µL, 100 µL, 200 µL, 1000 µL)	Sarstedt AG & Co., Germany
Biosphere® Plus Filter Tips (20 µL, 100 µL, 200 µL, 1000 µL)	Sarstedt AG & Co., Germany
Brain matrix	World Precision Instruments, USA
Bright field microscope Axiovert 40 CFL	Carl Zeiss AG, Germany
Cell strainer (70 µm)	Greiner Bio-One International GmbH, Germany
Centrifuge 5430, 5430 R, and multifuge 3 S-R	Eppendorf AG, Germany
Ceramic beads (1.4 mm, 325g)	VWR International, USA
Climate incubator MKKL1200	Flohr Instruments, Netherlands
Combitips advanced® (0.1 mL, 0.5 mL, 5 mL)	Eppendorf AG, Germany
Cotton swabs	Nobamed, Germany
Cover glasses	Th. Geyer GmbH, Germany
Cryostat CM3050 S	Leica Biosystems, Germany
Dräger Isoflurane Vapor® 19.3	Drägerwerk AG & Co. KGaA, Germany
Dremel® 200 Multitool System	Dremel, USA
Duomax 1030	Heidolph Instruments, Germany
ECGenie Clinic System	Mouse Specifics Inc., USA

ER-4000 receiver plates	PhilipsRespironics, USA
EVOS® FL Auto Imaging System	Thermo Fisher Scientific Inc., Germany
Feather disposable scalpel	Feather Safety Razor Co., Ltd., Japan
Fisherbrand™ Homogenizer Bead Mill 24	Fisher Scientific GmbH, Germany
G2 E-Mitter	PhilipsRespironics, USA
Glass capillaries (1.14 mm; 504949)	World Precision Instruments, USA
Glucometer	Bayer, Germany
Green Line Sealsafe Plus	Tecniplast S.p.A, Italy
Heating pad Themolux®	Witte + Sutor GmbH, Germany
Hood	Waldner Laboreinrichtungen GmbH & Co. KG, Germany
Infrared camera T335	FLIR Systems Termisk Systemteknik, Sweden
Inject® FLuerSolo	B. Braun SE, Germany
Inveon preclinical PET/CT system	Siemens, Germany
Magnetic Hotplate Stirrer VMS-C4	VWR International, Germany
Magnetic stirrer (Rct basic)	IKA®-Werke GmbH & Co. KG, Germany
Microscope slides Superfrost® Plus	Thermo Fisher Scientific Inc., Germany
Microtest plate transparent, flat bottom, 96 well	Sarstedt AG & Co., Germany
Microtome Blade MB35 Premier	Epredia Netherlands B.V., Netherlands
Multipette 8-channel (0.5-10 µL)	Eppendorf AG, Germany
Multipette® E3	Eppendorf AG, Germany
NanoDrop™ One C	Thermo Fisher Scientific Inc., Germany
Nanoliter 2020 injector	World Precision Instruments, USA
Parafilm	Sigma Aldrich Chemie GmbH, Germany
PCR strip of 8 200 µL	Sarstedt AG & Co., Germany
Permanent suture (EH7823H)	Ethicon, Germany
Pestle	Th. Geyer GmbH, Germany
pH-meter (PB-11)	Sartorius Lab Instruments GmbH & Co. KG, Germany
Pipette controller	Brand GmbH + Co. KG, Germany
Pipette Research® Plus (0.5-10 µL, 2-20 µL, 10-100µL, 20-200 µL, 100-1000 µL)	Eppendorf AG, Germany

Precision balance	VWR International, Germany
PV-1 Grantbio	Grant Instruments Ltd, UK
QuantStudio Applied Biosystems realtime PCR sytem	Thermo Fisher Scientific Inc., Germany
Razor blades	World Precision Instruments, Germany
Rectal thermometer probe BAT-12	Physitemp Inc., USA
SafeSeal tube (1.5 mL, 2 mL, 5 mL)	Sarstedt AG & Co., Germany
Screw cap micro tube 2 mL	Sarstedt AG & Co., Germany
Serological Pipette (5 mL, 10 mL, 25 mL, 50 mL)	Sarstedt AG & Co., Germany
SPECTROstar Nano Microplate Reader	BMG Labtech, Germany
Staining jar	Isolab Laborgeräte GmbH, Germany
Stereo microscope VWR® VisiScope® SZB250	VWR International, Germany
Stereotaxic apparatus (963205A, 957)	Kopf®, USA
TC dish 100, standard	Sarstedt AG & Co., Germany
TC plate, 6 well, standard F	Sarstedt AG & Co., Germany
TC plate, 24 well, standard F	Sarstedt AG & Co., Germany
Thermocycler PTC-200	Biozym Scientific GmbH, Germany
Thermomixer 5436	Eppendorf AG, Germany
Tissue punch	Fine Science Tools, USA
Titramax 100	Heidolph Instruments, Germany
TSE PhenoMaster	TSE Systems, Germany
Tubes (15 mL, 50 mL)	Sarstedt AG & Co., Germany
Twin mouse carrier	MEDRES, Germany
Water bath	Polyscience, USA
Weighing pans neoLab®	neoLab Migge GmbH, Germany

2.1.3 COMMERCIALLY AVAILABLE KITS

Table 3 consists of commercially available kits that were used for analysis in this study.

Table 3: Commercially available kits

Item	Catalog no.	Origin
Corticosterone ELISA	RE52211	Tecan, Switzerland
Glycogen assay kit	MAK016	Sigma Aldrich Chemie GmbH, Germany
GoTaq® qPCR Mastermix	M7112	Promega GmbH, Germany
RevertAid First Strand cDNA Synthesis kit	K1621	Thermo Fisher Scientific Inc., Germany
RNeasy® FFPE kit	73504	QIAGEN GmbH, Germany
RNeasy® fibrous tissue mini kit	74704	QIAGEN GmbH, Germany
RNeasy® lipid tissue mini kit	74804	QIAGEN GmbH, Germany
RNeasy® mini kit	74106	QIAGEN GmbH, Germany
Total T3 ELISA	DNOV053	NovaTec Immundiagnostica GmbH, Germany
Total T4 ELISA	EIA-1781	DRG Instruments GmbH, Germany

2.1.4 BUFFERS

Table 4 shows all buffers used in this study with chemicals and their respective concentration.

Table 4: Buffers

Buffer	Chemicals	Concentration / Amount
Cryo protection solution (CPS) 250 mL; pH = 7.4	Ethylene glycol	75 mL
	Glycerol	75 mL
	NaH_2PO_4 (0.1 M)	19 mL
	Na_2HPO_4 (0.1 M)	81 mL
Phosphate buffered saline (PBS) (10x) pH = 7.4	KCl	27 mM
	KH_2PO_4	17.6 mM
	Na_2HPO_4	188.8 mM
	NaCl	1370 mM
Sodium citrate buffer for antigen retrieval pH = 6.0	$C_6H_5Na_3O_7$	10mM

2.1.5 SOFTWARE

Table 5 lists all software used and its purpose for this study.

Table 5: Software

Software	Company	Use
CorVita	Mouse Specifics Inc., USA	ECG signal processing and analysis
FLIR Tools	FLIR Systems Termisk Systemteknik, Sweden	Infrared photography analysis
GraphPad PRISM 8	GraphPad Software Inc., USA	Statistical analysis
ImageJ 1.53k	National Institute of Health, USA	Hippocampal area analysis
Microsoft Office Excel	Microsoft, USA	Data preprocessing and statistical analysis
QuantStudio™ Design & Analysis v1.5.1	Thermo Fisher Scientific Inc., Germany	qPCR analysis
TSE PhenoMaster Software V6.5.3	TSE Systems, Germany	Recording of indirect calorimetry and analysis
Vital View 4.200.2	PhilipsRespironics, USA	Recording of telemetry data

2.2 METHODS

Animal husbandry

Male wild-type and tyrosine hydroxylase-Cre mice (Savitt et al., 2005) with a C57/6NCr background were bred at the Gemeinsame Tierhaltung (GTH) at the University of Lübeck. The animals started the experiments at an age of 3-6 months and were single housed with *ad libitum* access to standard chow diet (Altromin) and water following a 12/12-hour light/dark cycle at a constant temperature of 22°C. To monitor the wellbeing and growth of the animals, body weight was measured at least twice a week. In addition, food – and water intake were monitored to ensure sufficient nutrition by weighing left-over food and water. New food and water were provided at least every other week or as needed. All experimental protocols were approved by MLLEV (Ministerium für Landwirtschaft, ländliche Räume, Europa und Verbraucherschutz) Schleswig-Holstein (Germany) and adhered to the EU guidelines (210/63/EU).

Positron emission tomography (PET)/Computed tomography (CT) imaging

PET-CT scans were conducted by Dr. Heiko Backes and Dr. Anna-Lena Cremer at the Max Planck Institute for Metabolism Research in Cologne, Germany. They were performed within subject, once before treatment and once after two weeks of oral treatment with T3 (0.5 mL/L drinking water) as described previously (Backes et al., 2011) with an Inveon preclinical PET/CT system (Siemens). Mice were anaesthetised using isoflurane and put on a twin mouse-carrier (MEDRES) before cannulation in the tail vein using a 30G cannula that is connected to polythene tubing (ID = 0.28 mm) fixated with glue. After PET recording was started, an injection of 7-8 MBq of ^{18}F-Fluorodeoxyglucose (FDG) in 50-100 µL of saline was carried out and emission data was recorded for 45 minutes. Afterwards, a CT scan was conducted (180 projections / 360°, 200 ms, 80 kV, 500 µA) to correct the PET data. A standard glucometer (Bayer) was used to determine plasma glucose levels from tail vein blood. The data was then histogrammed in 12 x 30 s, 30 x 60 s, 3 x 120 s and 7 x 240 s time frames and full 3D binning was used to bin it. PET images were constructed according to the MAP-SP algorithm, which was provided by the manufacturer. Co-registration was done using image analysis software Vinci (Cízek et al., 2004) and a 3D mouse brain atlas according to the 2D Paxinos mouse brain atlas (Franklin & Paxinos, 2013).

Kinetic modelling

Kinetic modelling was conducted by Dr. Heiko Backes and Dr. Anna-Lena Cremer at the Max Planck Institute for Metabolism Research in Cologne, Germany. PET data from the aorta, identified in the first time frame image for each animal, were utilised to get an image-based input function. This input function was corrected for fractional volume effects, assuming a volume fraction of 0.619. A voxel-wise data fitting approach with a voxel size of 0.4 mm x 0.4 mm x 0.8 mm was applied to a kinetic model to generate parametric images of the ^{18}F-FDG kinetic constants (K1, k2, k3, k4). Changes in glucose transport were used as an indicator of neuronal activation, as tissue to plasma glucose concentration ratio (CE/CP) measures glucose transport with

$$\frac{CE}{CP} = \frac{K1}{\frac{k2 + k3}{0.26}}$$

(Backes et al., 2011; Jais et al., 2016) and this parameter is very robust for plasma glucose levels.

Stereotactic AAV injections and radiotelemetry transmitter implantation

Before entering the experiment, mice were matched according to age and body weight and sorted into control and treatment groups. Coordinates for injections into the ZI were calculated with the use of the Mouse Brain Atlas (Paxinos & Franklin, 2004) relative to the bregma: anterior-posterior: 1.00 mm; medial-lateral: ± 0.75 mm; dorsal-ventral: -4.60 mm. Carprofen (5 mg/kg s.c.; Pfizer Inc.) was injected as pain medication before the start of the surgery. Mice were put on a heating pad (Witte + Sutor GmbH) for warming and a rectal probe was inserted to monitor body temperature. Heart rate and breathing were monitored to ensure successful surgery. Mice were anaesthetised using isoflurane (Zoetis Inc.), and lidocaine (AstraZeneca) was used for local anaesthesia before opening the scalp and drilling holes into the skull for injection. 500 nL of AAV serotype 1 were injected bilaterally per side using either manual injections or a nanoliter 2020 injector (World Precision Instruments). Wild-type mice received AAVs expressing either control green fluorescent protein (EGFP) (2.17×10^{12} genome copies (GC)/mL) or mCherry and a dominant-negative TRα1R384C (2.81×10^{12} GC/mL), all under a CMV promotor. Tyrosine hydroxylase-Cre mice were injected with AAVs with FLEXOn constructs expressing either control mCherry (2.3×10^{10} GC/mL) under a CAG promotor or a dominant-negative TRα1R384C and mCherry (2.92×10^{12} GC/mL) under a CMV promotor (VectorBuilder GmbH). After closing up the incision site, mice were implanted with a radiotelemetry transmitter (G2 E-Mitter; PhilipsRespironics) into their abdomen to non-invasively record body temperature and locomotion activity. This was done by cutting into the abdominal skin after disinfection, separating the skin from the connective tissue and then cutting along the linea alba of the peritoneum to open the abdomen. The radiotelemetry transmitter was then sterilised and implanted into the cavity, after which both the peritoneum and the outer skin were closed separately with sutures. The animals were monitored while waking up in their cages and treated with Carprofen (5 mg/kg s.c.; Pfizer Inc.) 24 hours after the surgery. For optimal recovery, mice were fed with water-soaked food for 24 hours and they were allowed to recover for at least 14 days before any experimental recording started.

2.2.1 *IN VIVO* METHODS

Radiotelemetry recordings

For baseline measurements of core body temperature and locomotion activity, mice were placed into a climate chamber (Flohr Instruments) set to 22°C and 50% humidity. Each cage was put

onto its own radiotelemetry receiver plate (PhilipsRespironics) that continuously recorded body temperature and locomotion activity every 30 seconds. Baseline recordings were conducted for at least 3 days. Afterwards, the temperature was set to 10°C and body temperature and locomotion activity was recorded for 7 hours. Mice were then allowed to rest and recover for at least 24 hours before being placed back into the climate chamber at 30°C to record body temperature and locomotion activity for 3 hours.

Infrared thermography

To measure BAT activity and tail heat loss, infrared pictures were taken using a FLIR IR camera (FLIR). Vaseline was applied to the back hair to reveal the skin above the interscapular brown adipose tissue (iBAT) for more accurate data (Oelkrug & Mittag, 2021). Mice were allowed to roam freely at an ambient temperature of 22°C and infrared pictures of the iBAT, tail and lower back were captured within a timeframe of 5 minutes to minimise stress-related increase in temperatures.

Electrocardiograms (ECGs)

For measurements of ECGs and related parameters, electrode towers (ECGenie Clinic System; Mouse Specifics Inc.) were used. Mice were allowed to acclimate to the towers for 10 minutes on 2 consecutive days before the measurements took place. On the day of the recording, mice were accustomed to the tower for 10 minutes prior to the measurements. Heart rate was recorded for 10-20 minutes (ECGenie Clinic System; Mouse Specifics Inc., USA) and the data was analysed using the ECGenie software (ECGenie CorVita Software; Mouse Specifics Inc., USA).

Indirect calorimetry

Measurements of oxygen consumption and oxygen and carbon dioxide exchange were conducted with an open respirometry climate chamber (TSE Systems). Mice were allowed to train and acclimate to the chambers for three days before recording. For baseline recordings, the temperature was set to 22°C and parameters were measured for a period of at least 7 hours. During this time, mice had *ad libitum* access to food and water. Afterwards, the temperature was set to 30°C and recordings took place for 6 hours with no access to food or water to measure the

basal metabolic rate. The respiratory quotient (RQ), as a measure for which micronutrients the organism uses, was calculated using the following formula:

$$RQ = \frac{carbon\ dioxide\ produced}{oxygen\ consumed}$$

For each measurement, body weight was recorded once before placement into the climate chamber and once afterwards. Data was analysed with Microsoft Office Excel (Version 2402; Microsoft) and the TSE PhenoMaster Software (V6.5.3; TSE Systems).

Behavioural assays

To assess the anxiety phenotype of the animals, two behavioural assays were carried out. Mice were allowed to acclimate to the testing room for at least 1 hour prior to the experiment. For the open field test, lights were set to 30 lux and the animals were placed into the centre of the field, facing away from the experimenter and left unrestrained for 10 minutes. For the elevated plus maze, the light was set to 125 lux and the mice were put into the centre of the maze, facing away from the experimenter and left unrestrained for 5 minutes. The data were analysed with the ANY-maze tracking software (Stoelting Europe).

Sacrifice and organ collection

Before sacrifice, mice were allowed to acclimate to the room for at least an hour to reduce stress. The animals were sacrificed by cervical dislocation. Blood was collected from the trunk after cutting off the head and left to coagulate at room temperature for 2 minutes and then placed on ice for at least 30 minutes. This was followed by a centrifugation step at 1000g and 4°C for 10 minutes. The liquid phase was then transferred to a new tube and centrifuged again. The resulting serum (liquid phase) was then again transferred to a new tube and stored at -20°C. Brains were directly transferred to 4% paraformaldehyde (PFA) (VWR International) and stored at 4°C prior to further preparation. All other organs were snap-frozen using either liquid nitrogen or dry ice and stored at -80°C.

2.2.2 MOLECULAR METHODS

Immunohistochemistry and immunofluorescence

Fresh brains were collected after sacrifice and fixed in 4% PFA (VWR International) in H_2O for 24 hours at 4°C. After PFA fixation, brains were transferred to 30% sucrose (w/v in PBS) (Carl Roth GmbH + Co. KG) and incubated for at least 3 days at 4°C until they were fully saturated. Subsequently, the brains were frozen on dry ice and stored at -80°C. In preparation for immunostaining, a cryostat (Leica Biosystems) was used to cut the brains to a thickness of 40 µm at around -20°C. Sections were collected in 5 tubes with each tube containing sections 200 µm apart and then stored in cryo protection solution (CPS) at -20°C.

For immunohistochemistry, sections were incubated with 1% hydrogen peroxide (H_2O_2) in PBS (Sigma Aldrich Chemie GmbH) for 30 minutes before blocking with 5% normal goat serum (BIOZOL Diagnostics) and 4 drops/mL avidin (BIOZOL Diagnostics) in 0.3% Triton X-100 (Sigma Aldrich Chemie GmbH) in PBS for 1 hour at room temperature. Afterwards, they were incubated in primary antibody (Table 6) and 5% normal goat serum (BIOZOL Diagnostics) with 4 drops/mL biotin (BIOZOL Diagnostics) in 0.3% Triton X-100 (Sigma Aldrich Chemie GmbH) in PBS over night at 4°C. Sections were then incubated in secondary antibody (Table 7) in 0.3% Triton X-100 (Sigma Aldrich Chemie GmbH) in PBS for 1 hour at room temperature before incubation with 10 µL/mL avidin and 10 µL/mL biotinylated horseradish peroxidase (HRP) (BIOZOL Diagnostics) in 0.3% Triton X-100 (Sigma Aldrich Chemie GmbH) in PBS for 1 hour at room temperature. Subsequently, sections were incubated with 0.5 mg/mL 3,3'-diaminobenzidine (DAB) (Sigma Aldrich Chemie GmbH) in PBS and 0.1% H_2O_2 (Sigma Aldrich Chemie) for 1-5 minutes at room temperature until colour developed. The sections were then mounted on microscope slides (Thermo Fisher Scientific Inc.), left to dry over night at room temperature and mounted with Micromount Mounting Medium (Leica Biosystems Richmond, Inc.) and coverslips (Th. Geyer GmbH). For c-Fos staining, an additional antigen retrieval step in 10 mM Na-Citrate was carried out for 10 minutes at 80°C before inactivation of endogenous peroxidase activity.

For immunofluorescence, sections were blocked with 5% normal goat serum (BIOZOL Diagnostics) or normal donkey serum (BIOZOL Diagnostics) in 0.3% Triton X-100 (Sigma Aldrich Chemie GmbH) in PBS for 1 hour at room temperature before incubation in primary antibody (Table 6) with 5% normal goat serum (BIOZOL Diagnostics) or normal donkey serum (BIOZOL Diagnostics) in 0.3% Triton X-100 (Sigma Aldrich Chemie GmbH) in PBS over night at 4°C. Afterwards, sections were incubated in secondary antibody (Table 7) in 0.3% Triton X-100 (Sigma Aldrich Chemie GmbH) in PBS for 1 hour and subsequently mounted on slides with ProLong

Diamond Antifade Mountant with DAPI (LifeTechnologies) or Anti-Fade Fluorescence Mounting Medium (Abcam).

Sections were washed in either PBS or 0.1% Triton X-100 (Sigma Aldrich Chemie GmbH) in PBS in between incubations. All incubations were done while shaking.

Table 6: Primary antibodies

Target	Host	Dilution	Catalog no.	Origin
C-Fos	Rabbit	1:500	89065	Novus Biologicals, USA
GFP	Rabbit	1:1000	Ab290	Abcam, UK
GFAP	Chicken	1:500	Ab4674	Abcam, UK
mCherry	Goat	1:1000	AB0040	OriGene Technologies Inc., USA
NeuN	Mouse	1:500	Ab104224	Abcam, UK
Tyrosine hydroxylase	Mouse	1:1000	T2928	Sigma Aldrich Chemie GmbH, Germany

Table 7: Secondary antibodies

Target	Host	Conjugation	Dilution	Catalog no.	Origin
Goat	Donkey	Alexa Fluor™ 594	1:800	A-11058	Invitrogen, Thermo Fisher Scientific, USA
Mouse	Goat	Biotin	1:250	BA-9200	BIOZOL Diagnostics, Germany
Mouse	Donkey	Alexa Fluor™ 488	1:800	A-21202	Invitrogen, Thermo Fisher Scientific, USA
Mouse	Donkey	Alexa Fluor™ 594	1:800	A-21203	Invitrogen, Thermo Fisher Scientific, USA
Rabbit	Goat	Biotin	1:250	BA-1000	BIOZOL Diagnostics, Germany
Rabbit	Donkey	Alexa Fluor™ 488	1:800	A-21206	Invitrogen, Thermo Fisher Scientific, USA
Chicken	Donkey	DyLight™ 405 AffiniPure™	1:400	703-475-155	Jackson ImmunoResearch Labs, USA

H&E staining

Cut sections were washed in PBS and mounted onto slides before drying for 1 hour at room temperature and stored at -20°C. In preparation for H&E staining, the slides were taken out of the freezer and left to acclimate to room temperature for 20-30 minutes. Afterwards, the sections were stained in hematoxylin (1:5 in dH_2O; Sigma Aldrich Chemie GmbH) for 2 minutes and then washed in warm H_2O for 15 minutes and subsequently washed in dH_2O for 5 minutes while shaking. After washing, the sections were stained by dipping once in eosin (Carl Roth GmbH + Co. KG) containing 0.5 mL acetic acid (Carl Roth GmbH + Co. KG) per 100 mL. The sections were then washed again shortly in dH_2O before destaining in 70% Ethanol (Carl Roth GmbH + Co. KG) for 5 minutes and dehydrating in 100% Ethanol (Carl Roth GmbH + Co. KG) for 15 seconds. After drying, the slides were coverslipped with Micromount Mounting Medium (Leica Biosystems Richmond, Inc.).

Isolation of the Zona Incerta

Right brain hemispheres of the animals were collected fresh after sacrifice and frozen on dry ice. For dissection of the Zona Incerta, a brain matrix (World Precision Instruments) and tissue punches (World Precision Instruments) were used. The brain matrix was frozen 24 hours prior to the dissection at -20°C and then placed into ice and frozen gel packs for cooling. A glass plate was put onto a mixture of ice and dry ice and cleaned with RNase ZAP™ (Th. Geyer GmbH). The frozen brains were placed into the brain matrix and allowed to acclimate for 2-5 minutes before cutting with pre-chilled razor blades (World Precision Instruments). Cut sections were then placed onto the glass plate and the ZI was cut out using tissue punches with the help of the Mouse Brain Atlas (Paxinos & Franklin, 2004). The dissected ZI was placed into pre-chilled tubes and stored at -80°C.

Quantitative polymerase chain reaction (qPCR)

RNA was isolated from the respective snap-frozen tissues. For hepatic RNA, liver was ground using mortar and pestle with liquid nitrogen. The isolation was done using RNeasy mini kits according to the manufacturer's instructions (RNeasy FFPE kit, #73504 for hypothalamic brain sections; RNeasy mini kit, #74104 for liver; RNeasy fibrous tissue mini kit, #74704 for M. gastrocnemius; RNeasy lipid tissue mini kit, #74804 for adrenal glands, brain, iBAT and pituitary;

QIAGEN) with performance of a DNase digestion step. Concentration of RNA was measured using Nanodrop (Thermo Fisher Scientific Inc.). Afterwards, cDNA synthesis was carried out using RevertAid first strand cDNA synthesis kit (Thermo Fisher Scientific Inc.).

For qPCR, RNA was diluted with nuclease-free water to a final working concentration of 5 ng. The measurements were done with GoTaq Master Mix (Promega GmbH) and a real-time PCR system (QuantStudio Applied Biosystems; Thermo Fisher Scientific Inc.), the protocol can be found in Table 8. Primer specificity was ensured by measurement of a melting curve. Standard curves were calculated, and primer efficiency (E) was determined using the following formula (Pfaffl et al., 2004):

$$E = 10^{-\frac{1}{standard\ curve\ slope}}$$

NormFinder was used to select housekeeping genes for each tissue for qPCR analysis (Andersen et al., 2004) (Table 9). Primer sequences for each qPCR can be found in Table 10. Data were analysed employing the ΔΔCt method (Livak & Schmittgen, 2001) and a design & analysis software (QuantStudio™, Thermo Fisher Scientific Inc.). Primer efficiency was used for normalisation.

Table 8: PCR method

Temperature [°C]	Time [min]	Number of cycles
50	2	1
95	10	1
95	0.15	40
60	1	
95	0.15	1
60	0.3	1
95	0.15	1

Table 9: Housekeeping genes

Tissue	Housekeeping genes
Anterior pituitary	*Actb*
Adrenal glands	*Actb, Ppia*
Hypothalamus	*Actb, Rn18s*
Interscapular brown adipose tissue	*Hprt, Rplp0*
Liver	*Hprt, Ppid*
Muscle (M. gastrocnemius)	*Gapdh, Ppia*
Zona Incerta	*Actb*

Table 10: Genes used for qPCR with respective primer sequences

Gene	Abbreviation	Sequences 5'→3' (forward and reverse)
18S Ribosomal RNA	*Rn18s*	GCAATTATTCCCCATGAACG GGGACTTAATCAACGCAAGC
α 1a-adrenergic receptor	*Adra1a*	GAGGCATGGTGCGTATCCC CAGCAGCAGACCTGCAAAAA
ATPase sarcoplasmic/endoplasmic reticulum Ca^{2+} transporting 1	*Atp2a1*	TGTTTGTCCTATTTCGGGGTG AATCCGCACAAGCAGGTCTTC
ATPase sarcoplasmic/endoplasmic reticulum Ca^{2+} transporting 2	*Atp2a2*	TCCGCTACCTCATCTCATCC CAGGTCTGGAGGATTGAACC
ATPase sarcoplasmic/endoplasmic reticulum Ca^{2+} transporting 3	*Atp2a3*	CGTCGCTTCTCGGTGACAG AAGAGGTCCTCAAACTGCTCC
β 2-adrenergic receptor	*Adrb2*	GGGAACGACAGCGACTTCTT GCCAGGAGCATAACCGACAT
β 3-adrenergic receptor	*Ardb3*	AGAAACGGCTCTCTGGCTTTG TGGTTATGGTCTGTAGTCTCGG
β-actin	*Actb*	ACTGAGCTGCGTTTTACACCC TGCTCCAACCAACTGCTGTC
Catalase	*Cat*	AGCGACCAGATGAAGCAGTG TCCGCTCTCTGTCAAAGTGTG
Cell death inducing DFFA-like effector A	*Cidea*	TGACATTCATGGGATTGCAGA GGCCAGTTGTGATGACTAAGA

Corticotropin-releasing hormone	*Crh*	GAAAATGTGGCCCCAAGGA GCCACCCCTCAAGAATGAATT
Corticotropin-releasing hormone receptor	*Crhr*	GGGCAGCCCGTGTGAATTATT ATGACGGCAATGTGGTAGTGC
Cytochrome P450, family 11, subfamily b, polypeptide 1	*Cyp11b1*	AACCCAAATGTTCTGTCACCAA CAAAGTCCCTTGCTATCCCATC
Cytochrome P450, family 11, subfamily b, polypeptide 2	*Cyp11b2*	TGGCTGAAGATGATACAGATCCT CACTGTGCCTGAAAATGGGC
Deiodinase 2	*Dio2*	ATGGGACTCCTCAGCGTAGAC ACTCTCCGCGAGTGGACTT
Fatty acid synthase	*Fasn*	GGAGGTGGTGATAGCCGGTAT TGGGTAATCCATAGAGCCCAG
Glucocorticoid receptor	*Gr*	AGCTCCCCCTGGTAGAGAC GGTGAAGACGCAGAAACCTTG
Glucose-6-phosphate dehydrogenase	*G6dph*	ATGAAGCACACAGGCATTTGG TCCAGGTATAGCTGAAACAGTCC
Glutamate ionotropic receptor NMDA type subunit 2A	*Grin2a*	ACGTGACAGAACGCGAACTT TCAGTGCGGTTCATCAATAACG
Glycerinaldehyde-3-phosphate dehydrogenase	*Gapdh*	AGGTCGGTGTGAACGGATTTG TGTAGACCATGTAGTTGAGGTCA
Glycerol-3-phosphate dehydrogenase 2	*Gpd2*	GAAGGGGACTATTCTTGTGGGT GGATGTCAAATTCGGGTGTGT
Hairless	*Hr*	CGGAGACAATCATAGGAAGCAAG CCGGTCAGTACCCCTACCT
Hypoxanthine phosphoribosyltransferase	*Hprt*	GCAGTACAGCCCCAAAATGG AACAAAGTCTGGCCTGTATCCAA
Krüppel-like factor 9	*Klf9*	TTATTGCACGCTGGTCACTATC CTCATCGGGACTCTCCAGAC
Metallothionein 2	*Mt2*	GCCTGCAAATGCAAACAATGC AGCTGCACTTGTCGGAAGC
Myosin heavy chain 1	*Myh1*	CTCTTCCCGCTTTGGTAAGTT CAGGAGCATTTCGATTAGATCCG
Myosin heavy chain 4	*Myh4*	CTTTGCTTACGTCAGTCAAGGT AGCGCCTGTGAGCTTGTAAA

Myostatin	*Mstn*	CCCAGGACCAGGAGAAGATGGGC TCGACCGTGAGGGGGTAGCG
Peptidylprolyl isomerase A	*Ppia*	GAGCTGTTTGCAGACAAAGTTC CCCTGGCACATGAATCCTGG
Peptidylprolyl isomerase D	*Ppid*	TCACAACAGTTCCGACTCCTC ACCTCTACATTTTCAAGCGTCC
Peroxisome proliferator-activated receptor γ	*Pparγ*	TCGCTGATGCACTGCCTATG GAGAGGTCCACAGAGCTGATT
Peroxisome proliferator-activated receptor δ	*Pparδ*	TCCATCGTCAACAAAGACGGG ACTTGGGCTCAATGATGTCAC
Phosphodiesterase 10A	*Pde10a*	GGACAGAGACAAGCGAGATGA GGTGTGCTCTTGCTAGGCG
Phosphoenolpyruvate carboxykinase	*Pepck*	ATCTTTGGTGGCCGTAGACCT GCCAGTGGGCCAGGTATTT
Proopiomelanocortin	*Pomc*	TCATGACCTCCGAGAAGAGC GCCTTGGAATGAGAAGACC
PR domain 16	*Prdm16*	CCCCACATTCCGCTGTGAT CTCGCAATCCTTGCACTCA
Pyruvate kinase	*Pyrk*	TCAAGGCAGGGATGAACATTG CACGGGTCTGTAGCTGAGTG
Ribosomal protein lateral stalk subunit P0	*Rplp0*	TCGGGTCCTAGACCAGTGTTC AGATTCGGGATATGCTGTTGGC
Ryanodine receptor 1	*Ryr1*	CAGTTTTTGCGGACGGATGAT CACCGGCCTCCACAGTATTG
Sarcolipin	*Sln*	GAGGTGGAGAGACTGAGGTCCTTGG GAAGCTCGGGGCACACAGCAG
Stearoyl-Coa desaturase 1	*Scd1*	TTCTTGCGATACACTCTGGTGC CGGGATTGAATGTTCTTGTCGT
T-box 19	*Tbx19*	TCTCGCCTGCTTAACGTGG CCAGCCCTGTGACACTAATCTT
Thyroid hormone receptor α 1	*Tra1*	GTGACTGACCTCCGCATGAT ATCCTCAAAGACCTCCAGGAA
Thyroid hormone receptor β 1	*Trb1*	ACACCTTATCCAGGCCACTT GTGGTACCCTGTGGCTTTGT

Thyroid hormone receptor β 2	*Trb2*	CCAGAGGTACACGAAGTGTGC AGGTTTCCAGGGTAACTACAGG
Thyroid stimulating hormone β	*Tshb*	GGGCAAGCAGCATCCTTTTG GTGTCATACAATACCCAGCACAG
Thyrotropin-releasing hormone receptor	*Trhr*	GTCAGTGAAATGAACCAAACCG CACAATGCCCAGTCCACAAATA
Tyrosine aminotransferase	*Tat*	TGCTGGATGTTCGCGTCAATA CGGCTTCACCTTCATGTTGTC
Uncoupling protein 1	*Ucp1*	ACTCAGGATTGGCCTCTACG CCACACCTCCAGTCATTAAGC
Uncoupling protein 2	*Ucp2*	CGAAGCCTACAAGACCATTGC GTTGGCTTTCAGGAGAGTATCTTTG
Uncoupling protein 3	*Ucp3*	GAGATGGTGACCTACGACATCA GCGTTCATGTATCGGGTCTTTA

Serum T3, T4 and corticosterone

Total T3 (NovaTec Immundiagnostica), total T4 (DRG Diagnostics) and corticosterone (Tecan) serum concentrations were measured with enzyme-linked immunoabsorbent assays (ELISA) according to the manufacturers' instructions. A standard curve was generated using the mean absorbance values of the provided standards and their concentrations. Interpolation of this curve was used to determine the concentrations of the samples. If sample concentration was too high, a dilution with saline was performed.

Glycogen assay

The hepatic glycogen concentration was measured using a glycogen assay kit which is commercially available (Sigma Aldrich Chemie GmbH) with ground liver tissue according to the manufacturer's instructions. A standard curve was created by plotting the mean absorbance values of the provided standards against their concentrations. The sample concentrations were then determined by interpolating the data using linear regression. Finally, the sample concentrations were normalised to tissue weight.

Hippocampal volume

Brain sections were stained using H&E staining for visualisation of the hippocampus. Single areas (a_s) were determined using the ImageJ software (Version 1.53k; National Institue of Health). Single volumes (V_s) were calculated using the following formula:

$$V_s = a_s * 200\ \mu m$$

Total hippocampal volume was determined by adding up all single volumes.

2.3 Statistics and software

Prior to conducting statistical analysis, data were preprocessed using Excel (Microsoft). During preprocessing, data were normalised, and outliers were identified. Group comparisons were then made using GraphPad Prism 8 (GraphPad Software Inc.) or Excel (Microsoft) with paired and unpaired Student's t-test, ANCOVA or two-way ANOVA with Šídák's multiple comparison post hoc test. Further details are provided in Supplementary Table 1. Significance levels were defined as: *p < 0.05, **p < 0.01, ***p < 0.001. The results are expressed as mean ± standard error of the mean (SEM). Figures were designed using GraphPad Prism 8 (GraphPad Software Inc.) and Biorender.com.

3. RESULTS

3.1 THYROID HORMONE ACTIONS IN THE BRAIN

THs can not only act locally at target tissues but also centrally in the brain to have a myriad of effects (Warner & Mittag, 2012). While some of these effects, such as body temperature regulation (Sentis et al., 2024), have already been attributed to brain regions, others still remain elusive and the regions responsible for them are still unknown.

3.1.1 ACTIVATION OF THE ZONA INCERTA BY TREATMENT WITH THYROID HORMONES

To identify candidate regions for central thyroid hormone effects, PET/CT scans were conducted. Male mice were treated with 0.5 mg/L T3 in the drinking water for two weeks and brain scans with a ^{18}F-FDG radiotracer were carried out both before and after treatment. Radiotracer uptake visualised neuronal activation of brain regions by T3. With the help of the mouse brain atlas (Paxinos & Franklin, 2004), areas of the PET/CT scans could be annotated to brain regions. Among other areas including the hippocampus and the lateral hypothalamus, the Zona Incerta showed increased glucose uptake and therefore activation after T3 treatment (Fig. 5A). To further validate this, mouse brain sections were stained for c-Fos, a marker for early neuronal activation. Without T3 treatment, no c-Fos positive cells could be observed in the Zona Incerta. However, when mice were treated orally with 0.5 mg/L T3 for 24 h, neurons in the Zona Incerta were positive for c-Fos, indicating activation. Interestingly, this effect disappeared when the animals were treated with T3 for 12.5 days (Fig. 5B), as c-Fos only shows early activation and reduces expression with time (Hoffman et al., 1993).

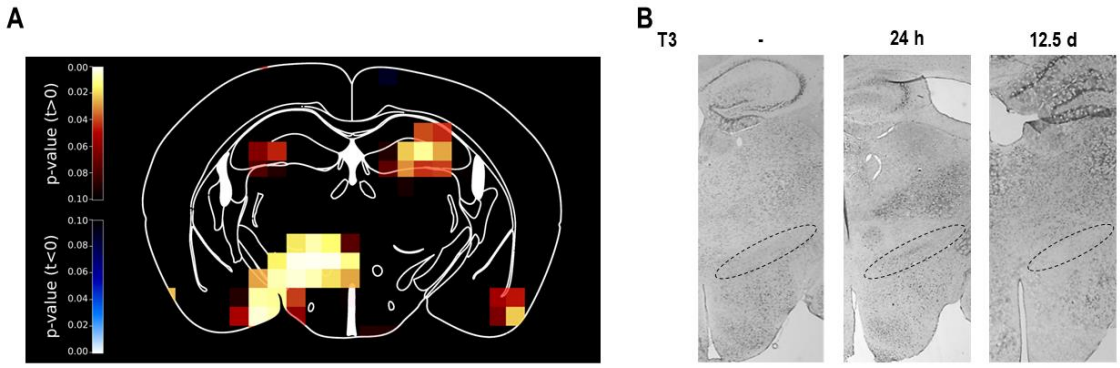

Figure 5: Neuronal activation of the Zona Incerta by treatment with T3 (0.5 mg/L) (A) *PET/CT scans of mouse brains after oral T3 treatment (n = 12). Highlighted areas indicate increased glucose uptake and therefore neuronal activation (data generated in collaboration with Dr. Heiko Backes and Dr. Anna-Lena Cremer, MPI Cologne).* ***(B)*** *Staining for c-Fos in mice treated with T3 for different periods of time. Circled region shows the Zona Incerta. Adapted from Maier et al., 2024, in press.*

Among all the brain regions activated, the ZI showed the highest amount of glucose uptake with the highest significance (Table 11).

Table 11: Glucose uptake of different brain regions upon T3 treatment. *Mice were treated with 0.5 mg/L T3 in the drinking water for 14 days. Shown is the glucose uptake at day 0 (before treatment) and at day 14 (after treatment) sorted from highest to lowest difference in glucose uptake. CPu = Caudate putamen; Hip = Hippocampus; LH = Lateral hypothalamus; MeP = Posterior medial amygdaloid nucleus; Pir = Piriform cortex; S1BF = Primary somatosensory barrel field; ZI = Zona incerta. Data generated in collaboration with Dr. Heiko Backes and Dr. Anna-Lena Cremer, MPI Cologne. Table adapted from Maier et al., 2024, in press.*

Brain region	Day 0	Day 14	Difference	% Difference	p
ZI	0.209705	0.2425832	0.0328782	15.67831	0.0004731
S1BF	0.2159847	0.2472484	0.0312637	14.4749605	0.000623
Hip2	0.2003379	0.2259333	0.0255954	12.7761148	0.002525
MeP	0.1863625	0.209289	0.0229265	12.3020994	0.003927
Hip1	0.2032275	0.2250936	0.0218661	10.7594199	0.0101
Hip3	0.2161788	0.2389415	0.0227627	10.5295709	0.01522
Pir	0.1887197	0.2075368	0.0188171	9.97092513	0.0213
Cpu	0.1857101	0.2042011	0.018491	9.95691672	0.007964
LH	0.2061208	0.2256911	0.0195703	9.49457794	0.01035

3.1.2 What are the effects of central TRα1 signalling in the Zona Incerta?

To analyse the effects of TH signalling specifically in the ZI, TRα1 signalling has been inhibited by injection of an AAV expressing a dominant-negative TRα1 into the ZI. Additionally, a radiotelemetry transmitter was implanted into the abdomen of the animals to non-invasively record core body temperature and locomotor activity for several days. For ideal expression of the virus, the animals were single housed to recover for two weeks before any data were recorded. After radiotelemetry measurements, infrared pictures were taken of iBAT, ear, tail and lower back, and an electrocardiogram was conducted. Furthermore, oxygen consumption was measured at 22°C, as well as at 30°C under fasting conditions to guarantee that BAT does not contribute to energy expenditure. Lastly, both an open field test and an elevated plus maze were carried out to analyse the animals' behaviour. After recovery for at least 48 hours, the mice were sacrificed by cervical dislocation (Fig. 6).

For analysis of metabolic pathways, as well as other molecular effects, several organs were collected after sacrifice: brain, pituitary, liver, iBAT, adrenal glands, and muscle (M. gastrocnemius). The organs were all snap-frozen and prepared for further analysis.

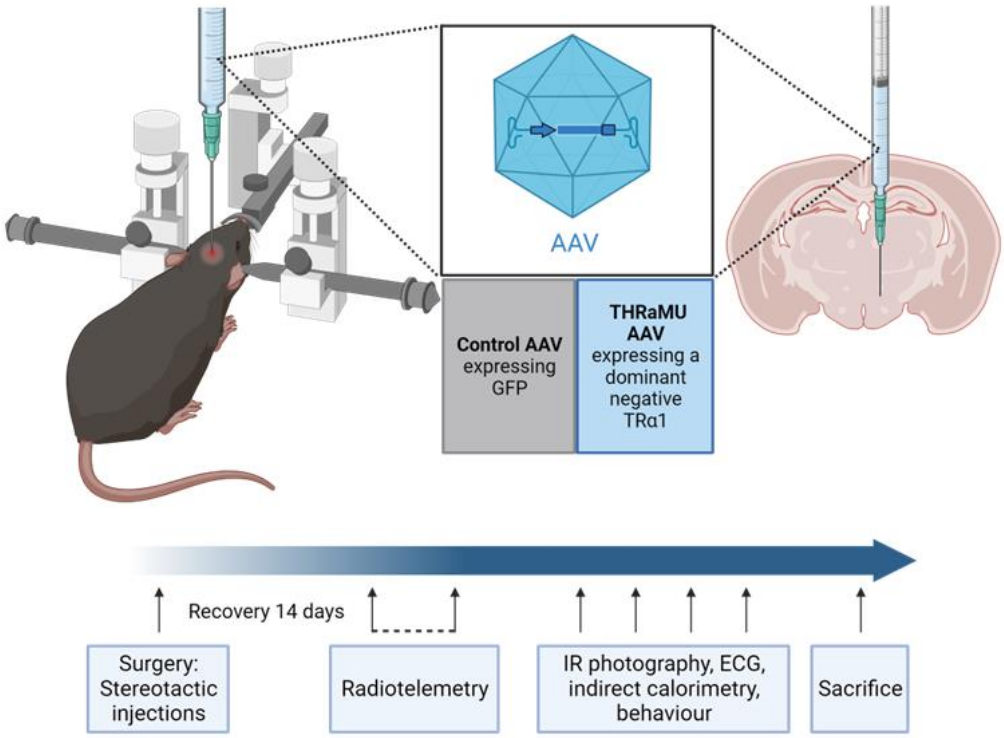

Figure 6: Experimental in vivo design to explore the effects of central TRα1 signalling in the Zona Incerta. *Figure generated with Biorender.com. Adapted from Maier et al., 2024, in press.*

3.1.2.1 Effects of TRα1 signalling inhibition on body weight and food intake

The injected AAVs express either EGFP (control virus) or mCherry (using an IRES after the dominant-negative TRα1) under the CMV promotor. By staining for either reporter gene, it was possible to validate the injection sites in each animal after sacrificing. mCherry or EGFP were expressed in neurons in the ZI, indicating successful injection, and some colocalization with tyrosine hydroxylase could be observed, which shows infection of dopaminergic neurons (representative, Fig. 7A).

In addition to validating the injection sites, it was also necessary to validate the inhibition of TRα1 signalling. For this, the ZI was isolated from the right brain hemispheres and gene expression for TR target genes was measured (Denver et al., 1997; Siemes et al., 2023; Thompson & Potter, 2000; Waters et al., 1997). This analysis showed significant reduction of Krüppel-like factor 9 (*Klf9*), as well as a trend for decreased expression of hairless (*Hr*). No difference could be observed in stearoyl-CoA denaturase (*Scd1*) or phosphodiesterase 10A (*Pde10a*) (Fig. 7B). Analysis of gene expression revealed significant increase in expression of thyroid hormone receptor α1 (*Tra1*) in mice lacking ZI TH signalling ($p = 0.0023$), and roughly 10 times higher expression of *Tra1* than thyroid hormone receptor β1 (*Trb1*) in controls. Thyroid hormone receptor β2 (*Trb2*) was not detectable (Fig. 7C).

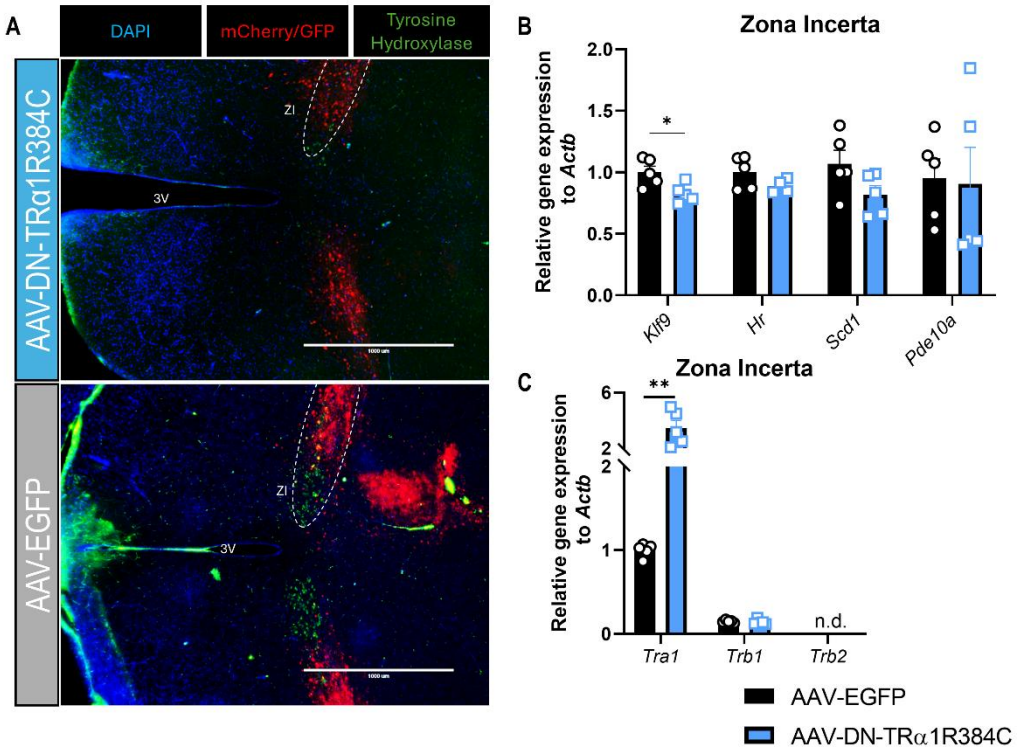

Figure 7: Validation of virus expression and successful TRα1 signalling inhibition. ***(A)*** *Staining of representative brain sections for either mCherry or GFP, and tyrosine hydroxylase as marker for the Zona Incerta. Circled area indicates Zona Incerta, scale bar is 1000 µm.* ***(B)*** *qPCR analysis of TR target genes in the Zona Incerta for control (n = 5) vs. dominant-negative TRα1 (n = 4-5) animals.* ***(C)*** *qPCR analysis of TRs in the Zona Incerta for control (n = 5) vs. dominant-negative TRα1 (n = 5) animals. Graphs show mean ± SEM; *p < 0.05, **p < 0.01 with unpaired Student's t-test, n.d.: not detectable. Actb: β-actin; Hr: Hairless; Klf9: Krüppel-like factor 9; Pde10a: Phosphodiesterase 10A; Scd1: Stearoyl-CoA denaturase 1; Tra1: Thyroid hormone receptor α1; Trb1: Thyroid hormone receptor β1; Trb2: Thyroid hormone receptor β2. Figure was adapted from Maier et al., 2024, in press.*

Co-staining for NeuN and GFAP, as markers for neurons and astrocytes respectively, as well as EGFP as a marker for injected control AAV showed co-localisation of NeuN and EGFP, but not GFAP (Fig. 8). This validates the serotype of the AAV and specificity to neurons instead of astrocytes, showing that injection of the AAV results in infection of neurons and that any observed effect is mediated by neurons and not astrocytes.

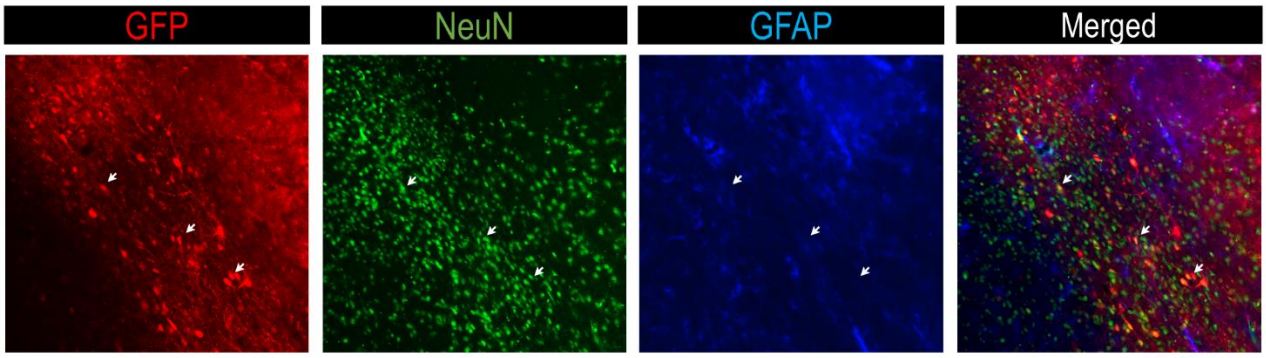

Figure 8: Cell-type specific infection of injected AAV. *Representative staining of brains injected with control AAV for EGFP, NeuN and GFAP. Arrows show GFP-positive and therefore infected cells. Figure was adapted from Maier et al., 2024, in press.*

Throughout the experiment, body weight, as well as food and water intake, were recorded to analyse the effects of TH signalling inhibition in the ZI. The results showed no difference in body weight change, as the starting weight and the end weight of the animals did not differ between the groups. However, due to growth of the animals, both groups weighed significantly more at the start of the experiment compared to the end (controls: p = 0.0016; dominant-negative TRα1: p = 0.0232) (Fig. 9A). In addition, there was no observable difference between food intake (Fig. 9B) or water intake (Fig. 9C).

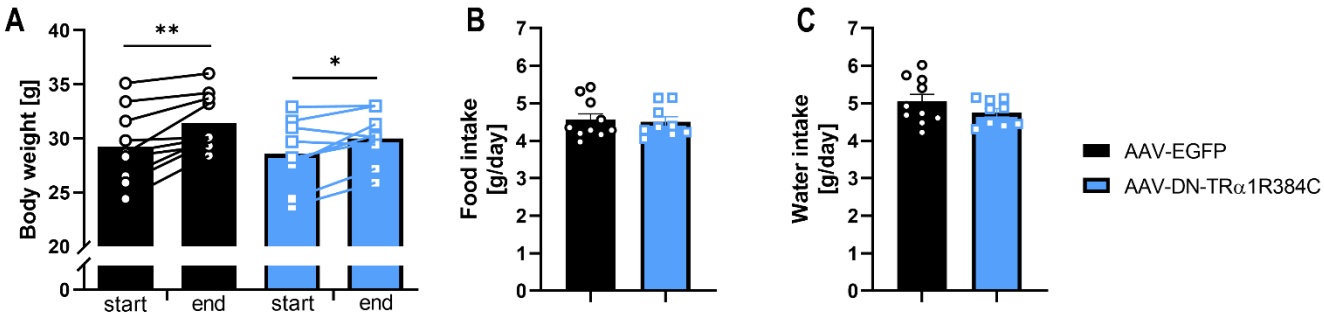

Figure 9: Body weight and food and water intake of mice with inhibited thyroid hormone signalling in the Zona Incerta. ***(A)*** *Start (two weeks post injections) and end weight of all animals.* ***(B)*** *Food intake throughout the experiment.* ***(C)*** *Water intake throughout the experiment. Data is represented as mean ±SEM for control (n = 10) vs. dominant-negative TRα1 (n = 9) animals; *p < 0.05, **p < 0.01 with paired Student's t-test. Adapted from Maier et al., 2024, in press.*

Since it is known that the PVN is involved in the regulation of TH release (Fekete & Lechan, 2014), total T3 and T4 levels were measured in the serum to rule out an effect of the infection on

the nearby PVN. The results showed that there was no difference in circulating TH levels between the two groups (Fig. 10A+B), which supports the findings, that the HPT axis is not affected.

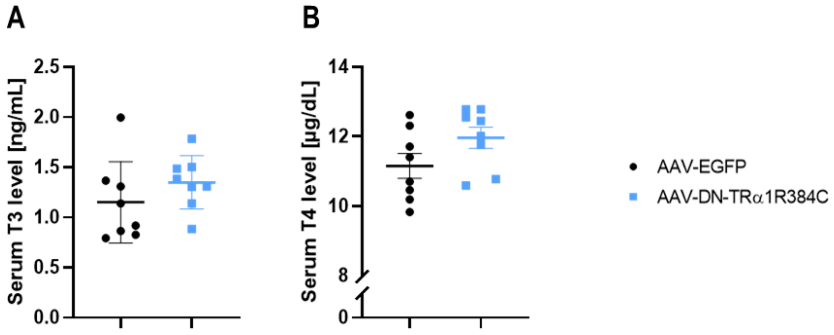

Figure 10: Circulating thyroid hormone levels of mice expressing a dominant-negative TRα1 compared to control mice. (A) *Total T3 level in the serum.* ***(B)*** *Total T4 level in the serum. Data is represented as mean ± SEM (n = 8 per group). Figure was adapted from Maier et al., 2024, in press.*

Taken together, expression of a dominant-negative TRα1R384C via AAV injection successfully downregulated TH signalling in the ZI without affecting the PVN and therefore circulating T3 and T4 levels. This inhibition did not alter body weight and had no effect on food and water intake.

3.1.2.2 Effects of TRα1 signalling inhibition on thermoregulation

Since THs are well-known to affect body temperature, as hyperthyroid patients often present with heat intolerance (De Leo et al., 2016) and hypothyroid patients often display cold intolerance (Chaker et al., 2017), body temperature was recorded non-invasively for several days using radiotelemetry transmitters. These transmitters also allowed for recording of locomotion activity. Body temperature and locomotion were recorded at different ambient temperatures: 22°C, 10°C and 30°C. No differences could be observed at either temperature. At 22°C, body temperature showed a difference of about 1°C between light and dark phases (Fig. 11A). Locomotion activity also did not differ, and as expected, was higher during the dark phases compared to the light phases (Fig. 11B). At 10°C, body temperature did not differ significantly between the groups (Fig. 11C). Again, locomotion activity was not altered by ZI TH inhibition (Fig. 11D). At 30°C, body temperature showed no difference between the groups (Fig. 11E). There was also no difference in locomotion activity (Fig. 11F).

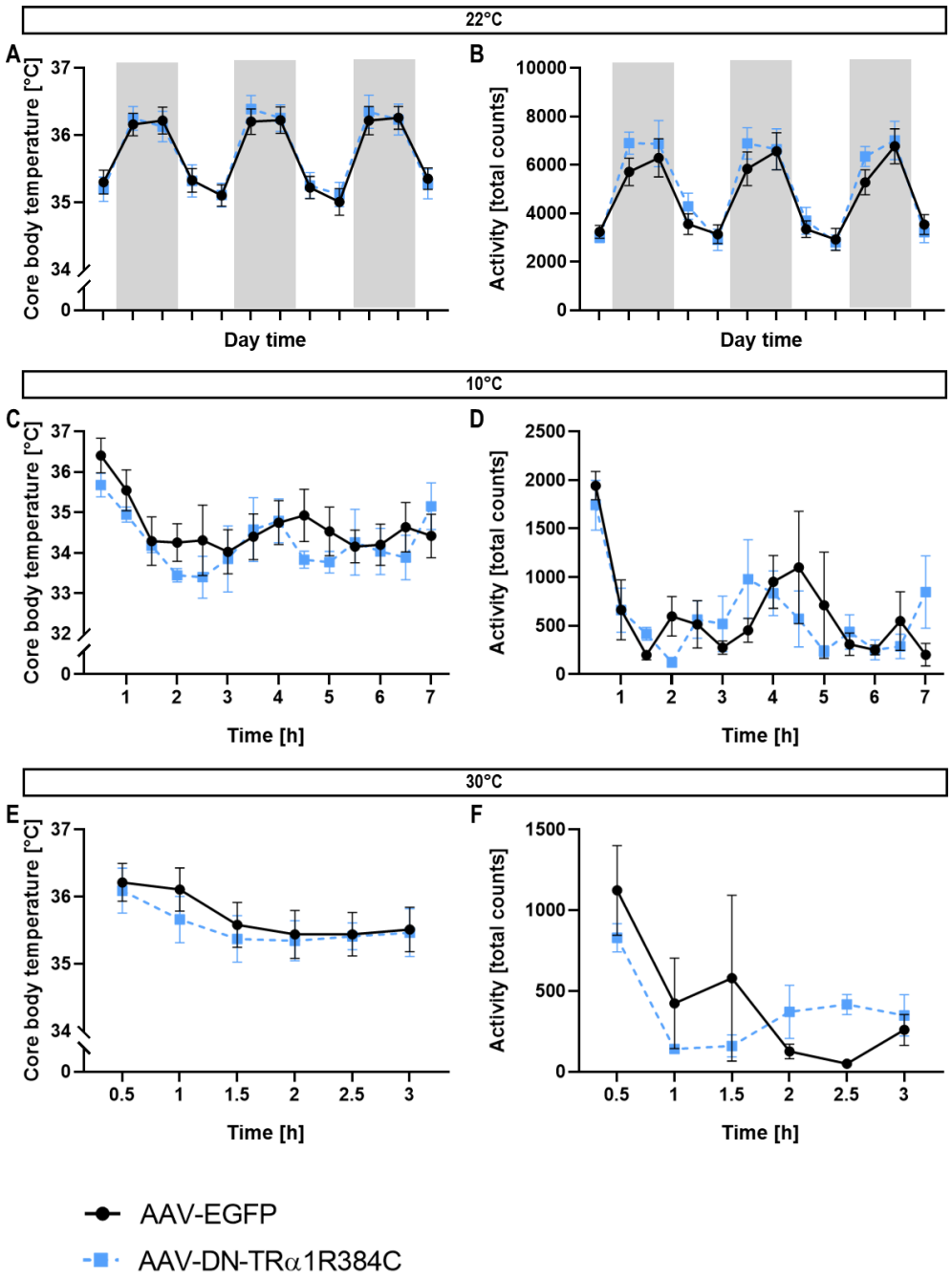

Figure 11: Effects of Zona Incerta thyroid hormone signalling inhibition on core body temperature and locomotion. ***(A-B)*** *Core body temperature* ***(A)*** *and locomotion activity* ***(B)*** *at 22°C ambient temperature for control (n = 10) vs. dominant-negative TRα1 mice (n = 9). Grey areas indicate dark phases.* ***(C-D)*** *Core body temperature* ***(C)*** *and locomotion activity* ***(D)*** *at 10°C ambient temperature for control vs. dominant-negative TRα1 animals.* ***(E-F)*** *Core body temperature* ***(E)*** *and locomotion activity* ***(F)*** *at 30°C ambient temperature for control vs. dominant-negative TRα1 animals. Data is represented as mean ± SEM, n = 4 per group unless otherwise stated. Adapted from Maier et al., 2024, in press.*

In addition to core body temperature measurements with radiotelemetry transmitters, infrared thermography was conducted at an ambient temperature of 22°C to analyse

temperatures of iBAT and tail (Fig. 12A). All temperatures were normalised to the lower back temperature. iBAT temperature did not differ between the groups, indicating no difference in BAT activity (Fig. 12B). This was further validated by gene expression analysis of thermogenic markers in the iBAT. The only marker that was differentially expressed was cell death inducing DFFA like effector A (*Cidea*), which showed slightly decreased gene expression with ZI TH signalling inhibition (Fig. 12C), indicating a lower level of browning in the iBAT (Rosell et al., 2014). Furthermore, inhibition of TH signalling in the ZI had no effect on tail temperature (Fig. 12B), suggesting no difference in tail heat loss.

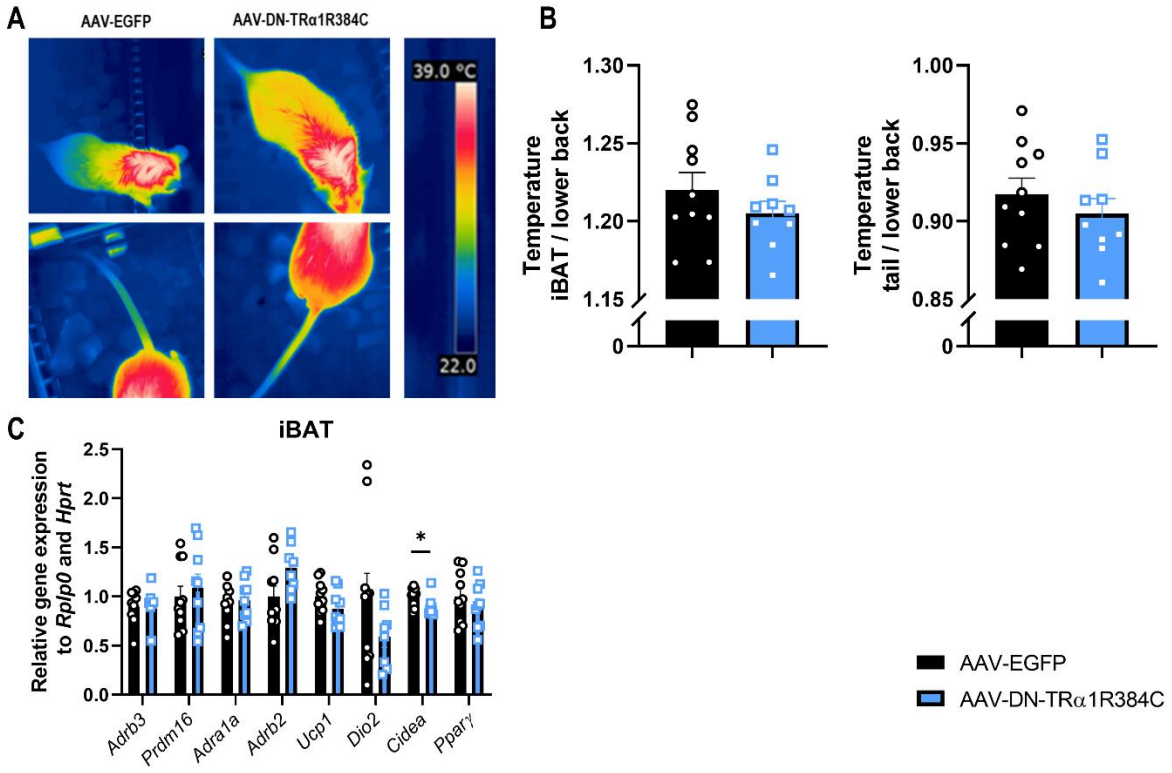

Figure 12: iBAT activity and tail heat loss in mice expressing a mutant TRα1 or control GFP. ***(A)*** *Representative infrared images of iBAT and tail.* ***(B)*** *iBAT and tail temperatures normalised to lower back temperature with infrared thermography for control animals (n =10) vs. dominant-negative TRα1 animals (n = 9).* ***(C)*** *Normalised gene expression of thermogenic genes in iBAT for control (n = 9-10) and dominant-negative TRα1 (n = 8-9) mice. Data is represented as mean ± SEM; *p < 0.05 with unpaired Student's t-test. Adra1a: α 1a-adrenergic receptor; Adrb2: β 2-adrenergic receptor; Adrb3: β 3-adrenergic receptor; Cidea: Cell death-inducing DFFA-like effector A; Dio2: Deiodinase2; Hprt: Hypoxanthine phosphoribosyltransferase; Pparγ: Peroxisome proliferator-activated receptor γ; Prdm16: PR domain 16; Rplp0: Ribosomal protein lateral stalk subunit P0; Ucp1: Uncoupling Protein 1. Figure was adapted from Maier et al., 2024, in press.*

In conclusion, inhibition of TH signalling in the ZI did not affect thermoregulation, as core body temperature, as well as iBAT and tail temperature were not significantly altered. Furthermore, it did not result in differentially expressed thermogenic genes except for *Cidea* in the iBAT and had no effect on locomotion activity.

3.1.2.3 Effects of TRα1 signalling inhibition on energy expenditure

The ability of THs to alter energy metabolism is already well established (Mullur et al., 2014). To investigate whether TH signalling in the ZI has any effect on energy expenditure, oxygen consumption was measured under resting conditions at 22°C, as well as under fasting conditions at 30°C using an indirect calorimetry system (TSE). The analysis showed no significant differences at 22°C (Fig. 13A+C) for increased normalised oxygen consumption ($p = 0.12$; Fig. 13B). Inhibition of ZI TH signalling also had no effect on the respiratory quotient (RQ) (Fig. 13D). At 30°C, oxygen consumption was elevated with ZI TH signalling inhibition as shown by normalising to body weight ($p = 0.003$; Fig. 13F) and ANCOVA analysis ($p = 0.028$; Fig. 13G). The RQ was again not affected (Fig. 13H). In addition to elevated oxygen consumption and therefore increased energy expenditure, dominant-negative TRα1 animals lost 4% of body weight during the fasting period, while the control animals only lost 2.8% ($p = 0.04$; Fig. 13I).

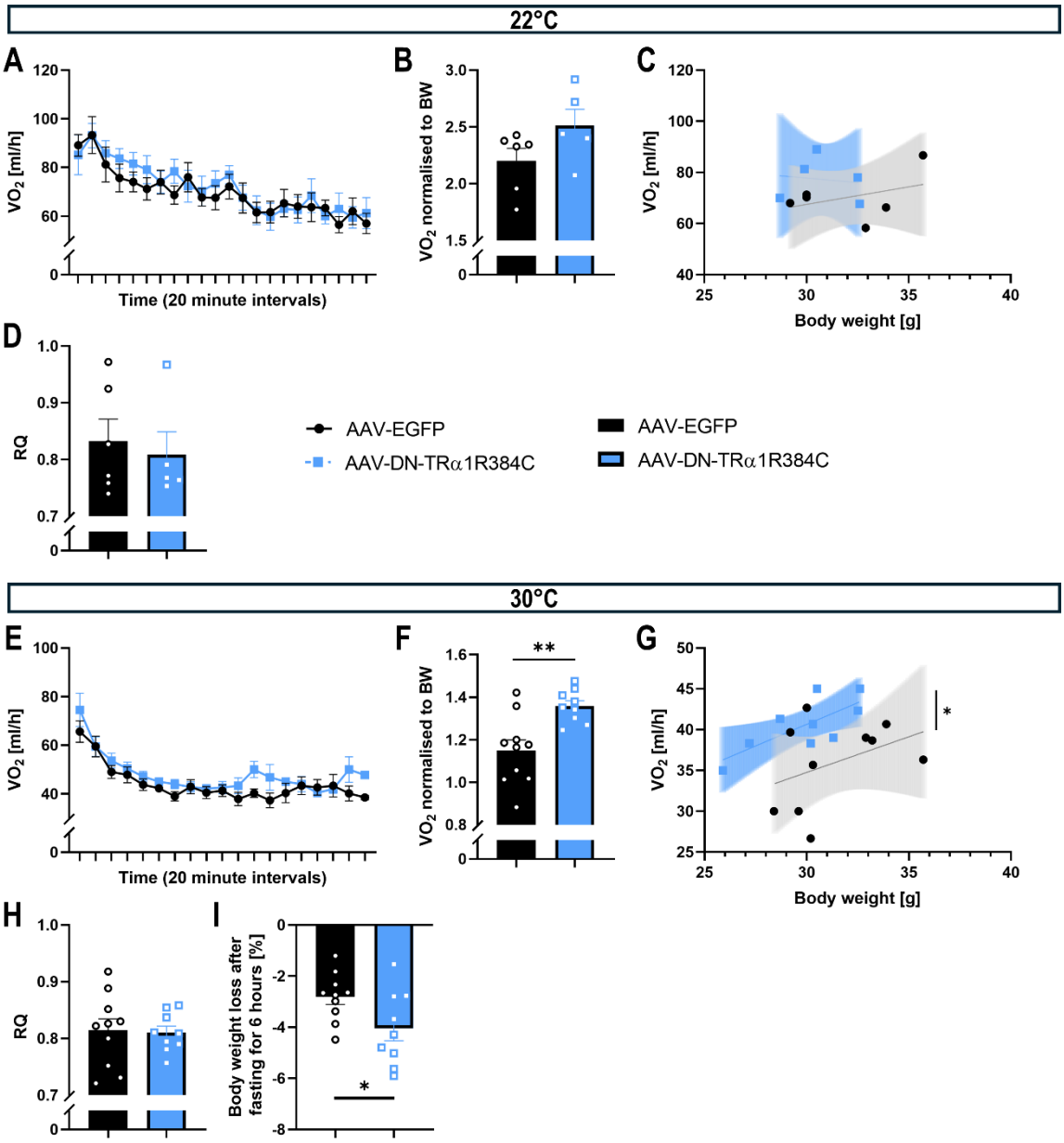

Figure 13: Effect of Zona Incerta thyroid hormone signalling inhibition on energy expenditure at different ambient temperatures. *Indirect calorimetry* ***(A-D)*** *at 22°C with* ad libitum *access to food and water and* ***(E-I)*** *at 30°C under fasting conditions. Control (n = 4-10) vs. dominant-negative TRα1 animals (n = 4-9).* ***(A+E)*** *Oxygen consumption over time measured in 20-minute intervals.* ***(B+F)*** *Oxygen consumption normalised to body weight; **p < 0.01 with Welch's t-test.* ***(C+G)*** *ANCOVA of oxygen consumption vs. body weight; *p < 0.05 with ANCOVA.* ***(D+H)*** *Respiratory quotient (RQ).* ***(I)*** *Body weight loss at 30°C under fasting conditions for 6 hours. *p < 0.05 with unpaired Student's t-test. Data is represented as mean ± SEM. Adapted from Maier et al., 2024, in press.*

To further characterise the metabolic phenotype of the dominant-negative TRα1 mice, expression analysis of metabolic genes has been conducted in the muscle and the liver.

Examination of m. gastrocnemius showed significantly decreased expression of Sarcolipin (*Sln*) ($p = 0.002$), a gene expressing an inhibitor of the sarco endoplasmic reticulum calcium ATPase (SERCA), while SERCA genes ATPase sarcoplasmic/endoplasmic reticulum Ca^{2+} transporting 1-3 (*Atp2a1*, *Atp2a2* and *Atp2a3)* were not affected. Other genes involved in calcium flux or muscle growth were also not altered (Fig. 14A). In the liver, no significant difference was found in gene expression of glucose and fatty acid metabolism genes (Fig. 14B). Moreover, hepatic glycogen content did not differ between the groups (Fig. 14C).

Collectively, these results show that inhibition of TH signalling in the ZI led to increased energy expenditure at 30°C and therefore increased body weight loss during fasting periods. While there was no difference in metabolic markers in the liver, it affected expression of *Sln* in the muscle.

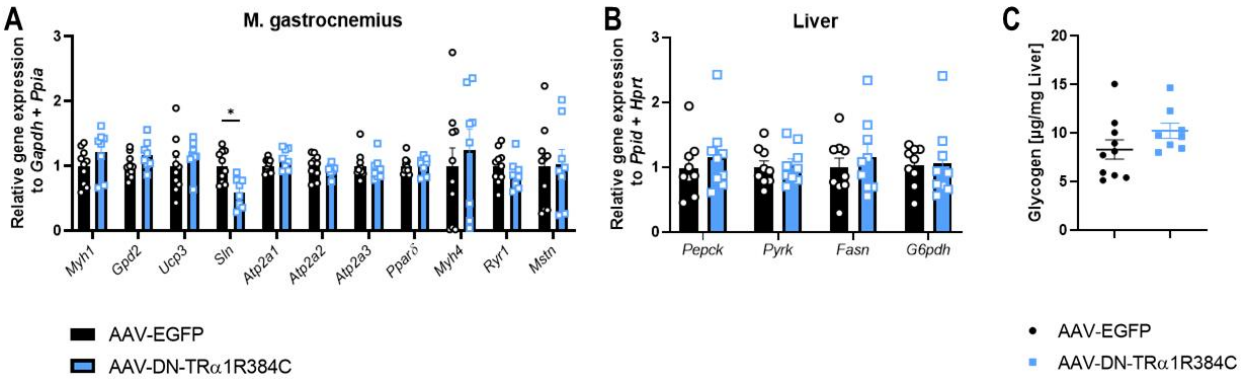

Figure 14: qPCR analysis of muscle and liver and glycogen content in mice expressing a dominant-negative TRα1 or control GFP. ***(A)*** *Relative gene expression in m. gastrocnemius for control (n = 10) vs. dominant-negative TRα1 animals (n = 8).* ***(B)*** *Relative gene expression in the liver for control vs. dominant-negative TRα1 animals (n = 9 per group).* ***(C)*** *Glycogen content in the liver normalised to liver weight. Data is represented as mean ± SEM; *p < 0.05 with unpaired Student's t-test. Atp2a1: ATPase sarcoplasmic/endoplasmic reticulum Ca^{2+} Transporting 1; Atp2a2: ATPase sarcoplasmic/endoplasmic reticulum Ca^{2+} Transporting 2; Atp2a3: ATPase sarcoplasmic/endoplasmic reticulum Ca^{2+} Transporting 3; Fasn: Fatty acid synthase; Gapdh: Glycerinaldehyde-3-phosphate dehydrogenase; Gpd2: Glycerol-3-phosphate dehydrogenase; G6pdh: Glucose-6-phosphate dehydrogenase; Hprt: Hypoxanthine phosphoribosyltransferase; Mstn: Myostatin; Myh1: Myosin heavy chain 1; Myh4: Myosin heavy chain 4; Pepck: Phosphoenolpyruvate carboxykinase; Pparδ: Peroxisome proliferator-activated receptor δ; Ppia: Peptidylprolyl isomerase A; Ppid: Peptidylprolyl isomerase D; Pyrk: Pyruvate kinase; Ryr1: Ryanodine receptor 1; Sln: Sarcolipin; Ucp3: Uncoupling protein 3. Figure was adapted from Maier et al., 2024, in press.*

3.1.2.4 Effects of TRα1 signalling inhibition on the behavioural phenotype

Since the ZI has been implicated in the modulation of anxiety and fear generalisation (Z. Li et al., 2021; Venkataraman et al., 2019), two behavioural tests were conducted to test for possible anxiety behaviour, namely an open field test and an elevated plus maze. For the open field test, mice were observed for 10 minutes. While inhibition of TH signalling in the ZI did not have a significant effect on time spent in the centre or in the outer zones of the open field during the first 5 minutes (Fig. 15A), it resulted in significantly more time spent in the outer zone during the last 5 minutes ($p = 0.039$; Fig. 15B). Moreover, there was no observable difference in mean speed or distance (Fig. 15A+B) between the two groups. In the elevated plus maze, mice were observed for 5 minutes and ZI TH signalling inhibition caused significantly more time spent on the open arms ($p = 0.03$), where control animals spent 6% of time and dominant-negative TRα1 animals 22%. However, no difference in entry ratio of the open or closed arms could be observed (Fig. 15C).

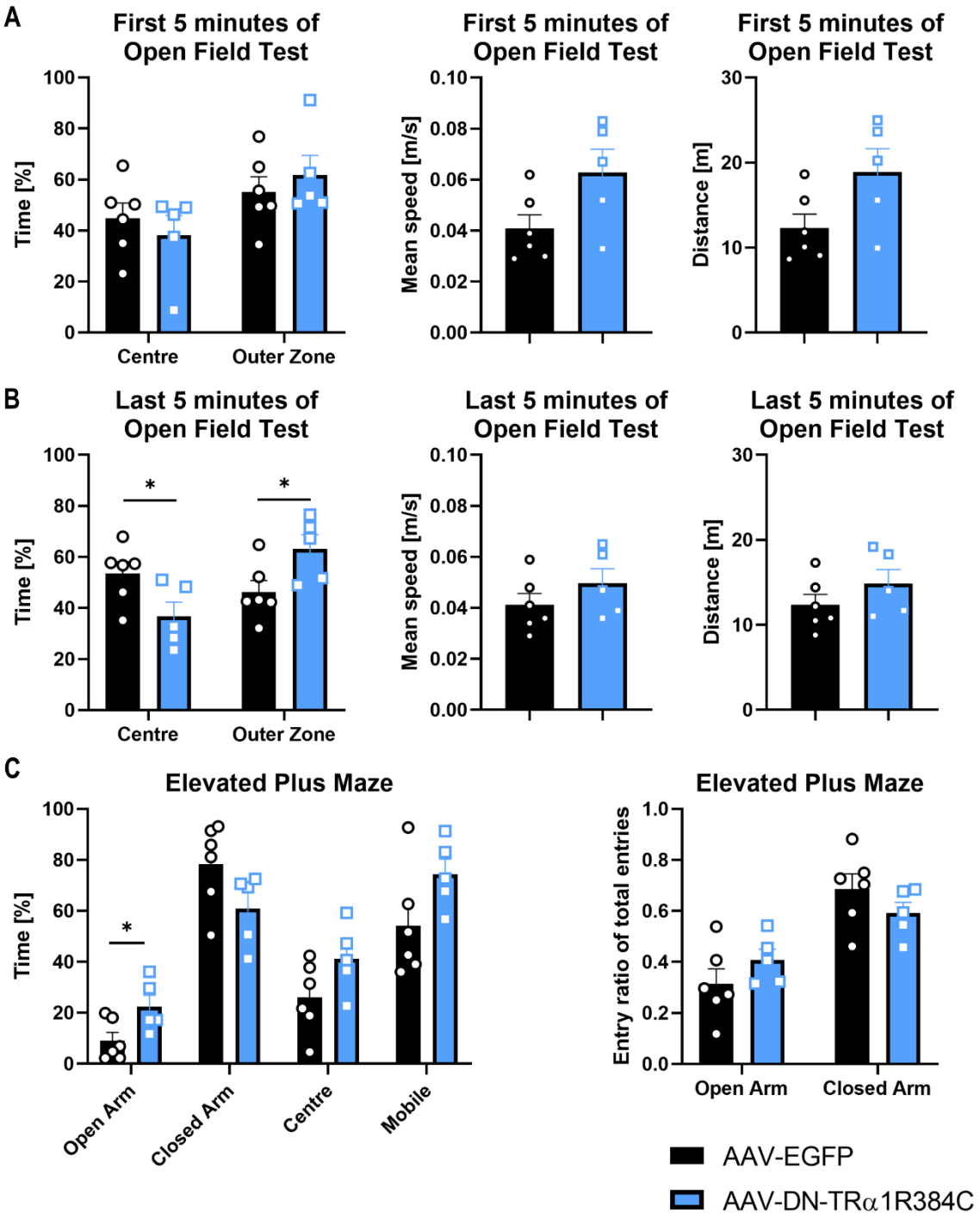

Figure 15: ***Effects of Zona Incerta thyroid hormone signalling inhibition on anxiety behaviour.*** ***(A)*** *First 5 minutes of the open field test. Relative time spent in the centre vs. the outer zone of the open field, as well as mean speed and distance.* ***(B)*** *Last 5 minutes of the open field test. Relative time spent in the centre vs. the outer zone of the open field, as well as mean speed and distance.* ***(C)*** *Elevated plus maze. Relative time spent in different areas of the elevated plus maze and entry ratios of open and closed arms. Data is represented as mean ± SEM for control (n = 6) vs. dominant-negative TRα1 animals (n = 5); *p < 0.05 with unpaired Student's t-test. Adapted from Maier et al., 2024, in press.*

To analyse anxiety and stress on a molecular level, circulating glucocorticoid levels were measured in the serum. The results showed increased levels of corticosterone in mice with inhibited ZI TH signalling (p = 0.003; Fig. 16A). However, gene expression levels of the glucocorticoid receptor (*Gr*) and its target genes in the liver did not reveal any significant differences (Fig. 16B), and *Gr* was also not differentially expressed in the muscle (Fig. 16C).

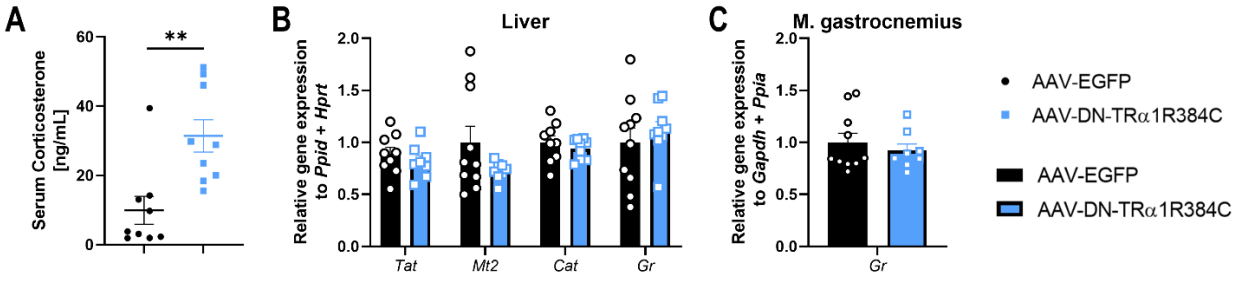

Figure 16: Serum glucocorticoid levels and qPCR analysis of liver and muscle in mice expressing a mutant TRα1 or control GFP. (A) *Level of corticosterone in the serum of control vs. dominant-negative TRα1 animals (n = 9 per group).* ***(B)*** *Relative gene expression of glucocorticoid receptor target genes in the liver for control (n = 9-10) and dominant-negative TRα1 animals (n =8-9).* ***(C)*** *Relative gene expression of the glucocorticoid receptor in the muscle for control (n = 10) vs. dominant-negative TRα1 mice (n = 8). Data is represented as mean ± SEM; **p < 0.01 with unpaired Student's t-test. Cat: Catalse; Gapdh: Glycerinaldehyde-3-phosphate dehydrogenase; Gr: Glucocorticoid receptor; Hprt: Hypoxanthine Phosphoribosyltransferase; Mt2: Metallothionein 2; Ppia: Peptidylprolyl isomerase A; Ppid: Peptidylprolyl isomerase D; Tat: Tyrosine aminotransferase. Figure was adapted from Maier et al., 2024, in press.*

To investigate the cause for the rise in serum corticosterone, genes involved in the HPA axis were analysed in the hypothalamus, the anterior pituitary and the adrenal glands. The results showed no effect of ZI TH signalling inhibition on the expression of hypothalamic corticotropin-releasing hormone (*Crh*) (Fig. 17A), nor corticotropin-releasing hormone receptor (*Crhr*), T-box 19 (*Tbx19*) or proopiomelanocortin (*Pomc*) in the anterior pituitary (Fig. 17B) or cytochrome P450, family 11, subfamily b, polypeptide 1 and 2 (*Cyp11b1* and *Cyp11b2*) in the adrenal glands (Fig 17C). Additionally, there was no difference in gene expression of thyrotropin-releasing hormone receptor (*Trhr*) in the anterior pituitary. However, expression of thyroid stimulation hormone subunit β (*Tshb*) was elevated (Fig. 17B).

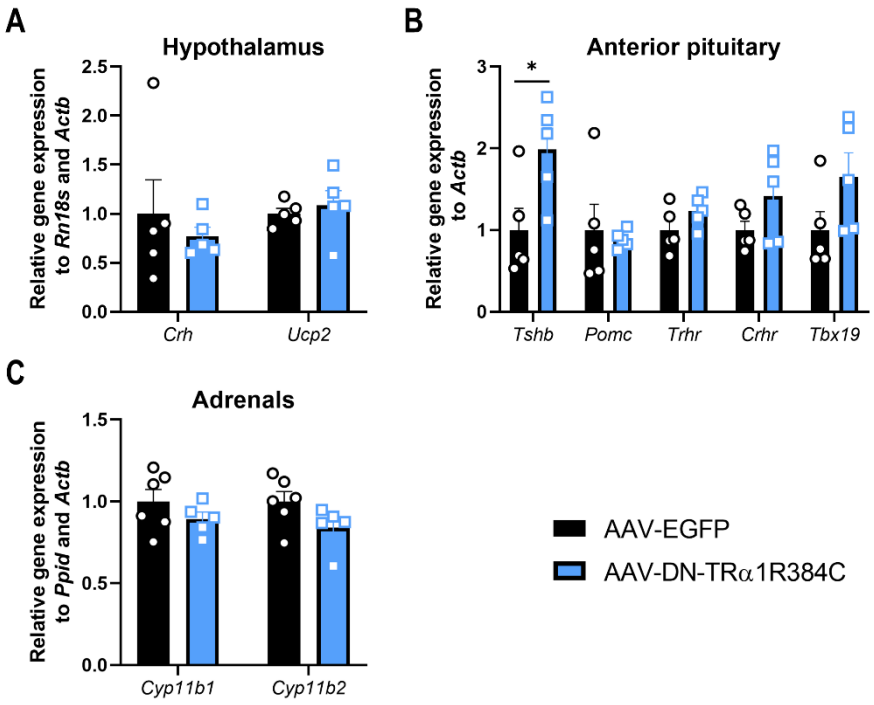

Figure 17: Effects of Zona Incerta thyroid hormone signalling inhibition on the HPA axis. ***(A)*** *Relative gene expression of HPA axis related genes in the hypothalamus.* ***(B)*** *Relative gene expression of genes related to the HPA and HPT axes in the anterior pituitary.* ***(C)*** *Relative gene expression for genes involved in glucocorticoid synthesis in the adrenal glands. Data is represented as mean ± SEM for control (n = 5-6) and dominant-negative TRα1 (n = 5) animals. *p < 0.05 with unpaired Student's t-test. Actb: β-actin; Crh: Corticotropin releasing hormone; Crhr: Corticotropin releasing hormone receptor; Cyp11b1: Cytochrome P450 family 11 subfamily b member 1; Cyp11b2: Cytochrome P450 family 11 subfamily b member 2; Ppid: Peptidylprolyl isomerase D; Pomc: Proopiomelanocortin; Rn18s: 18S ribosomal RNA; Tbx19: T-box 19; Trhr: Thyrotropin releasing hormone receptor; Tshb: Thyroid stimulating hormone subunit β. Adapted from Maier et al., 2024, in press.*

Since anxiety and stress can also affect heart rate and related parameters (Y.-C. Cheng et al., 2022), and thyroid diseases can present with changes in heart rate (Dore et al., 2023; Mittag, Davis, et al., 2010), ECGs were performed. The results showed no difference in overall ECG outcome (Fig. 18A+B, representative). Further analysis revealed no impact on heart rate (Fig. 18C), heart rate variability (Fig. 18D) and R amplitude (Fig. 18E). Additional parameters, such as interval times (Fig. 18F), also showed no effect of TH signalling inhibition in the ZI.

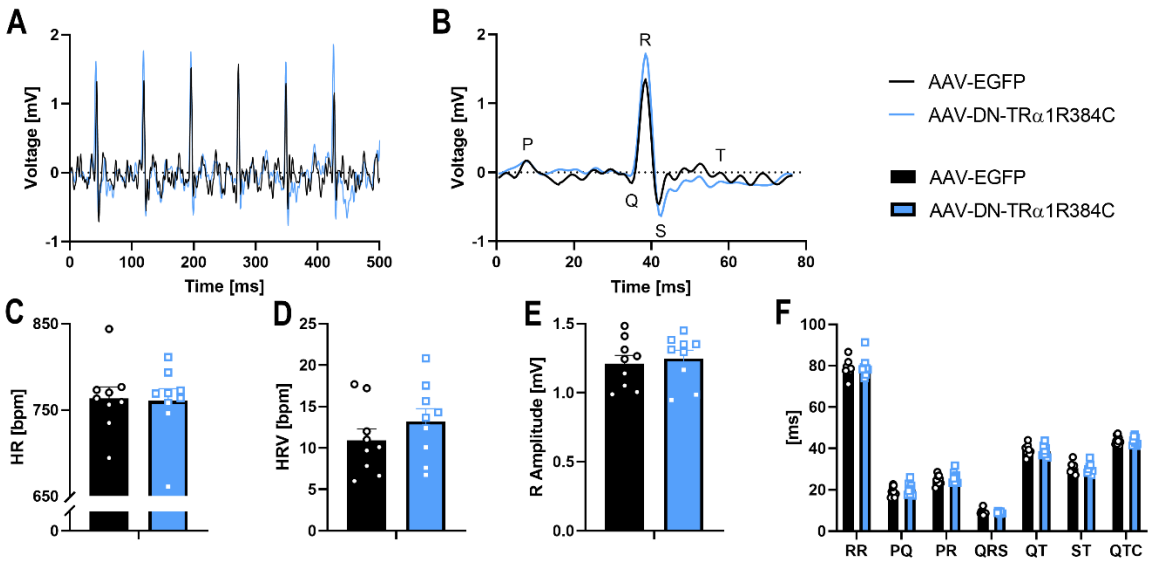

Figure 18: Electrocardiogram data for mice expressing either a dominant-negative TRα1 or control GFP. (A-B) *Representative ECG for control vs. dominant-negative TRα1 mice.* ***(C)*** *Heart rate.* ***(D)*** *Heart rate variability.* ***(E)*** *R amplitude.* ***(F)*** *ECG interval lengths. Data is represented as mean ± SEM for control vs. dominant-negative TRα1 animals (n = 9 per group). HR: Heart rate; HRV: Heart rate variability. Figure was adapted from Maier et al., 2024, in press.*

Taken together, inhibition of ZI TH signalling resulted in a partial anxiety phenotype, as it caused more time spent in the corners of the open field test, as well as less time spent in the centre in the last 5 minutes. Conversely, inhibition also led to increased time spent on the open arms of the elevated plus maze. While glucocorticoid receptor target genes and genes involved in the HPA axis were not differentially expressed, inhibition of TH signalling in the ZI resulted in increased serum corticosterone levels. It did not affect ECG parameters.

3.2 The role of dopaminergic neurons in the Zona Incerta

The ZI consists of several different neuron populations, such as γ-aminobutyric acid (GABA)ergic neurons (Lin et al., 1990), glutamatergic neurons (Heise & Mitrofanis, 2004) and dopaminergic neurons (Wagner et al., 1995). It remains unknown which neurons mediate the effects of central TRα1 action in the ZI.

3.2.1 The effect of T3 on Zona Incerta dopaminergic neurons

Since previous studies have shown that dopaminergic neurons in the ZI have an impact on energy expenditure and body weight (Folgueira et al., 2019), the cell number of these neurons was analysed under different conditions. The ZI of wild-type, TRα1R384C mutants and T3 treated wild-type mice was stained with tyrosine hydroxylase to visualise the dopaminergic neurons (Fig. 19A). The results showed that there was no difference between the conditions in terms of cell count, as it ranged from 250 to 300 in all groups (Fig. 19B).

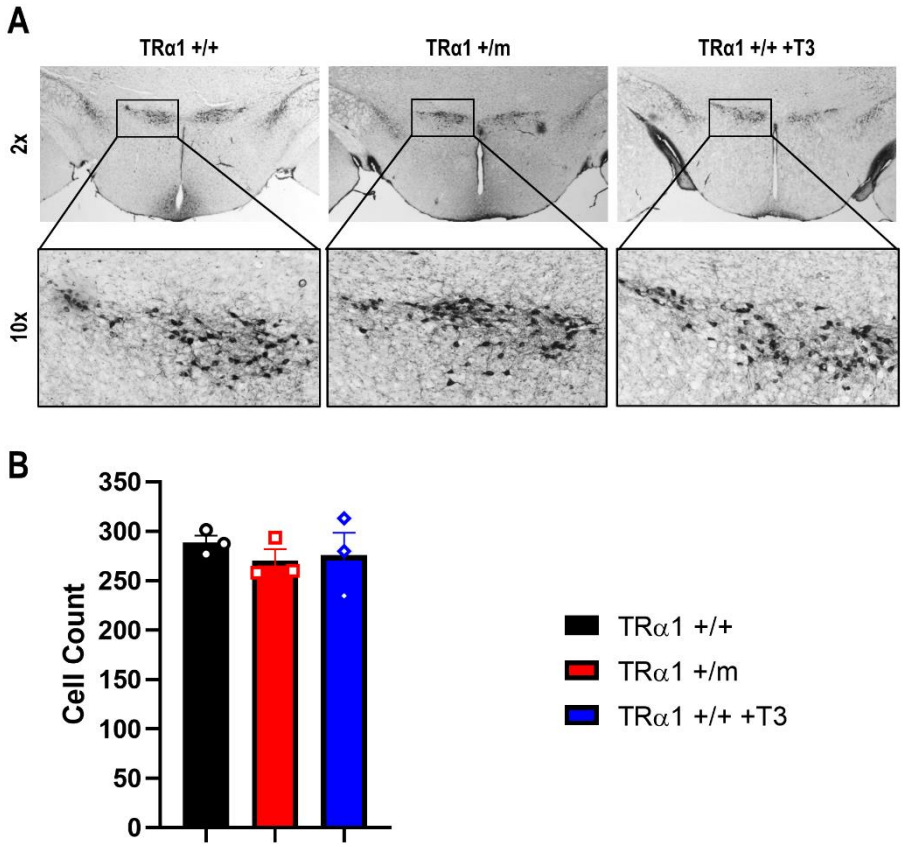

***Figure 19: Dopaminergic neurons in the Zona Incerta**. **(A)** Representative images of staining for tyrosine hydroxylase in the ZI of wild-type, TRα1R384C mutant and T3 treated wild-type animals. **(B)** Cell count of dopaminergic neurons in the ZI. Data is represented as mean ± SEM (n = 3 per group). Adapted from Maier et al., 2024, in press.*

3.2.2 What are the effects of TRα1 signalling in dopaminergic neurons of the Zona Incerta?

To further analyse TRα1 signalling in the ZI in more detail, the previous experimental set-up has been adjusted to allow for specific infection of dopaminergic neurons. For this, tyrosine hydroxylase-Cre mice were used instead of wild-type mice, and the AAV injected into the ZI contained a FLEXOn construct to express the dominant-negative TRα1R384C only upon Cre recombination in dopaminergic neurons. As in the previous experimental set-up, animals recovered for 14 days post surgery, which consisted of AAV injection and implantation of a radiotelemetry transmitter, before data was recorded. Radiotelemetry measurements were carried out at 22°C, 30°C and 10°C, and infrared photography, as well as ECGs and behaviour tests were conducted at 22°C. For energy expenditure, indirect calorimetry was carried out at 22°C during fasting conditions (Fig. 20). All animals were sacrificed by cervical dislocation and brain, pituitary, iBAT, liver and muscle (M. gastrocnemius) were collected for further molecular analysis.

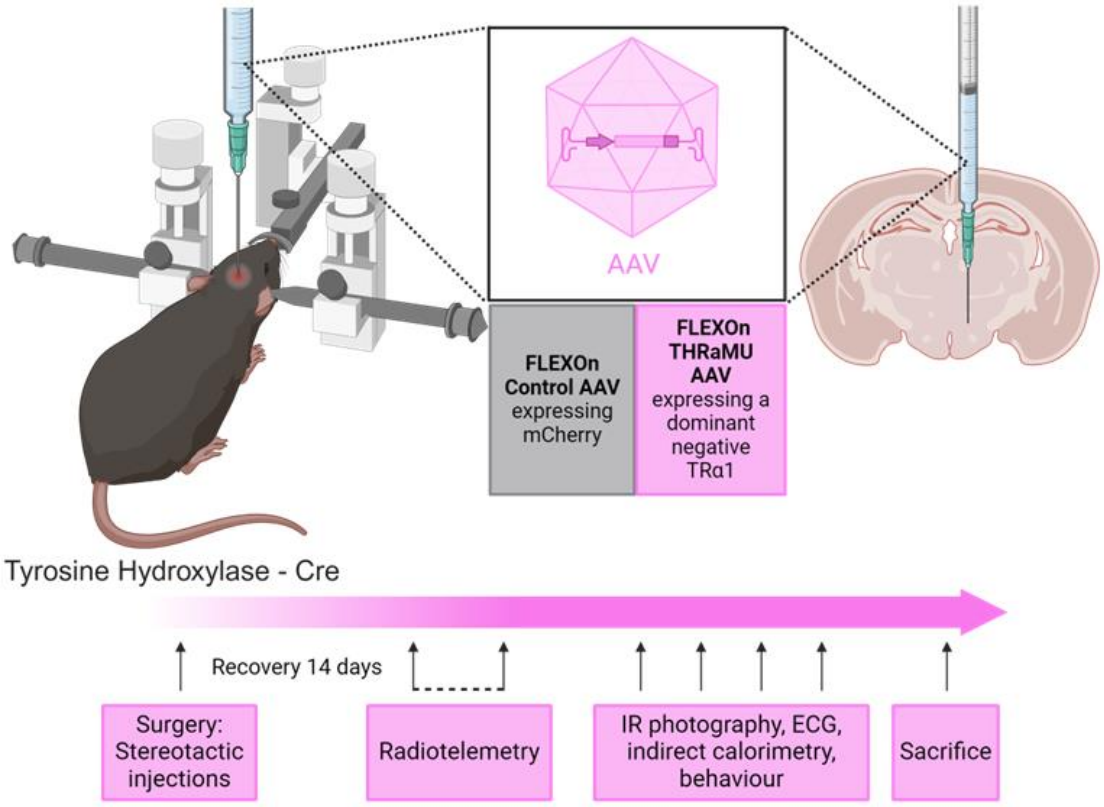

Figure 20: Experimental design to investigate the role of dopaminergic neuron thyroid hormone signalling in the Zona Incerta. *Figure created using Biorender.com. Adapted from Maier et al., 2024, in press.*

Confirmation of injection sites was achieved by staining for mCherry, a marker gene expressed by both the control virus and the dominant-negative TRα1 virus, as well as tyrosine hydroxylase to visualise co-localisation and show infection of the targeted neurons. The images showed mCherry positive cells in the Zona Incerta of all animals (Fig. 21A) and double staining with tyrosine hydroxylase (Fig. 21B), indicating expression of the virus in dopaminergic neurons.

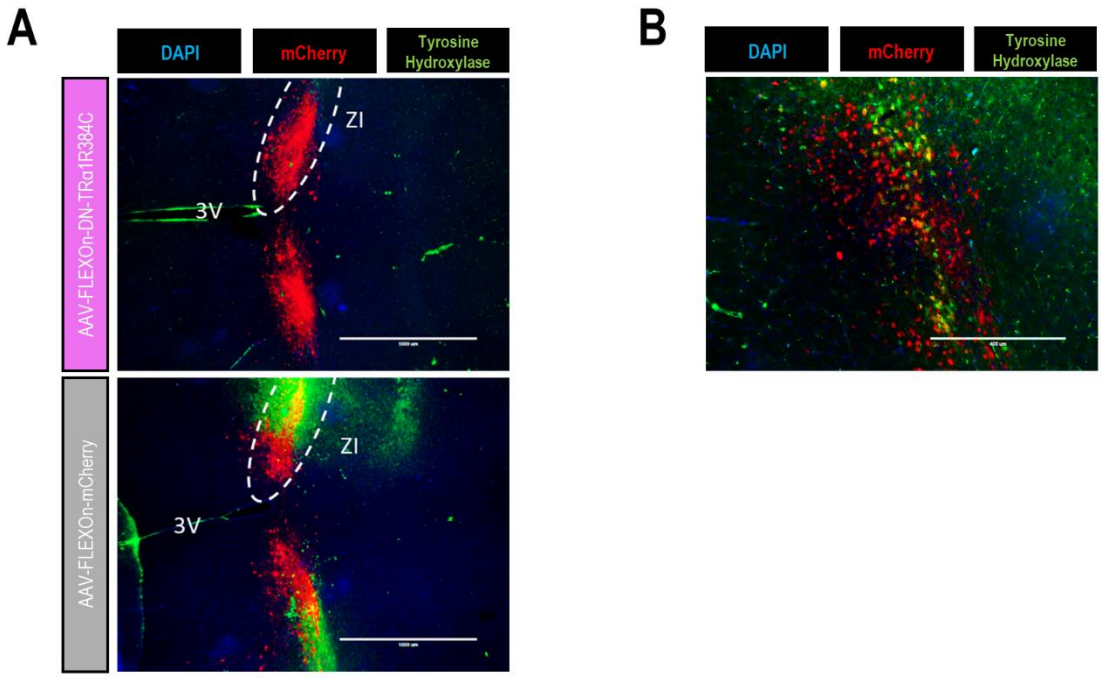

Figure 21: Virus injection site confirmation. (A-B) *Representative images of staining for mCherry and tyrosine hydroxylase, circled area indicates ZI. Scale bar is 1000 µm* ***(B)*** *Close up image of ZI. Scale bar is 400 µm. Adapted from Maier et al., 2024, in press.*

3.2.2.1 Body weight, food intake and water intake

Body weight, food intake and water intake were recorded throughout the experiment to characterise the general phenotype of mice with inhibited dopaminergic neuron TH signalling in the ZI. The data showed no difference in body weight or body weight change (Fig. 22A), and also no effect on food intake (Fig. 22B). Interestingly, inhibition of thyroid hormone signalling resulted in an increased water intake from 4.5 g (control) to 5.1 g (dominant-negative) per day (Fig 22C, $p = 0.0451$).

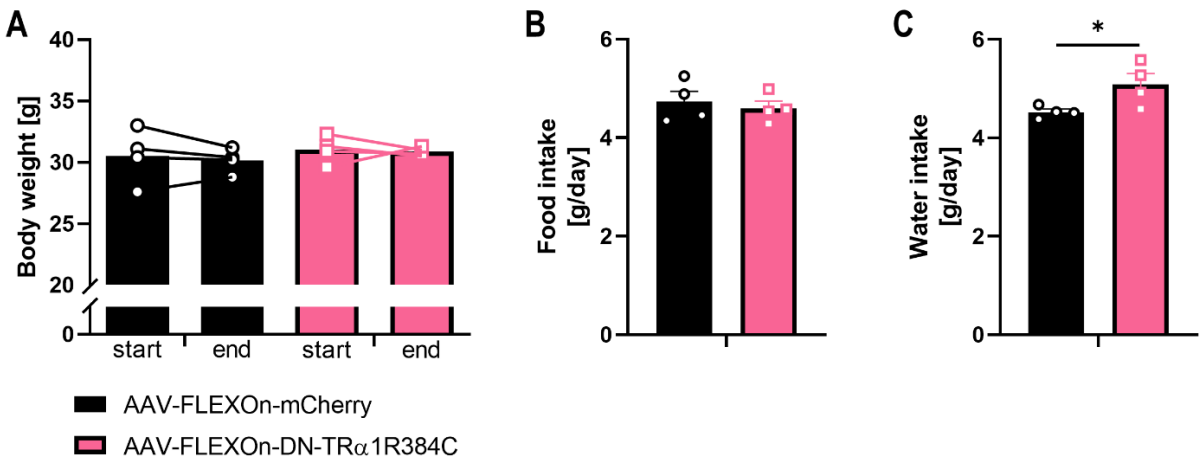

Figure 22: Effects of thyroid hormone signalling inhibition in the dopaminergic neurons of the Zona Incerta on body weight and food and water intake. ***(A)*** *Body weight at start (2 weeks post AAV injection) and end of experiment.* ***(B)*** *Food intake per day.* ***(C)*** *Water intake per day. Data is represented as mean ± SEM for control vs. dominant-negative TRα1 animals (n = 4 per group); *p < 0.05 with unpaired Student's t-test. Figure was adapted from Maier et al., 2024, in press.*

3.2.2.2 THERMOREGULATION

Dopaminergic neurons of the ZI have been implicated in the control of body temperature (Folgueira et al., 2019). Therefore, core body temperature, as well as locomotion activity, was recorded for several days at different ambient temperatures. The results showed no significant differences in body temperature at 22°C (Fig. 23A), 10°C (Fig. 23C) or 30°C (Fig. 23E) between the two groups. Furthermore, inhibition of dopaminergic neuron TH signalling in the ZI did not affect locomotion activity at either ambient temperature (Fig. 23B+D+F).

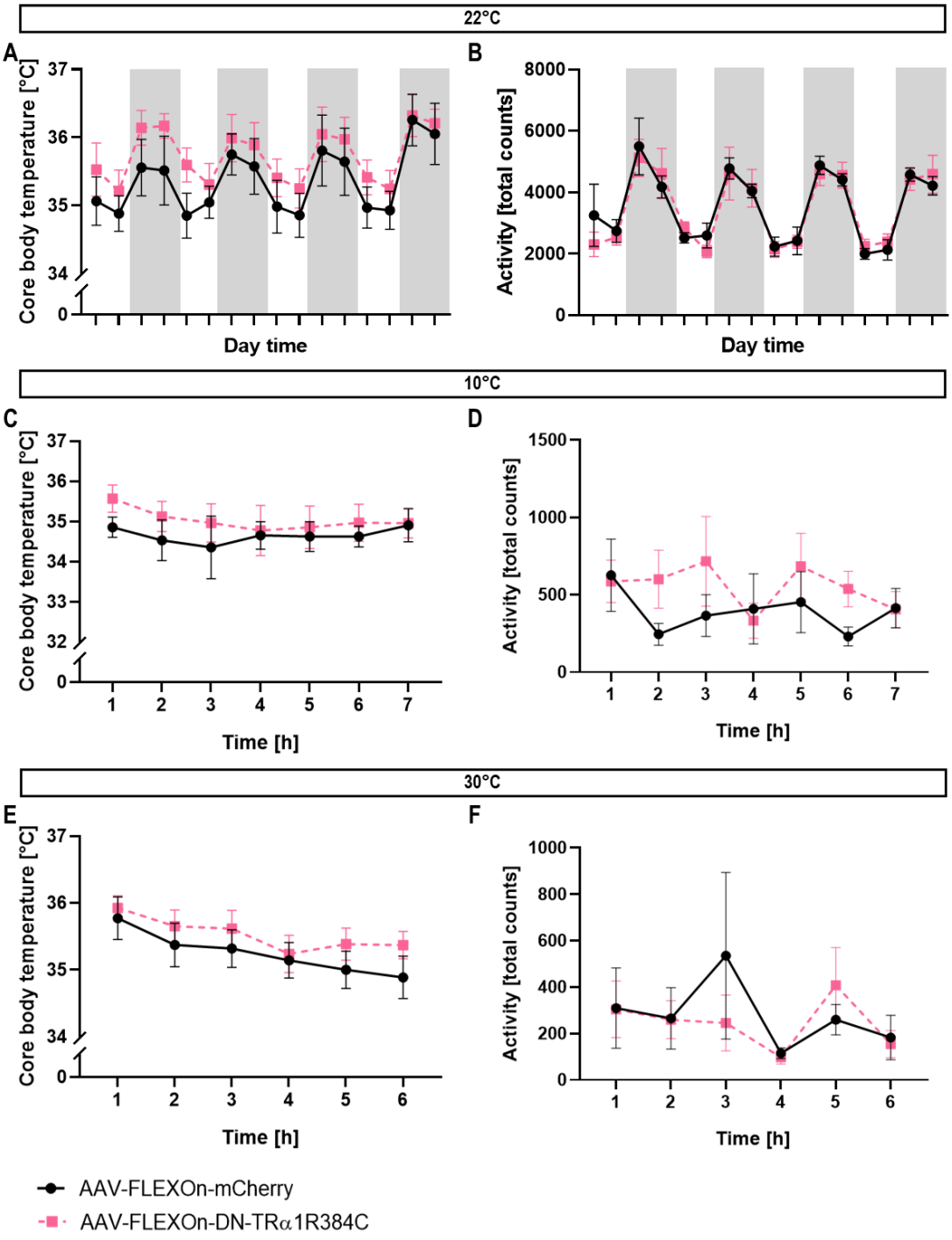

Figure 23: Body temperature and locomotion activity at different ambient temperatures in mice lacking thyroid hormone signalling in Zona Incerta dopaminergic neurons or control mice. ***(A-B)*** *Core body temperature* ***(A)*** *and locomotion activity* ***(B)*** *at 22°C ambient temperature for control vs. dominant-negative TRα1 animals, grey areas indicate dark phases.* ***(C-D)*** *Core body temperature* ***(C)*** *and locomotion activity* ***(D)*** *at 10°C ambient temperature for control vs. dominant-negative TRα1 animals.* ***(E-F)*** *Core body temperature* ***(E)*** *and locomotion activity* ***(F)*** *at 30°C ambient temperature for control vs. dominant-negative TRα1 animals. Data is represented as mean ± SEM (n = 4 per group). Adapted from Maier et al., 2024, in press.*

In addition to radiotelemetry measurements, infrared thermography was conducted at 22°C. Infrared pictures were taken of the iBAT, tail and lower back (Fig. 24A). The results again showed no effect of dopaminergic neuron TH signalling inhibition in the ZI on iBAT and tail temperatures (Fig. 24B).

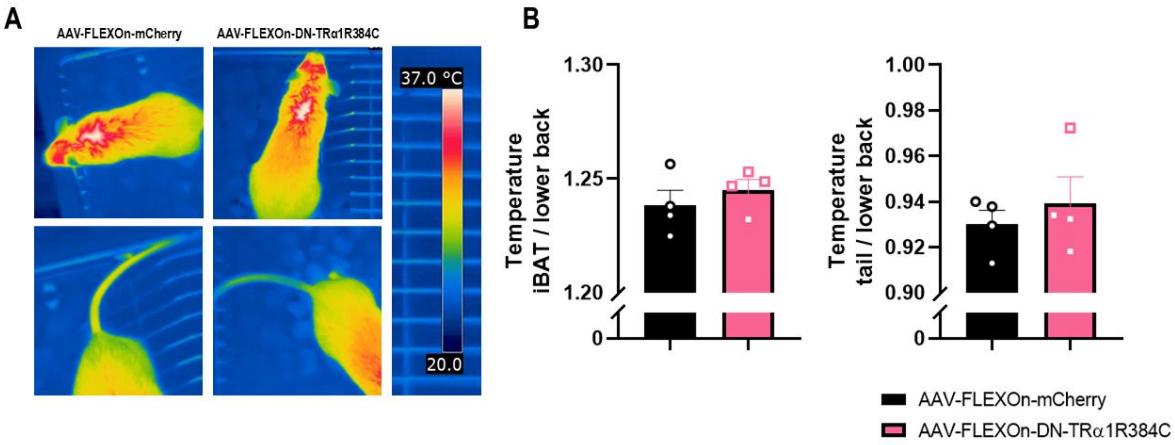

Figure 24: Infrared thermography of iBAT and tail in mice expressing either a mutant TRα1 or control mCherry in the dopaminergic neurons of the Zona Incerta. (A) *Representative infrared images of iBAT and tail.* ***(B)*** *iBAT and tail temperatures normalised to lower back temperature with infrared thermography. Data is represented as mean ± SEM for control vs. dominant-negative TRα1 animals (n = 4 per group). iBAT: Interscapular brown adipose tissue. Figure was adapted from Maier et al., 2024, in press.*

Taken together, these results show that inhibition of TH signalling in the dopaminergic neurons of the ZI did not affect core body, iBAT and tail temperature or locomotion activity.

3.2.2.3 Energy expenditure

Since previous results showed an effect of general TH signalling inhibition in the ZI on energy expenditure, oxygen consumption was measured for dopaminergic neuron specific inhibition of TH signalling at 22°C under fasting conditions. The results showed no significant difference in oxygen consumption (Fig. 25A-B). Furthermore, the RQ did not differ between the groups (Fig 25C). Unlike with general TH signalling inhibition, there was no effect on body weight loss during fasting conditions (Fig. 25D).

In conclusion, inhibition of TH signalling in the dopaminergic neurons of the ZI did not affect energy expenditure.

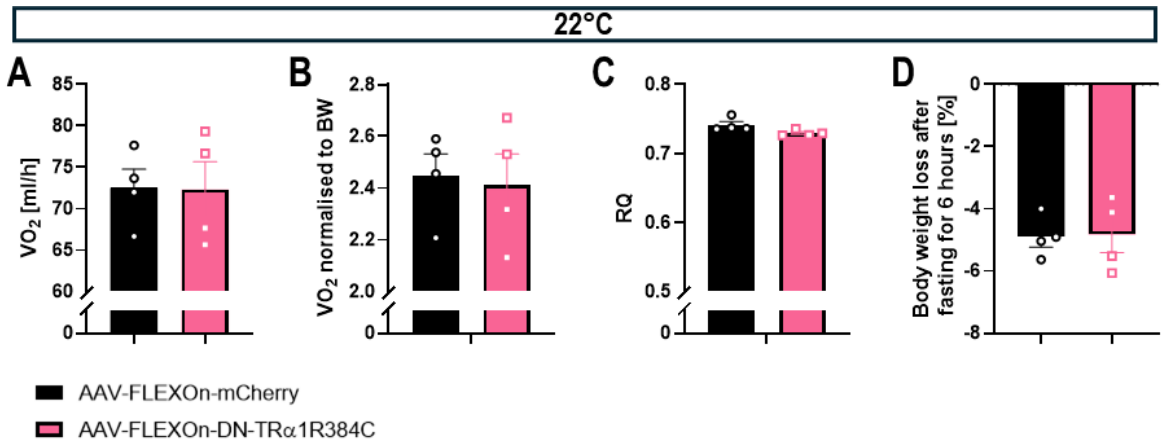

Figure 25: Effects of thyroid hormone signalling inhibition in the dopaminergic neurons of the Zona Incerta on energy expenditure at 22°C under fasting conditions. ***(A)*** *Oxygen consumption.* ***(B)*** *Oxygen consumption normalised to body weight.* ***(C)*** *Respiratory quotient.* ***(D)*** *Body weight loss after a fasting period of 6 hours. Data is represented as mean ± SEM for control vs. dominant-negative animals (n = 4 per group). Adapted from Maier et al., 2024, in press.*

3.2.2.4 Behaviour

In order to characterise the effect of dopaminergic neuron TH inhibition in the ZI on the behaviour phenotype, two anxiety behaviour tests were carried out. There were no significant differences between the groups in the open field test in terms of time spent in the centre or the outer zones, as well as time spent immobile or mobile (Fig. 26A). Furthermore, inhibition of TH signalling did not lead to any difference in mean speed (Fig. 26B), or distance travelled (Fig. 26C). In addition to the open field test, the animals were also subjected to an elevated plus maze. This test further showed no effect on exploratory behaviour, as there was no difference between the groups in time spent on open or closed arms (Fig. 26D). On a molecular level, inhibition of TH signalling in the dopaminergic neurons of the ZI did not lead to any change in serum levels of the glucocorticoid corticosterone (Fig. 26E).

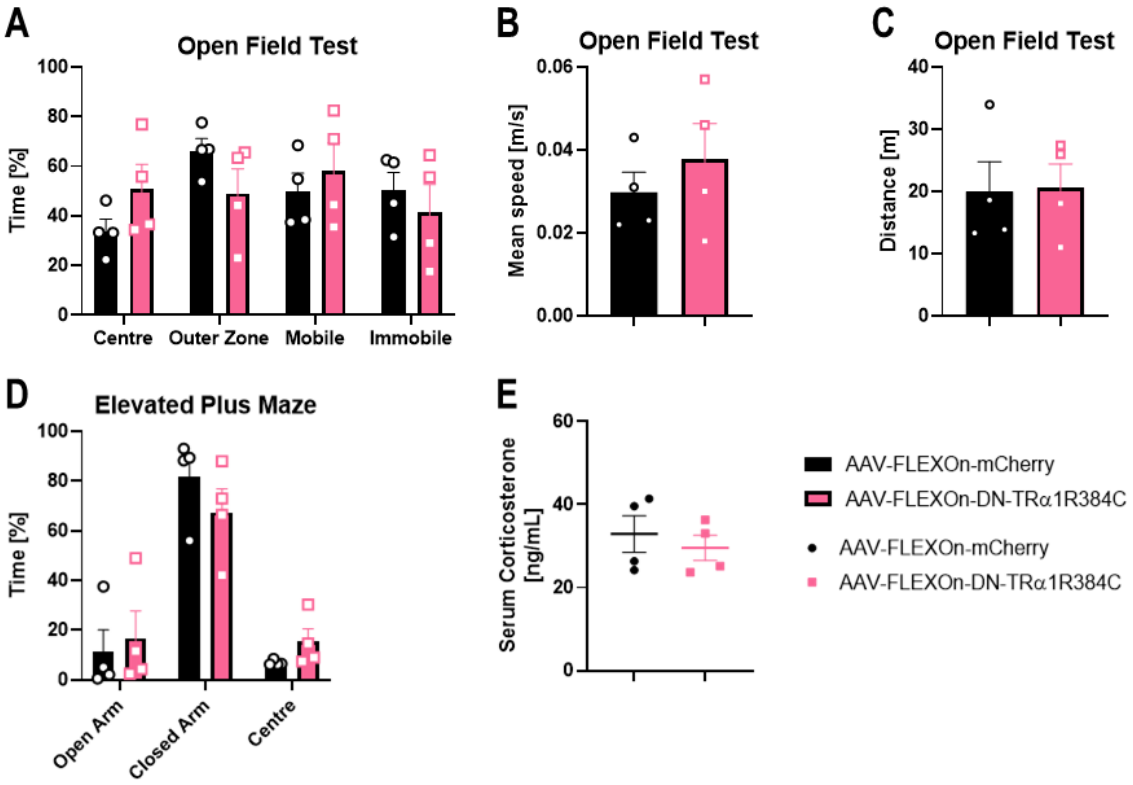

Figure 26: Anxiety behaviour and glucocorticoids in mice lacking thyroid hormone signalling in Zona Incerta dopaminergic neurons or control mice. ***(A)*** *Relative time spent in different areas of the open field.* ***(B)*** *Mean speed in the open field.* ***(C)*** *Distance travelled in the open field.* ***(D)*** *Relative time spent in different areas of the elevated plus maze.* ***(E)*** *Level of corticosterone in the serum. Data is represented as mean ± SEM for control vs. dominant-negative TRα1 animals (n = 4 per group). Figure was adapted from Maier et al., 2024, in press.*

In addition to behavioural anxiety tests, ECGs were conducted to measure any change in heart rate or related parameters. Inhibition of TH signalling in the dopaminergic neurons of the ZI did not have an effect on any parameter recorded in the ECG (Fig. 27A+B). Moreover, there were no significant differences in related parameters, such as heart rate (Fig. 27C), heart rate variability (Fig. 27D), R amplitude (Fig. 27E) or interval length (Fig. 27F).

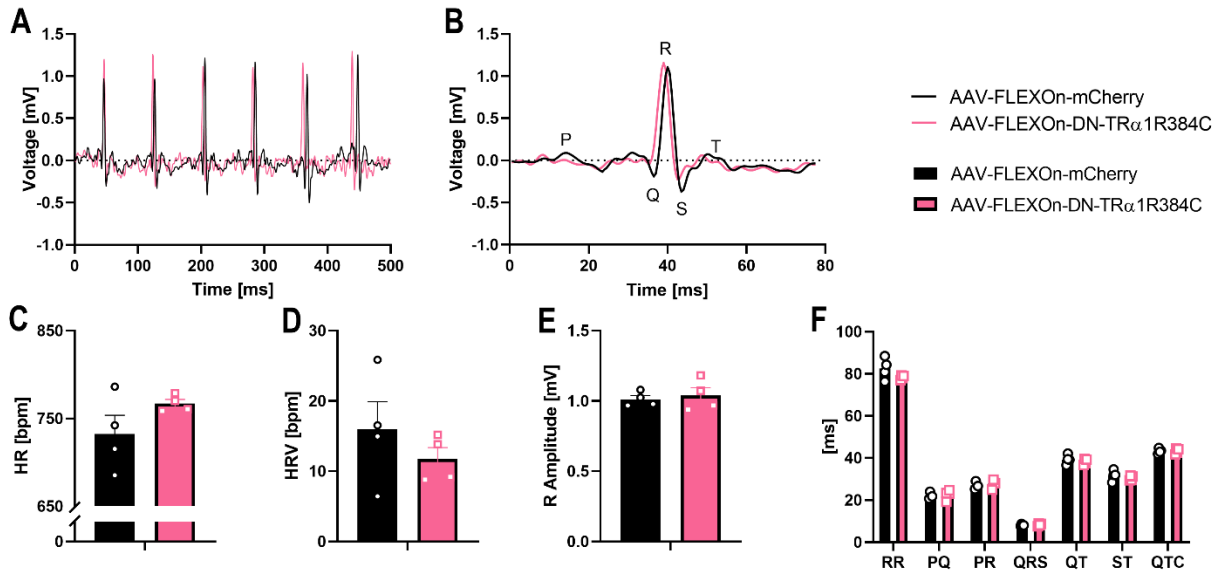

Figure 27: Effects of thyroid hormone signalling inhibition in the dopaminergic neurons of the Zona Incerta on electrocardiogram data. (A-B) *Representative ECG for control vs. dominant-negative TRα1 mice.* ***(C)*** *Heart rate.* ***(D)*** *Heart rate variability.* ***(E)*** *R amplitude.* ***(F)*** *ECG interval lengths. Data is represented as mean ± SEM for control vs. dominant-negative TRα1 animals (n = 4 per group). HR: Heart rate; HRV: Heart rate variability. Adapted from Maier et al., 2024, in press.*

In conclusion, inhibition of dopaminergic neuron TH signalling in the ZI did not lead to any changes in anxiety, as there were no differences in the open field test and the elevated plus maze. Furthermore, glucocorticoid levels did not differ, and ECGs showed no difference between the two groups.

4. Discussion

It has previously been established that THs do not solely act in the periphery but can also act centrally in the brain to have many effects on the organism, in addition to their effects on brain development (Alcaide Martin & Mayerl, 2023). While some of these effects have already been studied and a corresponding brain region for its T3 action has been identified, some effects remain poorly understood. Therefore, this thesis aimed to investigate which brain region is responsible for some of the other T3 mediated effects.

4.1 Effects of Thyroid Hormones on the brain

To first gather more information regarding which brain regions were affected by T3, PET/CT scans of mouse brains were conducted before and after T3 treatment. This gives insight into which brain regions show neuronal activation upon interaction with THs and could be responsible for some of the observed central effects. The results showed activity in several regions throughout the brain. Different areas of the hippocampus showed activation. The hippocampus is known to be involved in memory and imagination (Knierim, 2015), which gives rise to speculation about possible effects of THs in the hippocampus. Recent studies showed that hypothalamic TRα1 signalling controls the central regulation of body temperature (Sentis et al., 2024), which is in line with the findings of this study, showing that the lateral hypothalamus (LH) is activated upon treatment with T3. Most interestingly, they showed that the ZI was activated, indicating a possible role of the ZI in T3 mediated central effects. Moreover, the ZI had the highest increase in glucose uptake in the PET/CT scans among all activated brain regions, suggesting a high sensibility to T3.

The ZI is a brain region in the subthalamus that receives inputs from many different regions and vice versa projects to multiple areas in the brain, such as the thalamus and hypothalamus, as well as the brain stem and spinal cord (Mitrofanis, 2005; Romanowski et al., 1985) (Fig. 28). It is a relatively large region with neuronal populations that express a multitude of neuronal markers, including parvalbumin, tyrosine hydroxylase, GABA, glutamic acid decarboxylase (GAD) and somatostatin (Kolmac & Mitrofanis, 1999; Nicolelis et al., 1995).

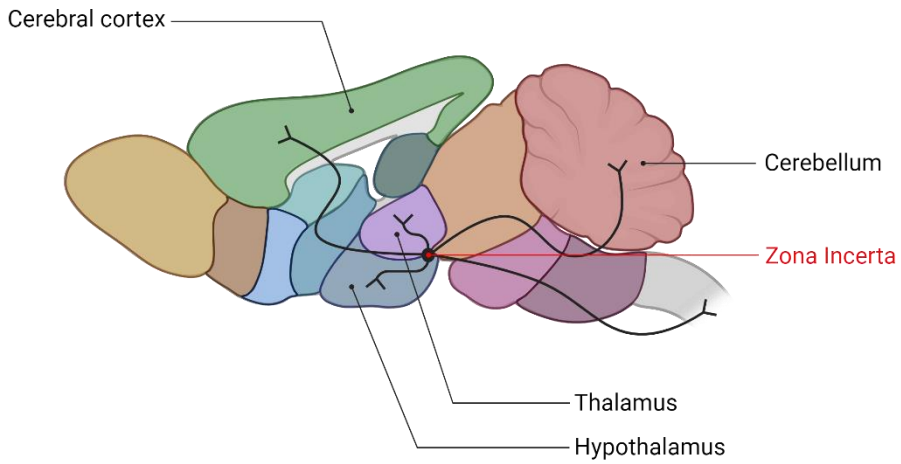

Figure 28: Efferent connections of the Zona Incerta. *The Zona Incerta, located in the subthalamus, projects to many regions throughout the brain, including the cortex, cerebellum, thalamus, hypothalamus, brain stem and spinal cord. Figure created with Biorender.com.*

The precise function of the ZI still remains largely unknown. Due to its connections to the cerebral cortex, many have proposed an involvement of the ZI in motor function and movement (Chometton et al., 2021), which also stems from projections to the spinal cord. In fact, studies in mice have shown that glutamatergic neurons of the ZI regulate motor symptoms found in Parkinson's disease (PD) (L.-X. Li et al., 2021). Moreover, deep brain stimulation of the ZI in PD patients ameliorates typical PD symptoms, such as bradykinesia, tremors and muscle rigidity (Ossowska, 2020). Interestingly, PD patients receiving ZI deep brain stimulation also reported that it mitigated their anxiety (Burrows et al., 2012), suggesting a possible role of the ZI in mood control, which is in agreements with the findings of this study. Furthermore, the ZI has been implicated in behaviour (Wang et al., 2020), food seeking motivation (Ye et al., 2023), pain (J. Li et al., 2023), visceral activity and arousal (Mitrofanis, 2005).

One of the neuron populations found in the ZI are dopaminergic neurons. These neurons produce dopamine, which is an important neurotransmitter (Juárez Olguín et al., 2016), and have been the target of some studies of ZI function.

It has been shown that hypothyroidism can cause alterations in neurotransmitter levels, such as GABA (Salas-Lucia, 2024), and that hyperthyroidism can affect connectivity between brain regions (Liu et al., 2020; W. Zhang et al., 2014), indicating that THs may also play a role in modulation of neuron populations. While the ZI consists of mainly inhibitory neurons, it also contains dopaminergic neuron populations (Björklund et al., 1975). Therefore, brains of mice with different TRα1 genotypes were stained for dopaminergic neurons, to elucidate the role of THs in the modulation of dopaminergic neuron populations. However, there was no difference in dopaminergic neuron cell number between wild-type mice, TRα1 mutant mice and T3 treated

wild-type mice. It can be concluded, that THs do not affect the cell number of dopaminergic neurons in the ZI, neither during development, nor during adult life. In addition, selective inhibition of TH signalling in only dopaminergic neurons of the ZI did not result in any effect that was tested for, indicating that dopaminergic neurons of the ZI are not involved in TH mediated central effects. Apart from dopaminergic neurons, there are several other neuronal populations, such as parvalbumin neurons, GABAergic neurons and glutamatergic neurons (Kolmac & Mitrofanis, 1999; Nicolelis et al., 1995). Further studies are needed to identify the neuron population that is responsible for the TH mediated effect in the ZI. While there are several studies on the effects of ZI stimulation, most of them are general and not specific to a type of neuron (Lu et al., 2021). However, a recent study showed that stimulation of GABAergic neurons of the ZI improved motor function in a mouse model of PD (F et al., 2023), implicating GABAergic neurons as a promising target for further research.

In summary, this study shows that THs activate multiple brain regions, among which is the ZI, a region in the subthalamus. The ZI contains dopaminergic neuron populations, which are not regulated by THs, as TH status does not affect the number of dopaminergic neurons.

4.2 Effects of TRα1 signalling in the Zona Incerta on body weight and thermoregulation

It is important to note that THs can exert many of their effects directly in the brain. THs are transported past the blood brain barrier via transporters, mainly the monocarboxylate transporter 8 (MCT8) (Bernal et al., 2015). Precise locations for central actions of THs and their connection to a defined phenotype still remain elusive. A recent study has shown that stimulation of dopaminergic neurons in the ZI results in body weight loss and an increase in iBAT activation, as evidenced by elevated iBAT temperature and levels of uncoupling protein 1 (UCP1) (Folgueira et al., 2019). Based on these findings and the phenotype of hypothyroidism, it was expected to find a decrease in body temperature and iBAT activation when TH signalling is inhibited in the ZI.

In order to investigate this, AAVs expressing the dominant-negative TRα1 were injected into the ZI, which causes inhibition of TH signalling specifically in the ZI. In contrast to what was expected, this inhibition did not lead to any significant changes in body weight or body temperature, neither core body temperature, nor BAT or tail temperature, showing that the ZI is not involved in the regulation of body temperature through BAT activation. This is in line with a recent study, which implicates the hypothalamus as the region for regulation of body temperature through central TH action (Sentis et al., 2024).

THs are important regulators of metabolism, as hypo- and hyperthyroidism often cause unwanted fluctuations in weight (Chaker et al., 2017; De Leo et al., 2016). This is due to their influence on many regulatory pathways. THs can influence metabolism on many levels, such as in the liver, the muscle and the BAT. Therefore it can alter thermogenesis and body weight, as well as regulation of cholesterol and triglycerides, and carbohydrate metabolism (Mullur et al., 2014). In terms of regulation of body weight specifically, THs affect energy expenditure and alter the basal metabolic rate (BMR) (Kim, 2008), which in turn leads to alterations in body weight. Additionally, THs influence intake of fat and carbohydrates and can affect body composition (Roef et al., 2012). Furthermore, hypothyroid obese patients show a decrease in leptin levels (El Amrousy et al., 2022), and TSH directly affects the secretion of leptin (Menendez et al., 2003), indicating a relationship between THs and leptin, a hormone that is involved in the control of body weight (Klok et al., 2007). By modulating UCP1 expression, THs affect thermogenesis, another important factor for energy expenditure (Sentis et al., 2021).

Mice heterozygous for TRα1R384C show a decreased core body temperature when housed at room temperature, which is caused by increased heat loss via the tail (Warner & Mittag, 2014). THs are known to influence body temperature by affecting thermogenesis. Thermogenesis is the production of heat within the body through various pathways. There are different forms of thermogenesis, shivering thermogenesis and non-shivering thermogenesis. Non-shivering thermogenesis can occur in different organs, such as the BAT (Himms-Hagen, 1984) and the muscle (Nowack et al., 2017). In the context of thermogenesis, it is important to note that the thermoneutral zone, a range of temperatures at which the organism does not need to use energy to maintain body temperature (Kingma et al., 2012), is at around 30°C in mice (Ganeshan & Chawla, 2017).

BAT is activated during cold exposure through innervation of the sympathetic nervous system (SNS). This elevates intracellular levels of cyclic adenosine monophosphate (cAMP), which in turn activates protein kinase A (PKA) to induce lipolysis of triglycerides (TAG) into free fatty acids (FFA). FFA are fuel for β-oxidation, where they are converted into acetyl coenzyme A (acetyl-CoA) that is oxidised to nicotinamide adenine dinucleotide (NADH) and flavin adenine dinucleotide (FADH2) in the tricarboxylic acid (TCA) cycle. This is the basis for the electron transport chain, which creates a proton gradient. BAT expresses UCP1, a protein that uncouples the electron transport chain to decrease ATP production efficiency during oxidative phosphorylation (OXPHOS), which results in the generation of heat (Cannon & Nedergaard, 2004; Yau & Yen, 2020). THs regulate UCP1 content in BAT, as TH signalling induces *Ucp1* expression, therefore being a major regulator of thermogenesis in BAT (Sentis et al., 2021). In this study, *Ucp1*

gene expression was not altered, which is in line with the findings that iBAT temperature was not increased. Therefore, it can be said that BAT activity is not mediated by TH signalling in the ZI.

Non-shivering thermogenesis does not only take place in adipose tissue but also in muscle via the uncoupling of the sarcoendoplasmic reticulum calcium ATPase (SERCA) activity. SERCA is an ATPase that hydrolyses ATP to generate energy. However, it has been shown that the energy produced by ATP hydrolysis is also partly dissipated as heat (Lervik et al., 2012). Given that the results of this thesis did not find elevated body temperature, nor increased SERCA genes, it can be said that muscle non-shivering thermogenesis is not controlled by ZI TRα1 signalling.

It has been shown previously, that THs can act in the hypothalamus to regulate energy balance by increasing SNS innervation (López et al., 2010). Moreover, hypothalamic TH signalling can also affect body temperature (Sentis et al., 2024). Therefore, it is likely that regulation of body weight and body temperature by THs is due to TH action in the hypothalamus, and the ZI does not contribute to these modulations, as shown by the results of this study.

In sum, while the ZI is activated by THs, TH signalling in the ZI does not influence body weight or body temperature. Furthermore, it does not affect BAT activity and observed body temperature phenotypes in full body TRα1 mutants are most likely due to TH action in the hypothalamus and not in the ZI. However, it remains to be seen whether the ZI could possibly play a role in hypothalamic based regulation of body temperature, as the ZI shows connections to the hypothalamus and the direct pathways of this regulation are still not fully understood.

4.3 Effects of TRα1 signalling in the Zona Incerta on energy expenditure

The ability of THs to modulate energy homeostasis is well established (Iwen et al., 2013, 2018; Vaitkus et al., 2015). TH-mediated uncoupling of the electron transport chain via UCP1 decreases the production of ATP, which naturally increases energy expenditure (Lowell & Spiegelman, 2000). Additionally, THs can affect the arcuate nucleus (ARC), which plays a key role in the control of energy expenditure via melanocortin type 4 receptor (MC4R) neurons and POMC neurons (Iwen et al., 2018; Krashes et al., 2016).

THs are key regulators of metabolic pathways and the BMR. The BMR is the amount of energy needed to sustain the body under basal conditions while awake and not affected by stress or other factors (Henry, 2005). T3 can increase mitochondrial activity by modulating proton leaks and increasing heat production, known as thermogenesis, thereby altering cellular oxygen consumption and ATP production (S.-Y. Cheng et al., 2010).

Interestingly THs are also able to affect the number of mitochondria by influencing the expression of PPAR gamma coactivator-1 (PGC1) and the mitochondrial transcription factor A, both mitochondrial transcription factors (S.-Y. Cheng et al., 2010). It is also known, that there are TRs located in the mitochondrial matrix (Andersson & Vennström, 1997; Casas et al., 1999).

TH related changes in BMR can result in weight changes (Maciak et al., 2020) and intolerance to heat or cold (Maeda et al., 2007). This is in line with the findings of this study, as inhibition of TH signalling in the ZI led to an increase in BMR. Since there was no observable difference in *Ucp1* gene expression in the iBAT, this increase is most likely due to muscle metabolism. Further studies to analyse the state and number of mitochondria could give more insight into how ZI TH signalling alters the BMR.

Additionally, studies showed that SERCA is active even during resting phases and contributes to the resting metabolic rate (I. C. Smith et al., 2013). SERCA controls Ca^{2+} concentrations by transporting cytosolic Ca^{2+} back into the sarcoendoplasmic reticulum (SR). During this process, SERCA can generate heat. This activity is regulated in part by Sarcolipin (SLN), which uncouples SERCA Ca^{2+} transport from ATP hydrolysis. This causes accumulation of Ca^{2+} in the cytosol of skeletal muscle. Binding of SLN to SERCA induces higher ATP utilisation and results in increased heat generation (Bal et al., 2012; Bal & Periasamy, 2020; Pant et al., 2016; Sahoo et al., 2013). Studies have shown that THs can have an effect on the expression of *Sln* (Minamisawa et al., 2006; Nicolaisen et al., 2020). Interestingly, since SERCA contributes to resting metabolic rate, SLN also affects whole body metabolism. Overexpression of SLN in mice leads to decreased weight gain, while knockout of SLN induces increased weight gain (Bal et al., 2012; Bal & Periasamy, 2020). This shows that SLN activity could protect from diet-induced obesity by promoting fat oxidation (Pant et al., 2016). However, the results of this study could not show any changes in SERCA genes, indicating that TH signalling in the ZI does not influence the expression of SERCA directly.

Previous studies have shown that T3 reduces *Sln* expression in atria of mice (Minamisawa et al., 2006), and loss of function of soleus TRα1 results in increased gene expression of *Sln* (Nicolaisen et al., 2020). Furthermore, treatment with T3 results in decreased expression of *Sln* in skeletal muscle (Johann et al., 2019), indicating that THs play a role in the regulation of *Sln* expression and therefore SERCA activity. Inhibition of TH signalling in the ZI resulted in a decrease in *Sln* expression in the m. gastrocnemius, which stands in contrast to the literature indicating that T3 decreases *Sln* expression. In this context, it is always important to note the differences between direct local actions of THs and central actions of THs, as action in the brain does not translate to local action at the organ. The most well-known example for this is the negative

feedback loop of T3 and T4, that have stimulating effects on organs such as the BAT but inhibitory effects on the hypothalamus (Ortiga-Carvalho et al., 2016). It has also been reported that increased energy expenditure is often due to an increased expression of *Sln* in skeletal muscle, as overexpression of *Sln* leads to higher energy expenditure in mice (Maurya & Periasamy, 2015). Interestingly, this study shows increased energy expenditure with decreased expression of *Sln*, suggesting another mechanism of energy expenditure increase is taking place. However, genes involved in fatty acid oxidation, glycolysis or gluconeogenesis were not differentially expressed in the liver and the hepatic glycogen content was also not affected. It is possible that other regulators of SERCA, such as phospholamban (PLN), are responsible for the modulation of energy expenditure (Gorski et al., 2017). It was furthermore shown that the injected AAV successfully targeted neurons and not astrocytes, which implies that the observed effects are due to a neuron population of the ZI.

While energy expenditure under basal conditions in this study was not altered, inhibition of TH signalling in the ZI resulted in increased oxygen consumption and subsequent body weight loss during fasting conditions at 30°C. 30°C ambient temperature is the thermoneutral zone for mice (Ganeshan & Chawla, 2017), in which BAT thermogenesis is not taking place (Johann et al., 2019; Sentis et al., 2021). Therefore, measurements at thermoneutrality allow for investigation of energy expenditure without the influence of BAT. Additionally, mice were fasted to eliminate diet-induced thermogenesis (Saito et al., 2020). However, this gives rise to the possibility of body weight loss being due to increased water loss instead of changes in body composition (Jensen et al., 2013). Polyuria, which is defined as an increased excretion of urine, is common in dogs with Cushing's syndrome, suggesting a possible connection between elevated glucocorticoids and body weight loss (Wehner et al., 2021). Glucocorticoids are closely linked to mineralocorticoids, both of which are steroid hormones. Since mineralocorticoids influence salt intake, it is known that elevated levels of mineralocorticoids can induce polyuria (Kurimoto et al., 2023). The effect of glucocorticoids on urine excretion is less well studied, but it has been shown that glucocorticoids can increase the volume of urine and cause hypertension (Baylis et al., 1990; Haack et al., 1977). However, the observed effects often coincide with increased water intake (Thunhorst et al., 2007), which could not be observed in this study. By measuring urine excretion with metabolic cages, further studies could elucidate the role of glucocorticoids, and therefore possibly TH signalling in the ZI, in polyuria. However, whether polyuria is the cause of decreased body weight in this study cannot be verified and needs to be further tested. The data of this study suggests that the observed increase in energy expenditure is due to alterations in muscle metabolism.

In conclusion, this study implicates TH signalling in the ZI in the regulation of muscle metabolism and therefore energy expenditure. While the precise mechanisms behind the increase in energy expenditure remain elusive, it has been shown that the ZI is involved in modulating oxygen consumption via TH action.

4.4 Effects of TRα1 signalling in the Zona Incerta on anxiety and stress

One system that THs interact with is the HPA axis, a system involved in anxiety and stress. Anxiety is a feeling of fear that, when excessive, can lead to the development of an anxiety disorder. Anxiety disorders are often characterised by intense feelings of extreme worry and can also be caused by high amounts of psychological stress (Bartlett et al., 2017). Patients suffering from anxiety disorders have been shown to present with a hyperactivity of the HPA axis, which is thought to be caused by chronic stress (Arborelius et al., 1999; Tafet & Nemeroff, 2016). There are different forms of stress, acute stress and chronic stress. Recent studies show that the physiological outcome of acute and chronic stress differ, as both forms result in an increase in energy expenditure, but only chronic stress decreases body weight, which was also observed in this study. In addition, chronic repeated stress does not induce an anxiety phenotype, while chronic variable stress does. Furthermore, corticosterone increase is higher with acute stress than with chronic stress, compared to control conditions (Kuti et al., 2022). THs can influence the production and the release of glucocorticoids by enhancing the sensitivity of the adrenal glands to ACTH (Sánchez-Franco et al., 1989). It has also been shown that hypothyroidism can lead to decreased levels of ACTH and cortisol *in utero,* indicating that THs play a role in the development of organs involved in the HPA axis (Camm et al., 2021), and that long-term hypothyroidism in rats leads to decreased levels of CRH and ACTH-induced cortisol release (Johnson et al., 2012). Vice versa, cortisol can affect THs by modulating deiodinase enzymes (Heyma & Larkins, 1982; Paragliola et al., 2021). These enzymes convert T4 to the more active form T3. Additionally, glucocorticoids can alter TH metabolism by inhibiting the pituitary directly (Ahlquist et al., 1989).

Moreover, THs can interact with insulin and affect glucose metabolism by enhancing insulin sensitivity and glucose uptake (S.-Y. Cheng et al., 2010; Mullur et al., 2014).

Inhibition of TH signalling in the ZI resulted in an increase in serum corticosterone, which indicates elevated levels of stress.

Interestingly, inhibition of TH signalling in the ZI did not alter *Crh* expression in the hypothalamus, *Pomc* expression in the anterior pituitary or GR target gene expression in the liver.

This indicates that the elevation in corticosterone serum levels is not due to a resetting of the HPA axis in its entirety but rather represents an acute phenomenon, such as an excessive endocrine response (Tran & Gellner, 2023).

Interestingly, studies showed that adult onset hypothyroidism can cause decreased hippocampal volumes, which is associated with altered mood and increased anxiety, as it is a marker for long-term alterations in glucocorticoid levels (Baumann et al., 2019; Cooke et al., 2014; Salas-Lucia, 2024; T. Zhang et al., 2024), which would be expected in this study, as TH signalling is inhibited in the ZI and corticosterone levels are elevated. However, the results of this study showed no alterations in hippocampal volume, which could be due to the short-term alteration of stress in this experimental set-up. Further studies with a longer experimental paradigm could help clarify whether the lack of hippocampal volume alterations in this study are due to non-involvement of the ZI or insufficient duration of TH signalling inhibition.

The ZI has previously been implicated in the modulation of fear generalisation and anxiety (Z. Li et al., 2021; Venkataraman et al., 2019), and deep-brain stimulation of the ZI in patients suffering from PD results in self-reported amelioration of their anxiety (Burrows et al., 2012). This is reflected in this study, as inhibition of TH signalling in the ZI resulted in more time spent in the outer zones during the last 5 minutes of an open field test. However, there was no difference in line crossings in the elevated plus maze, indicated no change in exploratory behaviour, which is usually part of classic mouse anxiety and has been observed previously during stimulation of ZI neurons (Hormigo et al., 2023; Sharma et al., 2024). This suggests that, although the initial exploratory behaviour in a novel environment is unchanged, the animals acclimate to the new surroundings more slowly than the controls and habituation is impaired (Bailey & Crawley, 2009). Mice carrying the TRα1R384C mutation show severe anxiety without alterations in corticosterone levels (Mittag, Davis, et al., 2010) in both the open field test and the elevated plus maze. However, in contrast to TRα1R384C expression in only the ZI, they show decreased travel distance and massive freezing, which implies that other brain regions involved in motor function could be responsible for this phenotype (Venero et al., 2005). Interestingly, a study shows that testicular feminization in mice results in increased anxiety, along with elevated levels of corticosterone, which suggests a possible role of the androgen receptor in modulation of anxiety and the HPA axis (Zuloaga et al., 2008). This gives rise to the assumption that the HPA axis can be regulated in multiple ways that are not yet fully understood and further studies looking into changes related to the androgen receptor would be of interest.

In summary, this study implicates TH signalling in the ZI in the modulation of anxiety and stress, as inhibition of TH signalling resulted in elevated corticosterone levels and a partial anxiety

phenotype with impaired habituation. This phenotype is similar to that of chronic repeated stress rather than acute stress and is most likely due to an increased endocrine response. However, further studies are needed to fully understand the mechanism behind the alteration of stress and anxiety by THs in the ZI. To test this, it would be of interest to repeat this study with additional treatment with T3 to investigate the reversibility of this phenotype, as T3 treatment can reactivate the mutated TRα1 that was expressed in the ZI. Additionally, more behaviour tests need to be carried out to fully characterise the anxiety phenotype. A novel object recognition test could give more insights into the ability to habituate to new environments, and a marble burying test could further show if inhibition of TH signalling in the ZI has effects on obsessive compulsory behaviour. As stress often causes hypertension (Farah et al., 2004), measurements of blood pressure throughout the experiment could be of use. Analysis of more endpoints, such as sleeping patterns, pain suppression, serum ketone body levels, and changes in neurotransmission of serotonin and dopamine can give more insights into the anxiety phenotype (Patchev & Patchev, 2006). Furthermore, ACTH levels in serum and urine could elucidate the role of the HPA axis in the observed chronic stress-like state. By purposely stressing the animals, such as with bright lights or odors that originate from predators (Patchev & Patchev, 2006), it would be possible to more closely observe potential differences in stress responses. It would further be of interest to test the effects of overexpression of TRα1 to see how the phenotype changes when TH signalling in the ZI is increased compared to decreased TH signalling. Lastly, a conditional model for TH signalling in the ZI of other neuronal populations, such as GABAergic neurons or glutamatergic neurons, is needed to show which neurons mediate the observed effects.

5. Conclusion and Outlook

In summary, this thesis demonstrates the involvement of the Zona Incerta in central effects of thyroid hormones. Inhibition of TRα1 signalling specifically in the ZI leads to a chronic stress-like state, including impaired habituation and increased levels of serum corticosterone. Furthermore, it elevates the BMR (Fig. 29). Since many neuroanatomical substrates of central TH action are still poorly understood, this thesis contributes valuable information to the general understanding of TH action.

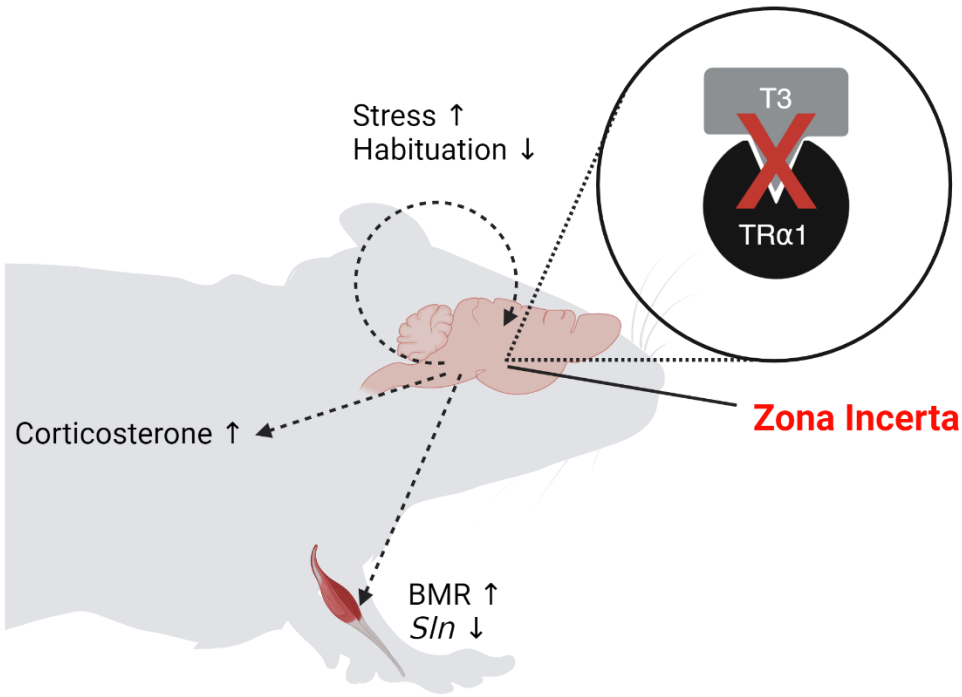

Figure 29: Effects of thyroid hormone signalling inhibition in the Zona Incerta on the organism. *Expression of a mutant TRα1 in the ZI results in a chronic stress-like state with increased corticosterone levels and BMR. BMR: Basal metabolic rate; Sln: Sarcolipin. Figure was created using Biorender.com.*

However, the exact mechanisms behind the alterations of the stress state through TH signalling in the ZI remain ambiguous. The effects are most likely mediated by muscle metabolism, as elevation of energy expenditure can be observed during fasting at thermoneutrality and gene expression of genes generally involved in energy expenditure (Asahi et al., 2003; Bal et al., 2012; Maurya & Periasamy, 2015) is altered. Additionally, corticosterone levels are increased without any change in gene expression of *Pomc* or *Crh*, showing an endocrine

change rather than an effect on the HPA axis as a whole. Since the mutant TRα1 that was introduced into the ZI is reactivatable, further studies with T3 treatment need to be performed to elucidate the role of the ZI in central TH actions and test for reversibility of the phenotype. Furthermore, as the hypothalamus has been implicated as a region responsible for TH mediated alteration of the body temperature set point (Sentis et al., 2024), additional studies with more brain regions identified in the PET/CT scans need to be conducted to fully understand which brain regions mediate which central effects of TH.

By showing that the ZI is involved in TH-mediated control of mood and energy expenditure, this study can help to gain more insight into the cause for mood disorders in patients suffering from hypo- and hyperthyroidism (Bathla et al., 2016; Fischer & Ehlert, 2018; Nuguru et al., 2022). In addition, the presented results of this study can extend the knowledge of the hypothyroid phenotype in humans that sometimes includes elevated levels of glucocorticoids (Sinha et al., 2023) and the development of anxiety disorders (Wiersinga, 2014) and can postulate a possible role of the ZI in these effects. It is well known that THs can influence mood, and this thesis now demonstrates a better understanding of the processes behind these effects. Therefore, this study could help find new therapies for the treatment of mood disorders, such as depression and anxiety disorders.

6. References

Ahlquist, J. A., Franklyn, J. A., Ramsden, D. B., & Sheppard, M. C. (1989). The influence of dexamethasone on serum thyrotrophin and thyrotrophin synthesis in the rat. *Molecular and Cellular Endocrinology*, *64*(1), 55–61. https://doi.org/10.1016/0303-7207(89)90064-6

Alcaide Martin, A., & Mayerl, S. (2023). Local Thyroid Hormone Action in Brain Development. *International Journal of Molecular Sciences*, *24*(15), 12352. https://doi.org/10.3390/ijms241512352

American Psychiatric Association. (2013). *Diagnostic and statistical manual of mental disorders: DSM-5*. (5th Edition). American Psychiatric Association.

Andersen, C. L., Jensen, J. L., & Ørntoft, T. F. (2004). Normalization of real-time quantitative reverse transcription-PCR data: A model-based variance estimation approach to identify genes suited for normalization, applied to bladder and colon cancer data sets. *Cancer Research*, *64*(15), 5245–5250. https://doi.org/10.1158/0008-5472.CAN-04-0496

Andersson, M. L., & Vennström, B. (1997). Chicken thyroid hormone receptor alpha requires the N-terminal amino acids for exclusive nuclear localization. *FEBS Letters*, *416*(3), 291–296. https://doi.org/10.1016/s0014-5793(97)01223-4

Arborelius, L., Owens, M. J., Plotsky, P. M., & Nemeroff, C. B. (1999). The role of corticotropin-releasing factor in depression and anxiety disorders. *The Journal of Endocrinology*, *160*(1), 1–12. https://doi.org/10.1677/joe.0.1600001

Asahi, M., Sugita, Y., Kurzydlowski, K., De Leon, S., Tada, M., Toyoshima, C., & MacLennan, D. H. (2003). Sarcolipin regulates sarco(endo)plasmic reticulum Ca2+-ATPase (SERCA) by binding to transmembrane helices alone or in association with phospholamban. *Proceedings of the National Academy of Sciences of the United States of America*, *100*(9), 5040–5045. https://doi.org/10.1073/pnas.0330962100

Backes, H., Walberer, M., Endepols, H., Neumaier, B., Graf, R., Wienhard, K., & Mies, G. (2011). Whiskers Area as Extracerebral Reference Tissue for Quantification of Rat Brain Metabolism Using 18F-FDG PET: Application to Focal Cerebral Ischemia. *Journal of Nuclear Medicine*, *52*(8), 1252–1260. https://doi.org/10.2967/jnumed.110.085266

Bailey, K. R., & Crawley, J. N. (2009). Anxiety-Related Behaviors in Mice. In J. J. Buccafusco (Ed.), *Methods of Behavior Analysis in Neuroscience* (2nd ed.). CRC Press/Taylor & Francis. http://www.ncbi.nlm.nih.gov/books/NBK5221/

Bal, N. C., Maurya, S. K., Sopariwala, D. H., Sahoo, S. K., Gupta, S. C., Shaikh, S. A., Pant, M., Rowland, L. A., Bombardier, E., Goonasekera, S. A., Tupling, A. R., Molkentin, J. D., & Periasamy, M. (2012). Sarcolipin is a newly identified regulator of muscle-based

thermogenesis in mammals. *Nature Medicine*, *18*(10), Article 10. https://doi.org/10.1038/nm.2897

Bal, N. C., & Periasamy, M. (2020). Uncoupling of sarcoendoplasmic reticulum calcium ATPase pump activity by sarcolipin as the basis for muscle non-shivering thermogenesis. *Philosophical Transactions of the Royal Society of London. Series B, Biological Sciences*, *375*(1793), 20190135. https://doi.org/10.1098/rstb.2019.0135

Bartlett, A. A., Singh, R., & Hunter, R. G. (2017). Anxiety and Epigenetics. *Advances in Experimental Medicine and Biology*, *978*, 145–166. https://doi.org/10.1007/978-3-319-53889-1_8

Bathla, M., Singh, M., & Relan, P. (2016). Prevalence of anxiety and depressive symptoms among patients with hypothyroidism. *Indian Journal of Endocrinology and Metabolism*, *20*(4), 468–474. https://doi.org/10.4103/2230-8210.183476

Baumann, P., Schriever, S. C., Kullmann, S., Zimprich, A., Feuchtinger, A., Amarie, O., Peter, A., Walch, A., Gailus-Durner, V., Fuchs, H., Hrabě de Angelis, M., Wurst, W., Tschöp, M. H., Heni, M., Hölter, S. M., & Pfluger, P. T. (2019). Dusp8 affects hippocampal size and behavior in mice and humans. *Scientific Reports*, *9*(1), 19483. https://doi.org/10.1038/s41598-019-55527-7

Baylis, C., Handa, R. K., & Sorkin, M. (1990). Glucocorticoids and control of glomerular filtration rate. *Seminars in Nephrology*, *10*(4), 320–329.

Bernal, J., Guadaño-Ferraz, A., & Morte, B. (2015). Thyroid hormone transporters—Functions and clinical implications. *Nature Reviews. Endocrinology*, *11*(7), 406–417. https://doi.org/10.1038/nrendo.2015.66

Björklund, A., Lindvall, O., & Nobin, A. (1975). Evidence of an incerto-hypothalamic dopamine neurone system in the rat. *Brain Research*, *89*(1), 29–42. https://doi.org/10.1016/0006-8993(75)90131-6

Bochukova, E., Schoenmakers, N., Agostini, M., Schoenmakers, E., Rajanayagam, O., Keogh, J. M., Henning, E., Reinemund, J., Gevers, E., Sarri, M., Downes, K., Offiah, A., Albanese, A., Halsall, D., Schwabe, J. W. R., Bain, M., Lindley, K., Muntoni, F., Vargha-Khadem, F., … Chatterjee, K. (2012). A mutation in the thyroid hormone receptor alpha gene. *The New England Journal of Medicine*, *366*(3), 243–249. https://doi.org/10.1056/NEJMoa1110296

Brent, G. A. (2012). Mechanisms of thyroid hormone action. *The Journal of Clinical Investigation*, *122*(9), 3035–3043. https://doi.org/10.1172/JCI60047

Burrows, A. M., Ravin, P. D., Novak, P., Peters, M. L. B., Dessureau, B., Swearer, J., & Pilitsis, J. G. (2012). Limbic and motor function comparison of deep brain stimulation of the zona incerta and subthalamic nucleus. *Neurosurgery*, *70*(1 Suppl Operative), 125–130; discussion 130-131. https://doi.org/10.1227/NEU.0b013e318232fdac

Camm, E. J., Inzani, I., De Blasio, M. J., Davies, K. L., Lloyd, I. R., Wooding, F. B. P., Blache, D., Fowden, A. L., & Forhead, A. J. (2021). Thyroid Hormone Deficiency Suppresses Fetal Pituitary-Adrenal Function Near Term: Implications for the Control of Fetal Maturation and Parturition. *Thyroid: Official Journal of the American Thyroid Association*, *31*(6), 861–869. https://doi.org/10.1089/thy.2020.0534

Cannon, B., & Nedergaard, J. (2004). Brown adipose tissue: Function and physiological significance. *Physiological Reviews*, *84*(1), 277–359. https://doi.org/10.1152/physrev.00015.2003

Casas, F., Rochard, P., Rodier, A., Cassar-Malek, I., Marchal-Victorion, S., Wiesner, R. J., Cabello, G., & Wrutniak, C. (1999). A variant form of the nuclear triiodothyronine receptor c-ErbAalpha1 plays a direct role in regulation of mitochondrial RNA synthesis. *Molecular and Cellular Biology*, *19*(12), 7913–7924. https://doi.org/10.1128/MCB.19.12.7913

Chaker, L., Bianco, A. C., Jonklaas, J., & Peeters, R. P. (2017). Hypothyroidism. *Lancet (London, England)*, *390*(10101), 1550–1562. https://doi.org/10.1016/S0140-6736(17)30703-1

Cheng, S.-Y., Leonard, J. L., & Davis, P. J. (2010). Molecular Aspects of Thyroid Hormone Actions. *Endocrine Reviews*, *31*(2), 139–170. https://doi.org/10.1210/er.2009-0007

Cheng, X., Zhang, H., Guan, S., Zhao, Q., & Shan, Y. (2023). Receptor modulators associated with the hypothalamus -pituitary-thyroid axis. *Frontiers in Pharmacology*, *14*, 1291856. https://doi.org/10.3389/fphar.2023.1291856

Cheng, Y.-C., Su, M.-I., Liu, C.-W., Huang, Y.-C., & Huang, W.-L. (2022). Heart rate variability in patients with anxiety disorders: A systematic review and meta-analysis. *Psychiatry and Clinical Neurosciences*, *76*(7), 292–302. https://doi.org/10.1111/pcn.13356

Chometton, S., Barbier, M., & Risold, P.-Y. (2021). The zona incerta system: Involvement in attention and movement. *Handbook of Clinical Neurology*, *180*, 173–184. https://doi.org/10.1016/B978-0-12-820107-7.00011-2

Cízek, J., Herholz, K., Vollmar, S., Schrader, R., Klein, J., & Heiss, W.-D. (2004). Fast and robust registration of PET and MR images of human brain. *NeuroImage*, *22*(1), 434–442. https://doi.org/10.1016/j.neuroimage.2004.01.016

Cooke, G. E., Mullally, S., Correia, N., O'Mara, S. M., & Gibney, J. (2014). Hippocampal volume is decreased in adults with hypothyroidism. *Thyroid: Official Journal of the American Thyroid Association*, *24*(3), 433–440. https://doi.org/10.1089/thy.2013.0058

Crocq, M.-A. (2015). A history of anxiety: From Hippocrates to DSM. *Dialogues in Clinical Neuroscience*, *17*(3), 319–325.

De Leo, S., Lee, S. Y., & Braverman, L. E. (2016). Hyperthyroidism. *Lancet (London, England)*, *388*(10047), 906–918. https://doi.org/10.1016/S0140-6736(16)00278-6

Denver, R. J., Pavgi, S., & Shi, Y. B. (1997). Thyroid hormone-dependent gene expression program for Xenopus neural development. *The Journal of Biological Chemistry*, *272*(13), 8179–8188. https://doi.org/10.1074/jbc.272.13.8179

Dore, R., Watson, L., Hollidge, S., Krause, C., Sentis, S. C., Oelkrug, R., Geißler, C., Johann, K., Pedaran, M., Lyons, G., Lopez-Alcantara, N., Resch, J., Sayk, F., Iwen, K. A., Franke, A., Boysen, T. J., Dalley, J. W., Lorenz, K., Moran, C., … Mittag, J. (2023). Resistance to thyroid hormone induced tachycardia in RTHα syndrome. *Nature Communications*, *14*(1), 3312. https://doi.org/10.1038/s41467-023-38960-1

Dragoş, D., & Tănăsescu, M. (2010). The effect of stress on the defense systems. *Journal of Medicine and Life*, *3*(1), 10–18.

Duntas, L. H. (2016). NEW INSIGHTS INTO THE HYPOTHALAMIC-PITUITARY-THYROID AXIS. *Acta Endocrinologica (Bucharest)*, *12*(2), 125–129. https://doi.org/10.4183/aeb.2016.125

El Amrousy, D., El-Afify, D., & Salah, S. (2022). Insulin resistance, leptin and adiponectin in lean and hypothyroid children and adolescents with obesity. *BMC Pediatrics*, *22*(1), 245. https://doi.org/10.1186/s12887-022-03318-x

Evans, R. M., & Mangelsdorf, D. J. (2014). Nuclear Receptors, RXR & the Big Bang. *Cell*, *157*(1), 255–266. https://doi.org/10.1016/j.cell.2014.03.012

F, C., J, Q., Z, C., A, L., J, C., L, S., & J, X. (2023). Chemogenetic and optogenetic stimulation of zona incerta GABAergic neurons ameliorates motor impairment in Parkinson's disease. *iScience*, *26*(7). https://doi.org/10.1016/j.isci.2023.107149

Farah, V. M. A., Joaquim, L. F., Bernatova, I., & Morris, M. (2004). Acute and chronic stress influence blood pressure variability in mice. *Physiology & Behavior*, *83*(1), 135–142. https://doi.org/10.1016/j.physbeh.2004.08.004

Fekete, C., & Lechan, R. M. (2014). Central Regulation of Hypothalamic-Pituitary-Thyroid Axis Under Physiological and Pathophysiological Conditions. *Endocrine Reviews*, *35*(2), 159–194. https://doi.org/10.1210/er.2013-1087

Fischer, S., & Ehlert, U. (2018). Hypothalamic-pituitary-thyroid (HPT) axis functioning in anxiety disorders. A systematic review. *Depression and Anxiety*, *35*(1), 98–110. https://doi.org/10.1002/da.22692

Flynn, C. A., & Chen, Y. C. C. (2003). Antidepressants for generalized anxiety disorder. *American Family Physician*, *68*(9), 1757–1758.

Folgueira, C., Beiroa, D., Porteiro, B., Duquenne, M., Puighermanal, E., Fondevila, M. F., Barja-Fernández, S., Gallego, R., Hernández-Bautista, R., Castelao, C., Senra, A., Seoane-Collazo, P., Gómez-Lado, N., Aguiar, P., Guallar, D., Fidalgo, M., Romero-Pico, A., Adan, R., Blouet, C., … Nogueiras, R. (2019). Hypothalamic dopamine signalling regulates

brown fat thermogenesis. *Nature Metabolism*, *1*(8), 811–829. https://doi.org/10.1038/s42255-019-0099-7

Fraichard, A., Chassande, O., Plateroti, M., Roux, J. P., Trouillas, J., Dehay, C., Legrand, C., Gauthier, K., Kedinger, M., Malaval, L., Rousset, B., & Samarut, J. (1997). The T3R alpha gene encoding a thyroid hormone receptor is essential for post-natal development and thyroid hormone production. *The EMBO Journal*, *16*(14), 4412–4420. https://doi.org/10.1093/emboj/16.14.4412

Franklin, K. B. J., & Paxinos, G. (2013). *Paxinos and Franklin's The mouse brain in stereotaxic coordinates* (Fourth edition). Academic Press, an imprint of Elsevier.

Ganeshan, K., & Chawla, A. (2017). Warming the mouse to model human diseases. *Nature Reviews. Endocrinology*, *13*(8), 458–465. https://doi.org/10.1038/nrendo.2017.48

Goodwin, R. D., Weinberger, A. H., Kim, J. H., Wu, M., & Galea, S. (2020). Trends in anxiety among adults in the United States, 2008–2018: Rapid increases among young adults. *Journal of Psychiatric Research*, *130*, 441–446. https://doi.org/10.1016/j.jpsychires.2020.08.014

Gorski, P. A., Ceholski, D. K., & Young, H. S. (2017). Structure-Function Relationship of the SERCA Pump and Its Regulation by Phospholamban and Sarcolipin. *Advances in Experimental Medicine and Biology*, *981*, 77–119. https://doi.org/10.1007/978-3-319-55858-5_5

Guerri, G., Bressan, S., Sartori, M., Costantini, A., Benedetti, S., Agostini, F., Tezzele, S., Cecchin, S., Scaramuzza, A., & Bertelli, M. (2019). Hypothyroidism and hyperthyroidism. *Acta Bio Medica : Atenei Parmensis*, *90*(Suppl 10), 83–86. https://doi.org/10.23750/abm.v90i10-S.8765

Haack, D., Möhring, J., Möhring, B., Petri, M., & Hackenthal, E. (1977). Comparative study on development of corticosterone and DOCA hypertension in rats. *The American Journal of Physiology*, *233*(5), F403-411. https://doi.org/10.1152/ajprenal.1977.233.5.F403

Harris, A. R. C., Christianson, D., Smith, M. S., Fang, S.-L., Braverman, L. E., & Vagenakis, A. G. (1978). The Physiological Role of Thyrotropin-Releasing Hormone in the Regulation of Thyroid-Stimulating Hormone and Prolactin Secretion in the Rat. *Journal of Clinical Investigation*, *61*(2), 441–448.

Heise, C. E., & Mitrofanis, J. (2004). Evidence for a glutamatergic projection from the zona incerta to the basal ganglia of rats. *The Journal of Comparative Neurology*, *468*(4), 482–495. https://doi.org/10.1002/cne.10971

Henry, C. J. K. (2005). Basal metabolic rate studies in humans: Measurement and development of new equations. *Public Health Nutrition*, *8*(7A), 1133–1152. https://doi.org/10.1079/phn2005801

Heyma, P., & Larkins, R. G. (1982). Glucocorticoids decrease in conversion of thyroxine into 3, 5, 3'-tri-iodothyronine by isolated rat renal tubules. *Clinical Science (London, England: 1979)*, *62*(2), 215–220. https://doi.org/10.1042/cs0620215

Himms-Hagen, J. (1984). Nonshivering thermogenesis. *Brain Research Bulletin*, *12*(2), 151–160. https://doi.org/10.1016/0361-9230(84)90183-7

Hoffman, G. E., Smith, M. S., & Verbalis, J. G. (1993). C-Fos and related immediate early gene products as markers of activity in neuroendocrine systems. *Frontiers in Neuroendocrinology*, *14*(3), 173–213. https://doi.org/10.1006/frne.1993.1006

Hormigo, S., Zhou, J., Chabbert, D., Sajid, S., Busel, N., & Castro-Alamancos, M. (2023). Zona incerta distributes a broad movement signal that modulates behavior. *eLife*, *12*, RP89366. https://doi.org/10.7554/eLife.89366

Ishikawa, K., Taniguchi, Y., Inoue, K., Kurosumi, K., & Suzuki, M. (1988). Immunocytochemical delineation of thyrotrophic area: Origin of thyrotropin-releasing hormone in the median eminence. *Neuroendocrinology*, *47*(5), 384–388. https://doi.org/10.1159/000124943

Iwen, K. A., Oelkrug, R., & Brabant, G. (2018). Effects of thyroid hormones on thermogenesis and energy partitioning. *Journal of Molecular Endocrinology*, *60*(3), R157–R170. https://doi.org/10.1530/JME-17-0319

Iwen, K. A., Schröder, E., & Brabant, G. (2013). Thyroid Hormones and the Metabolic Syndrome. *European Thyroid Journal*, *2*(2), 83–92. https://doi.org/10.1159/000351249

Jais, A., Solas, M., Backes, H., Chaurasia, B., Kleinridders, A., Theurich, S., Mauer, J., Steculorum, S. M., Hampel, B., Goldau, J., Alber, J., Förster, C. Y., Eming, S. A., Schwaninger, M., Ferrara, N., Karsenty, G., & Brüning, J. C. (2016). Myeloid-Cell-Derived VEGF Maintains Brain Glucose Uptake and Limits Cognitive Impairment in Obesity. *Cell*, *165*(4), 882–895. https://doi.org/10.1016/j.cell.2016.03.033

Jeanneteau, F. D., Lambert, W. M., Ismaili, N., Bath, K. G., Lee, F. S., Garabedian, M. J., & Chao, M. V. (2012). BDNF and glucocorticoids regulate corticotrophin-releasing hormone (CRH) homeostasis in the hypothalamus. *Proceedings of the National Academy of Sciences*, *109*(4), 1305–1310. https://doi.org/10.1073/pnas.1114122109

Jensen, T. L., Kiersgaard, M. K., Sørensen, D. B., & Mikkelsen, L. F. (2013). Fasting of mice: A review. *Laboratory Animals*, *47*(4), 225–240. https://doi.org/10.1177/0023677213501659

Johann, K., Cremer, A. L., Fischer, A. W., Heine, M., Pensado, E. R., Resch, J., Nock, S., Virtue, S., Harder, L., Oelkrug, R., Astiz, M., Brabant, G., Warner, A., Vidal-Puig, A., Oster, H., Boelen, A., López, M., Heeren, J., Dalley, J. W., … Mittag, J. (2019). Thyroid-Hormone-Induced Browning of White Adipose Tissue Does Not Contribute to Thermogenesis and Glucose Consumption. *Cell Reports*, *27*(11), 3385-3400.e3. https://doi.org/10.1016/j.celrep.2019.05.054

Johnson, E. O., Calogero, A. E., Konstandi, M., Kamilaris, T. C., La Vignera, S., & Chrousos, G. P. (2012). Effects of short- and long-duration hypothyroidism on hypothalamic-pituitary-adrenal axis function in rats: In vitro and in situ studies. *Endocrine*, *42*(3), 684–693. https://doi.org/10.1007/s12020-012-9714-z

Juárez Olguín, H., Calderón Guzmán, D., Hernández García, E., & Barragán Mejía, G. (2016). The Role of Dopamine and Its Dysfunction as a Consequence of Oxidative Stress. *Oxidative Medicine and Cellular Longevity*, *2016*, 9730467. https://doi.org/10.1155/2016/9730467

Katz, D., & Lazar, M. A. (1993). Dominant negative activity of an endogenous thyroid hormone receptor variant (alpha 2) is due to competition for binding sites on target genes. *The Journal of Biological Chemistry*, *268*(28), 20904–20910.

Kim, B. (2008). Thyroid hormone as a determinant of energy expenditure and the basal metabolic rate. *Thyroid: Official Journal of the American Thyroid Association*, *18*(2), 141–144. https://doi.org/10.1089/thy.2007.0266

Kingma, B., Frijns, A., & van Marken Lichtenbelt, W. (2012). The thermoneutral zone: Implications for metabolic studies. *Frontiers in Bioscience (Elite Edition)*, *4*(5), 1975–1985. https://doi.org/10.2741/e518

Klok, M. D., Jakobsdottir, S., & Drent, M. L. (2007). The role of leptin and ghrelin in the regulation of food intake and body weight in humans: A review. *Obesity Reviews: An Official Journal of the International Association for the Study of Obesity*, *8*(1), 21–34. https://doi.org/10.1111/j.1467-789X.2006.00270.x

Knierim, J. J. (2015). The hippocampus. *Current Biology: CB*, *25*(23), R1116-1121. https://doi.org/10.1016/j.cub.2015.10.049

Kolber, B. J., Wieczorek, L., & Muglia, L. J. (2008). HPA axis dysregulation and behavioral analysis of mouse mutants with altered GR or MR function. *Stress (Amsterdam, Netherlands)*, *11*(5), 321–338. https://doi.org/10.1080/10253890701821081

Kolmac, C., & Mitrofanis, J. (1999). Distribution of various neurochemicals within the zona incerta: An immunocytochemical and histochemical study. *Anatomy and Embryology*, *199*(3), 265–280. https://doi.org/10.1007/s004290050227

Komada, M., Takao, K., & Miyakawa, T. (2008). Elevated Plus Maze for Mice. *Journal of Visualized Experiments : JoVE*, *22*, 1088. https://doi.org/10.3791/1088

Krashes, M. J., Lowell, B. B., & Garfield, A. S. (2016). Melanocortin-4 receptor-regulated energy homeostasis. *Nature Neuroscience*, *19*(2), 206–219. https://doi.org/10.1038/nn.4202

Kravets, I. (2016). Hyperthyroidism: Diagnosis and Treatment. *American Family Physician*, *93*(5), 363–370.

Kurimoto, J., Takagi, H., Miyata, T., Kawaguchi, Y., Hodai, Y., Tsumura, T., Hagiwara, D., Kobayashi, T., Yasuda, Y., Sugiyama, M., Onoue, T., Iwama, S., Suga, H., Banno, R.,

Katsuki, T., Ando, F., Uchida, S., & Arima, H. (2023). Mineralocorticoids induce polyuria by reducing apical aquaporin-2 expression of the kidney in partial vasopressin deficiency. *Endocrine Journal*, *70*(3), 295–304. https://doi.org/10.1507/endocrj.EJ22-0339

Kuti, D., Winkler, Z., Horváth, K., Juhász, B., Szilvásy-Szabó, A., Fekete, C., Ferenczi, S., & Kovács, K. J. (2022). The metabolic stress response: Adaptation to acute-, repeated- and chronic challenges in mice. *iScience*, *25*(8), 104693. https://doi.org/10.1016/j.isci.2022.104693

Lee, S. Y., & Pearce, E. N. (2023). Hyperthyroidism: A Review. *JAMA*, *330*(15), 1472–1483. https://doi.org/10.1001/jama.2023.19052

Lekurwale, V., Acharya, S., Shukla, S., & Kumar, S. (2023). Neuropsychiatric Manifestations of Thyroid Diseases. *Cureus*, *15*(1), e33987. https://doi.org/10.7759/cureus.33987

Lervik, A., Bresme, F., Kjelstrup, S., & Rubí, J. M. (2012). On the thermodynamic efficiency of Ca^{2+}-ATPase molecular machines. *Biophysical Journal*, *103*(6), 1218–1226. https://doi.org/10.1016/j.bpj.2012.07.057

Lezoualc'h, F., Hassan, A. H., Giraud, P., Loeffler, J. P., Lee, S. L., & Demeneix, B. A. (1992). Assignment of the beta-thyroid hormone receptor to 3,5,3'-triiodothyronine-dependent inhibition of transcription from the thyrotropin-releasing hormone promoter in chick hypothalamic neurons. *Molecular Endocrinology (Baltimore, Md.)*, *6*(11), 1797–1804. https://doi.org/10.1210/mend.6.11.1480171

Li, J., Peng, S., Zhang, Y., Ge, J., Gao, S., Zhu, Y., Bai, Y., Wu, S., & Huang, J. (2023). Glutamatergic Neurons in the Zona Incerta Modulate Pain and Itch Behaviors in Mice. *Molecular Neurobiology*, *60*(10), 5866–5877. https://doi.org/10.1007/s12035-023-03431-7

Li, L.-X., Li, Y.-L., Wu, J.-T., Song, J.-Z., & Li, X.-M. (2021). Glutamatergic Neurons in the Caudal Zona Incerta Regulate Parkinsonian Motor Symptoms in Mice. *Neuroscience Bulletin*, *38*(1), 1–15. https://doi.org/10.1007/s12264-021-00775-9

Li, Z., Rizzi, G., & Tan, K. R. (2021). Zona incerta subpopulations differentially encode and modulate anxiety. *Science Advances*, *7*(37), eabf6709. https://doi.org/10.1126/sciadv.abf6709

Lightman, S. L., Birnie, M. T., & Conway-Campbell, B. L. (2020). Dynamics of ACTH and Cortisol Secretion and Implications for Disease. *Endocrine Reviews*, *41*(3), bnaa002. https://doi.org/10.1210/endrev/bnaa002

Lin, C. S., Nicolelis, M. A., Schneider, J. S., & Chapin, J. K. (1990). A major direct GABAergic pathway from zona incerta to neocortex. *Science (New York, N.Y.)*, *248*(4962), 1553–1556. https://doi.org/10.1126/science.2360049

Lister, R. G. (1987). The use of a plus-maze to measure anxiety in the mouse. *Psychopharmacology*, *92*(2), 180–185. https://doi.org/10.1007/BF00177912

Liu, B., Wen, L., Ran, Q., Zhang, S., Hu, J., Gong, M., & Zhang, D. (2020). Dysregulation within the salience network and default mode network in hyperthyroid patients: A follow-up resting-state functional MRI study. *Brain Imaging and Behavior*, *14*(1), 30–41. https://doi.org/10.1007/s11682-018-9961-6

Livak, K. J., & Schmittgen, T. D. (2001). Analysis of relative gene expression data using real-time quantitative PCR and the 2(-Delta Delta C(T)) Method. *Methods (San Diego, Calif.)*, *25*(4), 402–408. https://doi.org/10.1006/meth.2001.1262

López, M., Varela, L., Vázquez, M. J., Rodríguez-Cuenca, S., González, C. R., Velagapudi, V. R., Morgan, D. A., Schoenmakers, E., Agassandian, K., Lage, R., de Morentin, P. B. M., Tovar, S., Nogueiras, R., Carling, D., Lelliott, C., Gallego, R., Orešič, M., Chatterjee, K., Saha, A. K., … Vidal-Puig, A. (2010). Hypothalamic AMPK and fatty acid metabolism mediate thyroid regulation of energy balance. *Nature Medicine*, *16*(9), 1001–1008. https://doi.org/10.1038/nm.2207

Lowell, B. B., & Spiegelman, B. M. (2000). Towards a molecular understanding of adaptive thermogenesis. *Nature*, *404*(6778), 652–660. https://doi.org/10.1038/35007527

Lu, C. W., Harper, D. E., Askari, A., Willsey, M. S., Vu, P. P., Schrepf, A. D., Harte, S. E., & Patil, P. G. (2021). Stimulation of zona incerta selectively modulates pain in humans. *Scientific Reports*, *11*, 8924. https://doi.org/10.1038/s41598-021-87873-w

Maciak, S., Sawicka, D., Sadowska, A., Prokopiuk, S., Buczyńska, S., Bartoszewicz, M., Niklińska, G., Konarzewski, M., & Car, H. (2020). Low basal metabolic rate as a risk factor for development of insulin resistance and type 2 diabetes. *BMJ Open Diabetes Research & Care*, *8*(1), e001381. https://doi.org/10.1136/bmjdrc-2020-001381

Maeda, T., Fukushima, T., Ishibashi, K., & Higuchi, S. (2007). Involvement of basal metabolic rate in determination of type of cold tolerance. *Journal of Physiological Anthropology*, *26*(3), 415–418. https://doi.org/10.2114/jpa2.26.415

Maurya, S. K., & Periasamy, M. (2015). Sarcolipin is a novel regulator of muscle metabolism and obesity. *Pharmacological Research*, *102*, 270–275. https://doi.org/10.1016/j.phrs.2015.10.020

McGrath, J. J., Al-Hamzawi, A., Alonso, J., Altwaijri, Y., Andrade, L. H., Bromet, E. J., Bruffaerts, R., de Almeida, J. M. C., Chardoul, S., Chiu, W. T., Degenhardt, L., Demler, O. V., Ferry, F., Gureje, O., Haro, J. M., Karam, E. G., Karam, G., Khaled, S. M., Kovess-Masfety, V., … WHO World Mental Health Survey Collaborators. (2023). Age of onset and cumulative risk of mental disorders: A cross-national analysis of population surveys from 29 countries. *The Lancet. Psychiatry*, *10*(9), 668–681. https://doi.org/10.1016/S2215-0366(23)00193-1

Menendez, C., Baldelli, R., Camiña, J. P., Escudero, B., Peino, R., Dieguez, C., & Casanueva, F. F. (2003). TSH stimulates leptin secretion by a direct effect on adipocytes. *The Journal of Endocrinology*, *176*(1), 7–12. https://doi.org/10.1677/joe.0.1760007

Minamisawa, S., Uemura, N., Sato, Y., Yokoyama, U., Yamaguchi, T., Inoue, K., Nakagome, M., Bai, Y., Hori, H., Shimizu, M., Mochizuki, S., & Ishikawa, Y. (2006). Post-transcriptional downregulation of sarcolipin mRNA by triiodothyronine in the atrial myocardium. *FEBS Letters*, *580*(9), 2247–2252. https://doi.org/10.1016/j.febslet.2006.03.032

Mitrofanis, J. (2005). Some certainty for the 'zone of uncertainty'? Exploring the function of the zona incerta. *Neuroscience*, *130*(1), 1–15. https://doi.org/10.1016/j.neuroscience.2004.08.017

Mittag, J. (2020). More Than Fever—Novel Concepts in the Regulation of Body Temperature by Thyroid Hormones. *Experimental and Clinical Endocrinology & Diabetes: Official Journal, German Society of Endocrinology [and] German Diabetes Association*, *128*(6–07), 428–431. https://doi.org/10.1055/a-1014-2510

Mittag, J., Davis, B., Vujovic, M., Arner, A., & Vennström, B. (2010). Adaptations of the autonomous nervous system controlling heart rate are impaired by a mutant thyroid hormone receptor-alpha1. *Endocrinology*, *151*(5), 2388–2395. https://doi.org/10.1210/en.2009-1201

Mittag, J., Wallis, K., & Vennström, B. (2010). Physiological consequences of the TRalpha1 aporeceptor state. *Heart Failure Reviews*, *15*(2), 111–115. https://doi.org/10.1007/s10741-008-9119-5

Moran, C., & Chatterjee, K. (2015). Resistance to thyroid hormone due to defective thyroid receptor alpha. *Best Practice & Research. Clinical Endocrinology & Metabolism*, *29*(4), 647–657. https://doi.org/10.1016/j.beem.2015.07.007

Mullur, R., Liu, Y.-Y., & Brent, G. A. (2014). Thyroid Hormone Regulation of Metabolism. *Physiological Reviews*, *94*(2), 355–382. https://doi.org/10.1152/physrev.00030.2013

Murrough, J. W., Yaqubi, S., Sayed, S., & Charney, D. S. (2015). Emerging Drugs for the Treatment of Anxiety. *Expert Opinion on Emerging Drugs*, *20*(3), 393–406. https://doi.org/10.1517/14728214.2015.1049996

Nicolaisen, T. S., Klein, A. B., Dmytriyeva, O., Lund, J., Ingerslev, L. R., Fritzen, A. M., Carl, C. S., Lundsgaard, A.-M., Frost, M., Ma, T., Schjerling, P., Gerhart-Hines, Z., Flamant, F., Gauthier, K., Larsen, S., Richter, E. A., Kiens, B., & Clemmensen, C. (2020). Thyroid hormone receptor α in skeletal muscle is essential for T3-mediated increase in energy expenditure. *FASEB Journal: Official Publication of the Federation of American Societies for Experimental Biology*, *34*(11), 15480–15491. https://doi.org/10.1096/fj.202001258RR

Nicolelis, M. A. L., Chapin, J. K., & Lin, R. C. S. (1995). Development of direct GABAergic projections from the zona incerta to the somatosensory cortex of the rat. *Neuroscience*, *65*(2), 609–631. https://doi.org/10.1016/0306-4522(94)00493-O

Nolen-Hoeksema, S., Larson, J., & Grayson, C. (1999). Explaining the gender difference in depressive symptoms. *Journal of Personality and Social Psychology*, *77*(5), 1061–1072. https://doi.org/10.1037//0022-3514.77.5.1061

Nowack, J., Giroud, S., Arnold, W., & Ruf, T. (2017). Muscle Non-shivering Thermogenesis and Its Role in the Evolution of Endothermy. *Frontiers in Physiology*, *8*, 889. https://doi.org/10.3389/fphys.2017.00889

Nuguru, S. P., Rachakonda, S., Sripathi, S., Khan, M. I., Patel, N., & Meda, R. T. (2022). Hypothyroidism and Depression: A Narrative Review. *Cureus*, *14*(8), e28201. https://doi.org/10.7759/cureus.28201

Oelkrug, R., & Mittag, J. (2021). An improved method for the precise unravelment of non-shivering brown fat thermokinetics. *Scientific Reports*, *11*(1), 4799. https://doi.org/10.1038/s41598-021-84200-1

Ortiga-Carvalho, T. M., Chiamolera, M. I., Pazos-Moura, C. C., & Wondisford, F. E. (2016). Hypothalamus-Pituitary-Thyroid Axis. *Comprehensive Physiology*, *6*(3), 1387–1428. https://doi.org/10.1002/cphy.c150027

Ortiga-Carvalho, T. M., Sidhaye, A. R., & Wondisford, F. E. (2014). Thyroid hormone receptors and resistance to thyroid hormone disorders. *Nature Reviews. Endocrinology*, *10*(10), 582–591. https://doi.org/10.1038/nrendo.2014.143

O'Shea, P. J., & Williams, G. R. (2002). Insight into the physiological actions of thyroid hormone receptors from genetically modified mice. *The Journal of Endocrinology*, *175*(3), 553–570. https://doi.org/10.1677/joe.0.1750553

Ossowska, K. (2020). Zona incerta as a therapeutic target in Parkinson's disease. *Journal of Neurology*, *267*(3), 591–606. https://doi.org/10.1007/s00415-019-09486-8

Pant, M., Bal, N. C., & Periasamy, M. (2016). Sarcolipin: A Key Thermogenic and Metabolic Regulator in Skeletal Muscle. *Trends in Endocrinology and Metabolism: TEM*, *27*(12), 881–892. https://doi.org/10.1016/j.tem.2016.08.006

Pappa, T., & Refetoff, S. (2021). Resistance to Thyroid Hormone Beta: A Focused Review. *Frontiers in Endocrinology*, *12*, 656551. https://doi.org/10.3389/fendo.2021.656551

Paragliola, R. M., Corsello, A., Papi, G., Pontecorvi, A., & Corsello, S. M. (2021). Cushing's Syndrome Effects on the Thyroid. *International Journal of Molecular Sciences*, *22*(6), 3131. https://doi.org/10.3390/ijms22063131

Patchev, V. K., & Patchev, A. V. (2006). Experimental models of stress. *Dialogues in Clinical Neuroscience*, *8*(4), 417–432.

Paxinos, G., & Franklin, K. B. J. (2004). *The Mouse Brain in Stereotaxic Coordinates: Compact Second Edition*. Gulf Professional Publishing.

Penninx, B. W., Pine, D. S., Holmes, E. A., & Reif, A. (2021). Anxiety disorders. *Lancet (London, England)*, *397*(10277), 914–927. https://doi.org/10.1016/S0140-6736(21)00359-7

Pfaffl, M. W., Tichopad, A., Prgomet, C., & Neuvians, T. P. (2004). Determination of stable housekeeping genes, differentially regulated target genes and sample integrity: BestKeeper--Excel-based tool using pair-wise correlations. *Biotechnology Letters*, *26*(6), 509–515. https://doi.org/10.1023/b:bile.0000019559.84305.47

Refetoff, S., DeWind, L. T., & DeGroot, L. J. (1967). Familial syndrome combining deaf-mutism, stuppled epiphyses, goiter and abnormally high PBI: Possible target organ refractoriness to thyroid hormone. *The Journal of Clinical Endocrinology and Metabolism*, *27*(2), 279–294. https://doi.org/10.1210/jcem-27-2-279

Rodgers, R. J., & Dalvi, A. (1997). Anxiety, defence and the elevated plus-maze. *Neuroscience & Biobehavioral Reviews*, *21*(6), 801–810. https://doi.org/10.1016/S0149-7634(96)00058-9

Roef, G., Lapauw, B., Goemaere, S., Zmierczak, H.-G., Toye, K., Kaufman, J.-M., & Taes, Y. (2012). Body composition and metabolic parameters are associated with variation in thyroid hormone levels among euthyroid young men. *European Journal of Endocrinology*, *167*(5), 719–726. https://doi.org/10.1530/EJE-12-0447

Romanowski, C. A., Mitchell, I. J., & Crossman, A. R. (1985). The organisation of the efferent projections of the zona incerta. *Journal of Anatomy*, *143*, 75–95.

Rosell, M., Kaforou, M., Frontini, A., Okolo, A., Chan, Y.-W., Nikolopoulou, E., Millership, S., Fenech, M. E., MacIntyre, D., Turner, J. O., Moore, J. D., Blackburn, E., Gullick, W. J., Cinti, S., Montana, G., Parker, M. G., & Christian, M. (2014). Brown and white adipose tissues: Intrinsic differences in gene expression and response to cold exposure in mice. *American Journal of Physiology. Endocrinology and Metabolism*, *306*(8), E945-964. https://doi.org/10.1152/ajpendo.00473.2013

Sahoo, S. K., Shaikh, S. A., Sopariwala, D. H., Bal, N. C., & Periasamy, M. (2013). Sarcolipin protein interaction with sarco(endo)plasmic reticulum Ca2+ ATPase (SERCA) is distinct from phospholamban protein, and only sarcolipin can promote uncoupling of the SERCA pump. *The Journal of Biological Chemistry*, *288*(10), 6881–6889. https://doi.org/10.1074/jbc.M112.436915

Saito, M., Matsushita, M., Yoneshiro, T., & Okamatsu-Ogura, Y. (2020). Brown Adipose Tissue, Diet-Induced Thermogenesis, and Thermogenic Food Ingredients: From Mice to Men. *Frontiers in Endocrinology*, *11*, 222. https://doi.org/10.3389/fendo.2020.00222

Salas-Lucia, F. (2024). Mapping Thyroid Hormone Action in the Human Brain. *Thyroid: Official Journal of the American Thyroid Association*, *34*(7), 815–826. https://doi.org/10.1089/thy.2024.0120

Sánchez-Franco, F., Fernández, L., Fernández, G., & Cacicedo, L. (1989). Thyroid hormone action on ACTH secretion. *Hormone and Metabolic Research = Hormon- Und Stoffwechselforschung = Hormones Et Metabolisme*, *21*(10), 550–552. https://doi.org/10.1055/s-2007-1009285

Savitt, J. M., Jang, S. S., Mu, W., Dawson, V. L., & Dawson, T. M. (2005). Bcl-x is required for proper development of the mouse substantia nigra. *The Journal of Neuroscience: The Official Journal of the Society for Neuroscience*, *25*(29), 6721–6728. https://doi.org/10.1523/JNEUROSCI.0760-05.2005

Segerson, T. P., Kauer, J., Wolfe, H. C., Mobtaker, H., Wu, P., Jackson, I. M., & Lechan, R. M. (1987). Thyroid hormone regulates TRH biosynthesis in the paraventricular nucleus of the rat hypothalamus. *Science (New York, N.Y.)*, *238*(4823), 78–80. https://doi.org/10.1126/science.3116669

Seibenhener, M. L., & Wooten, M. C. (2015). Use of the Open Field Maze to Measure Locomotor and Anxiety-like Behavior in Mice. *Journal of Visualized Experiments : JoVE*, *96*, 52434. https://doi.org/10.3791/52434

Sentis, S. C., Dore, R., Oelkrug, R., Kolms, B., Iwen, K. A., & Mittag, J. (2024). Hypothalamic Thyroid Hormone Receptor α1 Signaling Controls Body Temperature. *Thyroid: Official Journal of the American Thyroid Association*, *34*(2), 243–251. https://doi.org/10.1089/thy.2023.0513

Sentis, S. C., Oelkrug, R., & Mittag, J. (2021). Thyroid hormones in the regulation of brown adipose tissue thermogenesis. *Endocrine Connections*, *10*(2), R106–R115. https://doi.org/10.1530/EC-20-0562

Sharma, S., Badenhorst, C. A., Ashby, D. M., Di Vito, S. A., Tran, M. A., Ghavasieh, Z., Grewal, G. K., Belway, C. R., McGirr, A., & Whelan, P. J. (2024). Inhibitory medial zona incerta pathway drives exploratory behavior by inhibiting glutamatergic cuneiform neurons. *Nature Communications*, *15*(1), 1160. https://doi.org/10.1038/s41467-024-45288-x

Siemes, D., Vancamp, P., Markova, B., Spangenberg, P., Shevchuk, O., Siebels, B., Schlüter, H., Mayerl, S., Heuer, H., & Engel, D. R. (2023). Proteome Analysis of Thyroid Hormone Transporter Mct8/Oatp1c1-Deficient Mice Reveals Novel Dysregulated Target Molecules Involved in Locomotor Function. *Cells*, *12*(20), 2487. https://doi.org/10.3390/cells12202487

Sinha, S. R., Prakash, P., Keshari, J. R., Kumari, R., & Prakash, V. (2023). Assessment of Serum Cortisol Levels in Hypothyroidism Patients: A Cross-Sectional Study. *Cureus*, *15*(12), e50199. https://doi.org/10.7759/cureus.50199

Sjögren, M., Alkemade, A., Mittag, J., Nordström, K., Katz, A., Rozell, B., Westerblad, H., Arner, A., & Vennström, B. (2007). Hypermetabolism in mice caused by the central action of an unliganded thyroid hormone receptor alpha1. *The EMBO Journal*, *26*(21), 4535–4545. https://doi.org/10.1038/sj.emboj.7601882

Smith, I. C., Bombardier, E., Vigna, C., & Tupling, A. R. (2013). ATP consumption by sarcoplasmic reticulum Ca^{2+} pumps accounts for 40-50% of resting metabolic rate in mouse fast and slow twitch skeletal muscle. *PloS One*, *8*(7), e68924. https://doi.org/10.1371/journal.pone.0068924

Smith, S. M., & Vale, W. W. (2006). The role of the hypothalamic-pituitary-adrenal axis in neuroendocrine responses to stress. *Dialogues in Clinical Neuroscience*, *8*(4), 383–395.

Stein, D. J., Palk, A. C., & Kendler, K. S. (2021). What is a mental disorder? An exemplar-focused approach. *Psychological Medicine*, *51*(6), 894–901. https://doi.org/10.1017/S0033291721001185

Tafet, G. E., & Nemeroff, C. B. (2016). The Links Between Stress and Depression: Psychoneuroendocrinological, Genetic, and Environmental Interactions. *The Journal of Neuropsychiatry and Clinical Neurosciences*, *28*(2), 77–88. https://doi.org/10.1176/appi.neuropsych.15030053

Thompson, C. C., & Potter, G. B. (2000). Thyroid hormone action in neural development. *Cerebral Cortex (New York, N.Y.: 1991)*, *10*(10), 939–945. https://doi.org/10.1093/cercor/10.10.939

Thunhorst, R. L., Beltz, T. G., & Johnson, A. K. (2007). Glucocorticoids increase salt appetite by promoting water and sodium excretion. *American Journal of Physiology. Regulatory, Integrative and Comparative Physiology*, *293*(3), R1444–R1451. https://doi.org/10.1152/ajpregu.00294.2007

Tinnikov, A., Nordström, K., Thorén, P., Kindblom, J. M., Malin, S., Rozell, B., Adams, M., Rajanayagam, O., Pettersson, S., Ohlsson, C., Chatterjee, K., & Vennström, B. (2002). Retardation of post-natal development caused by a negatively acting thyroid hormone receptor alpha1. *The EMBO Journal*, *21*(19), 5079–5087. https://doi.org/10.1093/emboj/cdf523

Tran, I., & Gellner, A.-K. (2023). Long-term effects of chronic stress models in adult mice. *Journal of Neural Transmission (Vienna, Austria: 1996)*, *130*(9), 1133–1151. https://doi.org/10.1007/s00702-023-02598-6

Twenge, J. M., Cooper, A. B., Joiner, T. E., Duffy, M. E., & Binau, S. G. (2019). Age, period, and cohort trends in mood disorder indicators and suicide-related outcomes in a nationally representative dataset, 2005–2017. *Journal of Abnormal Psychology*, *128*(3), 185–199. https://doi.org/10.1037/abn0000410

Vaitkus, J. A., Farrar, J. S., & Celi, F. S. (2015). Thyroid Hormone Mediated Modulation of Energy Expenditure. *International Journal of Molecular Sciences*, *16*(7), 16158–16175. https://doi.org/10.3390/ijms160716158

Venero, C., Guadaño-Ferraz, A., Herrero, A. I., Nordström, K., Manzano, J., de Escobar, G. M., Bernal, J., & Vennström, B. (2005). Anxiety, memory impairment, and locomotor

dysfunction caused by a mutant thyroid hormone receptor α1 can be ameliorated by T3 treatment. *Genes & Development*, *19*(18), 2152–2163. https://doi.org/10.1101/gad.346105

Venkataraman, A., Brody, N., Reddi, P., Guo, J., Gordon Rainnie, D., & Dias, B. G. (2019). Modulation of fear generalization by the zona incerta. *Proceedings of the National Academy of Sciences*, *116*(18), 9072–9077. https://doi.org/10.1073/pnas.1820541116

Wagner, C. K., Eaton, M. J., Moore, K. E., & Lookingland, K. J. (1995). Efferent projections from the region of the medial zona incerta containing A13 dopaminergic neurons: A PHA-L anterograde tract-tracing study in the rat. *Brain Research*, *677*(2), 229–237. https://doi.org/10.1016/0006-8993(95)00128-D

Walker, E. R., McGee, R. E., & Druss, B. G. (2015). Mortality in Mental Disorders and Global Disease Burden Implications. *JAMA Psychiatry*, *72*(4), 334–341. https://doi.org/10.1001/jamapsychiatry.2014.2502

Walsh, R. N., & Cummins, R. A. (1976). The Open-Field Test: A critical review. *Psychological Bulletin*, *83*(3), 482–504.

Wang, X., Chou, X.-L., Zhang, L. I., & Tao, H. W. (2020). Zona Incerta: An Integrative Node for Global Behavioral Modulation. *Trends in Neurosciences*, *43*(2), 82–87. https://doi.org/10.1016/j.tins.2019.11.007

Warner, A., & Mittag, J. (2012). Thyroid hormone and the central control of homeostasis. *Journal of Molecular Endocrinology*, *49*(1), R29–R35. https://doi.org/10.1530/JME-12-0068

Warner, A., & Mittag, J. (2014). Brown fat and vascular heat dissipation: The new cautionary tail. *Adipocyte*, *3*(3), 221–223. https://doi.org/10.4161/adip.28815

Warner, A., Rahman, A., Solsjö, P., Gottschling, K., Davis, B., Vennström, B., Arner, A., & Mittag, J. (2013). Inappropriate heat dissipation ignites brown fat thermogenesis in mice with a mutant thyroid hormone receptor α1. *Proceedings of the National Academy of Sciences of the United States of America*, *110*(40), 16241–16246. https://doi.org/10.1073/pnas.1310300110

Wassner, A. J. (2018). Congenital Hypothyroidism. *Clinics in Perinatology*, *45*(1), 1–18. https://doi.org/10.1016/j.clp.2017.10.004

Waters, K. M., Miller, C. W., & Ntambi, J. M. (1997). Localization of a negative thyroid hormone-response region in hepatic stearoyl-CoA desaturase gene 1. *Biochemical and Biophysical Research Communications*, *233*(3), 838–843. https://doi.org/10.1006/bbrc.1997.6550

Watkins, E. R. (2008). Constructive and unconstructive repetitive thought. *Psychological Bulletin*, *134*(2), 163–206. https://doi.org/10.1037/0033-2909.134.2.163

Weetman, A. P. (2021). An update on the pathogenesis of Hashimoto's thyroiditis. *Journal of Endocrinological Investigation*, *44*(5), 883–890. https://doi.org/10.1007/s40618-020-01477-1

Wehner, A., Glöckner, S., Weiss, B., Ballhausen, D., Stockhaus, C., Zablotski, Y., & Hartmann, K. (2021). Association between ACTH stimulation test results and clinical signs in dogs with hyperadrenocorticism treated with trilostane. *Veterinary Journal (London, England: 1997)*, *276*, 105740. https://doi.org/10.1016/j.tvjl.2021.105740

Wiersinga, W. M. (2014). Paradigm shifts in thyroid hormone replacement therapies for hypothyroidism. *Nature Reviews. Endocrinology*, *10*(3), 164–174. https://doi.org/10.1038/nrendo.2013.258

Wikström, L., Johansson, C., Saltó, C., Barlow, C., Campos Barros, A., Baas, F., Forrest, D., Thorén, P., & Vennström, B. (1998). Abnormal heart rate and body temperature in mice lacking thyroid hormone receptor alpha 1. *The EMBO Journal*, *17*(2), 455–461. https://doi.org/10.1093/emboj/17.2.455

Williams, G. R. (2000). Cloning and Characterization of Two Novel Thyroid Hormone Receptor β Isoforms. *Molecular and Cellular Biology*, *20*(22), 8329–8342.

Yaribeygi, H., Panahi, Y., Sahraei, H., Johnston, T. P., & Sahebkar, A. (2017). The impact of stress on body function: A review. *EXCLI Journal*, *16*, 1057–1072. https://doi.org/10.17179/excli2017-480

Yau, W. W., & Yen, P. M. (2020). Thermogenesis in Adipose Tissue Activated by Thyroid Hormone. *International Journal of Molecular Sciences*, *21*(8), 3020. https://doi.org/10.3390/ijms21083020

Ye, Q., Nunez, J., & Zhang, X. (2023). Zona incerta dopamine neurons encode motivational vigor in food seeking. *Science Advances*, *9*(46), eadi5326. https://doi.org/10.1126/sciadv.adi5326

Zhang, T., Zhao, L., Chen, C., Yang, C., Zhang, H., Su, W., Cao, J., Shi, Q., & Tian, L. (2024). Structural and Functional Alterations of Hippocampal Subfields in Patients With Adult-Onset Primary Hypothyroidism. *The Journal of Clinical Endocrinology and Metabolism*, *109*(7), 1707–1717. https://doi.org/10.1210/clinem/dgae070

Zhang, W., Liu, X., Zhang, Y., Song, L., Hou, J., Chen, B., He, M., Cai, P., & Lii, H. (2014). Disrupted functional connectivity of the hippocampus in patients with hyperthyroidism: Evidence from resting-state fMRI. *European Journal of Radiology*, *83*(10), 1907–1913. https://doi.org/10.1016/j.ejrad.2014.07.003

Zuloaga, D. G., Morris, J. A., Jordan, C. L., & Breedlove, S. M. (2008). Mice with the testicular feminization mutation demonstrate a role for androgen receptors in the regulation of anxiety-related behaviors and the hypothalamic-pituitary-adrenal axis. *Hormones and Behavior*, *54*(5), 758–766. https://doi.org/10.1016/j.yhbeh.2008.08.004

APPENDIX

STATISTICAL ANALYSIS

The following table S1 shows the used statistical tests and their respective results.Paired and unpaired Student's t-tests were used to analyse statistical significance between two groups. Two-way analysis of variance (ANOVA) tested significance between two groups with a time parameter, and analysis of covariance (ANCOVA) was used to identify covariates. Šídák's post hoc test was used for analysis of multiple comparisons

Supplementary Table 12: Statistical tests used in this study and their results

FIgure	**Genotype**	**Statistical test**		
7B	Dominant-negative TRα1 vs. control	Unpaired Student's t-test		
		Df	t	p
Klf9		8	2.879	0.0205
Hr		7	1.604	0.1527
Scd1		8	1.871	0.0982
Pde10a		8	0.1421	0.8905
7C	Dominant-negative TRα1 vs. control	Unpaired Student's t-test		
		Df	t	p
Tra1		8	4.388	0.0023
Trb1		8	0.6265	0.5484
9A	Start vs. end of experiment	Paired Student's t-test		
		Df	t	p
Control		9	4.444	0.0016
Dominant-negative TR α1		8	2.800	0.0232
9B+C	Dominant-negative TRα1 vs. control	Unpaired Student's t-test		
		Df	t	p
Food intake		17	0.2477	0.8073
Water intake		17	1.290	0.2145
10	Dominant-negative TRα1 vs. control	Unpaired Student's t-test		
		Df	t	p
T3		14	1.150	0.2694
T4		14	1.712	0.1090
11A	Dominant-negative TRα1 vs. control	2-way ANOVA with Šídák's multiple comparison post hoc test		
		Interaction	Genotype	Time

		F (11, 187) = 0.5134 p = 0.8928	F (11, 17) = 0.009033 p = 0.9254	F (11, 187) = 70.60 p < 0.0001
11B	Dominant-negative TRα1 vs. control	2-way ANOVA with Šídák's multiple comparison post hoc test		
		Interaction	Genotype	Time
		F (11,187) = 1.527 p = 0.1245	F (11, 17) = 0.2821 p = 0.6022	F (2.833, 48.16) = 56.20 p < 0.0001
11C	Dominant-negative TRα1 vs. control	2-way ANOVA with Šídák's multiple comparison post hoc test		
		Interaction	Genotype	Time
		F (13,78) = 0.9159 p = 0.5407	F (1, 6) = 0.4115 p = 0.5449	F (3.637, 21.82) = 4.857 p < 0.0001
11D	Dominant-negative TRα1 vs. control	2-way ANOVA with Šídák's multiple comparison post hoc test		
		Interaction	Genotype	Time
		F (13, 78) = 0.9957 p = 0.4636	F (1, 6) = 0.03272 p = 0.8624	F (3.179, 19.07) = 5.051 p = 0.0088
11E	Dominant-negative TRα1 vs. control	2-way ANOVA with Šídák's multiple comparison post hoc test		
		Interaction	Genotype	Time
		F (5, 30) = 1.587 p = 0.1938	F (1, 6) = 0.1297 p = 0.7311	F (2.907, 17.44) = 25.52 p < 0.0001
11F	Dominant-negative TRα1 vs. control	2-way ANOVA with Šídák's multiple comparison post hoc test		
		Interaction	Genotype	Time
		F (5, 30) = 1.559 p = 0.2020	F (1,6) = 0.09601 p = 0.7671	F (1.814, 10.89) = 4.778 p = 0.0349
12B	Dominant-negative TRα1 vs. control	Unpaired Student's t-test		
		Df	t	p
iBAT		17	1.067	0.3010
Tail		17	0.8622	0.4006
12C	Dominant-negative TRα1 vs. control	Unpaired Student's t-test		
		Df	t	p
Adrb3		15	0.2435	0.8109
Prdm16		17	0.5016	0.6224
Adra1a		16	0.3506	0.7304
Adrb2		16	2.062	0.0559
Ucp1		17	1.549	0.1397
Dio2		16	1.451	0.1660
Cidea		16	2.219	0.0413
Pparγ		17	0.8620	0.4007

13A	Dominant-negative TRα1 vs. control	Mixed-effects analysis with Šídák's multiple comparison post hoc test		
		Interaction	Genotype	Time
		F (21, 249) = 0.5673 p = 0.9376	F (1, 17) = 0.2171 p = 0.6472	F (5.145, 61.01) = 8.262 p < 0.0001
13B+D	Dominant-negative TRα1 vs. control	Unpaired Student's t-test		
		Df	t	p
VO_2		9	1.736	0.1166
RQ		9	0.4224	0.6826
13C	Dominant-negative TRα1 vs. control	ANCOVA		
		Covariate		Treatment
		Df = 1 F = 0.374923 p = 0.550893		Df = 1 F = 0.931676 p = 0.362696
13E	Dominant-negative TRα1 vs. control	Mixed-effects analysis with Šídák's multiple comparison post hoc test		
		Interaction	Genotype	Time
		F (18, 239) = 0.8123 p = 0.6851	F (1, 17) = 4.024 p = 0.0610	F (4.236, 56.24) = 14.81 p < 0.0001
13F+H+I	Dominant-negative TRα1 vs. control	Unpaired Student's t-test (Welch's correction for VO_2)		
		Df	t	p
VO_2		17	3.518	0.0029
RQ		17	0.1602	0.8746
Body weight loss		17	2.201	0.0418
13G	Dominant-negative TRα1 vs. control	ANCOVA		
		Covariate		Treatment
		Df = 1 F = 5.315105 p = 0.03827		Df = 1 F = 5.799781 p = 0.028447
14A	Dominant-negative TRα1 vs. control	Unpaired Student's t-test		
		Df	t	p
Myh1		16	1.483	0.1575
Gpd2		16	1.871	0.0797
Ucp3		16	0.9345	0.3639
Sln		16	3.591	0.0024
Atp2a1		16	1.729	0.1031
Atp2a2		16	0.8937	0.3847
Atp2a3		16	0,3931	0.6994
Pparδ		16	0.1503	0.8824
Myh4		16	0.5715	0.5756
Ryr1		16	1.100	0.2875
Mstn		16	0.09959	0.9219

14B	Dominant-negative TRα1 vs. control	Unpaired Student's t-test		
		Df	t	p
Pepck		16	0.7296	0.4762
Pyrk		16	0.2437	0.8105
Fasn		16	0.7046	0.4912
G6pdh		16	0.1253	0.9019
14C	Dominant-negative TRα1 vs. control	Unpaired Student's t-test		
		Df	t	p
Glycogen		16	1.469	0.1612
15A	Dominant-negative TRα1 vs. control	Unpaired Student's t-test		
First 5 minutes of Open Field Test		Df	t	p
Centre		9	0.6994	0.5020
Outer Zone		9	0.6962	0.5039
Mean speed		9	2.154	0.0596
Distance		9	2.140	0.0610
15B	Dominant-negative TRα1 vs. control	Unpaired Student's t-test		
Last 5 minutes of Open Field Test		Df	t	p
Centre		9	2.353	0.0431
Outer Zone		9	2.411	0.0392
Mean speed		9	1.176	0.2697
Distance		9	1.221	0.2531
15C	Dominant-negative TRα1 vs. control	Unpaired Student's t-test		
Elevated Plus Maze		Df	t	p
Open arm time		9	2.458	0.0363
Closed arm time		9	1.861	0.0957
Centre time		9	1.827	0.1009
Mobile time		9	1.830	0.1004
Open arm entries		9	1.252	0.2422
Closed arm entries		9	1.252	0.2422
16A	Dominant-negative TRα1 vs. control	Unpaired Student's t-test		
		Df	t	p
Corticosterone		16	3.496	0.0030
16B	Dominant-negative TRα1 vs. control	Unpaired Student's t-test		
		Df	t	p
Tat		15	0.8310	0.4190
Mt2		16	1.548	0.1412
Cat		16	0.8586	0.4032
GR		17	0.6804	0.5054
16C	Dominant-negative TRα1 vs. control	Unpaired Student's t-test		
		Df	t	p

GR		16	0.6939	0.4977
17A	Dominant-negative TRα1 vs. control	Unpaired Student's t-test		
		Df	t	p
Crh		8	0.6346	0.5434
Ucp2		8	0.5498	0.5974
17B	Dominant-negative TRα1 vs. control	Unpaired Student's t-test		
		Df	t	p
Tshb		8	2.610	0.0311
Pomc		8	0.3527	0.7334
Trhr		8	1.555	0.1586
Crhr		8	1.581	0.1525
Tbx19		8	1.757	0.1171
17C	Dominant-negative TRα1 vs. control	Unpaired Student's t-test		
		Df	t	p
Cyp11b1		9	1.196	0.2624
Cyp11b2		9	1.831	0.1003
18C-F	Dominant-negative TRα1 vs. control	Unpaired Student's t-test		
		Df	t	p
HR		16	0.1565	0.8776
HRV		16	1.107	0.2848
R amplitude		16	0.4531	0.6565
RR		16	0.2346	0.8175
PQ		16	0.8408	0.4128
PR		16	0.9387	0.3619
QRS		16	0.1186	0.9070
QT		16	0.1908	0.8511
ST		16	0.1563	0.8778
QTC		16	0.4049	0.6909
19B		Unpaired Student's t-test		
		Df	t	p
TRα1 +/m vs. TRα1 +/+		4	1.337	0.2521
TRα1 +/+ +T3 vs. TRα1 +/+		4	0.5328	0.6224
22A	Start vs. end of experiment	Paired Student's t-test		
		Df	t	p
Control		3	0.6026	0.5893
Dominant-negative TR α1		3	0.2285	0.8339
22B+C	Dominant-negative TRα1 vs. control	Unpaired Student's t-test		
		Df	t	p
Food intake		6	0.5486	0.6031
Water intake		6	2.522	0.0451
23A	Dominant-negative TRα1 vs. control	2-way ANOVA with Šídák's multiple comparison post hoc test		
		Interaction	Genotype	Time

		F (15, 90) = 0.5723 p = 0.8888	F (1, 6) = 0.7594 p = 0.4170	F (15, 90) = 12.72 p < 0.0001
23B	Dominant-negative TRα1 vs. control	2-way ANOVA with Šídák's multiple comparison post hoc test		
		Interaction	Genotype	Time
		F (15, 90) = 0.4684 p = 0.9505	F (1, 6) = 0.02147 p = 0.8883	F (3.060, 18.36) = 18.20 p < 0.0001
23C	Dominant-negative TRα1 vs. control	2-way ANOVA with Šídák's multiple comparison post hoc test		
		Interaction	Genotype	Time
		F (6, 36) = 0.5321 p =0.7802	F (1, 6) = 0.4697 p = 0.5187	F (6, 36) = 1.075 p = 0.3954
23D	Dominant-negative TRα1 vs. control	2-way ANOVA with Šídák's multiple comparison post hoc test		
		Interaction	Genotype	Time
		F (6, 36) = 0.5851 p = 0.7398	F (1, 6) = 7.558 p = 0.0333	F (6, 36) = 0.5863 p = 0.7389
23E	Dominant-negative TRα1 vs. control	2-way ANOVA with Šídák's multiple comparison post hoc test		
		Interaction	Genotype	Time
		F (5, 30) = 0.9180 p = 0.4828	F (1, 6) = 0.6192 p = 0.4613	F (1.779, 10.67) = 13.54 p = 0.0015
23F	Dominant-negative TRα1 vs. control	2-way ANOVA with Šídák's multiple comparison post hoc test		
		Interaction	Genotype	Time
		F (5, 30) = 0.4433 p = 0.8147	F (1, 6) = 0.2191 p = 0.6563	F (2.055, 12.33) = 0.9965 p = 0.3992
24B	Dominant-negative TRα1 vs. control	Unpaired Student's t-test		
		Df	t	p
iBAT		6	0.8568	0.4245
Tail		6	0.6971	0.5118
25	Dominant-negative TRα1 vs. control	Unpaired Student's t-test		
		Df	t	p
VO_2		6	0.04120	0.9685
Normalised VO_2		6	0.2408	0.8177
RQ		6	2.163	0.0738
Fasting body weight loss		6	0.09286	0.9290
26A-C	Dominant-negative TRα1 vs. control	Unpaired Student's t-test		
Open Field Test		Df	t	p
Centre		6	1.553	0.1713
Outer zone		6	1.554	0.1712

Mobile		6	0.6460	0.5422
Immobile		6	0.6460	0.5422
Mean speed		6	0.8097	0.4490
Distance		6	0.1089	0.9169
26D	Dominant-negative TRα1 vs. control	Unpaired Student's t-test		
Elevated Plus Maze		Df	t	p
Open arm		6	0.3910	0.7093
Closed arm		6	1.115	0.3075
Centre		6	1.610	0.1585
26E	Dominant-negative TRα1 vs. control	Unpaired Student's t-test		
		Df	t	p
Corticosterone		6	0.6177	0.5595
27C-F	Dominant-negative TRα1 vs. control	Unpaired Student's t-test		
		Df	t	p
HR		6	1.584	0.1642
HRV		6	0.9768	0.3664
R amplitude		6	0.4545	0.6654
RR		6	1.599	0.1610
PQ		6	0.5116	0.6272
PR		6	0.6639	0.5314
QRS		6	0.6854	0.5187
QT		6	0.7906	0.4593
ST		6	0.9365	0.3852
QTC		6	0.02637	0.9798

ACKNOWLEDGEMENTS

This thesis would not have been possible without the support, guidance, and encouragement of many people. A project like this is always a team effort, relying on the help, advice, and collaboration of many who contribute in different ways. I am very thankful to everyone who has supported me throughout this journey.

First, I want to express my deepest gratitude to my supervisor Prof. Jens Mittag. His steady guidance, thoughtful feedback, and constant encouragement have been crucial in shaping this thesis. His sense of humour has helped to bring levity into the 3 years of this PhD project, even when times were tough. I feel very lucky to have had the chance to learn from him. A big thank you also to the entire research group surrounding him for some fun times during long office days and nice chats while eating delicious, homemade cakes.

I am also grateful to the postdoctoral researchers in our group, Dr. Riccardo Dore and Dr. Rebecca Oelkrug, for their mentorship. There was no problem that could not somehow be fixed by a fruitful discussion with them, and they always made time for me, especially when the equipment did not want to play by our rules. I am going to miss the impromptu office concerts dearly and can only hope to meet colleagues like them again.

I would also like to thank my co-supervisors, Dr. Helge Müller-Fielitz and Prof. Peter Kühnen, for their guidance and support throughout this project. Their feedback was always very valuable and allowed me to look at things with a new perspective, and to find the answers to many questions. I am also thankful to my collaborators in Cologne, Dr. Heiko Backes and Annika Glatzel, for their constant feedback and immense expertise. I would have been lost in the PET data without them and our meetings were always incredibly productive. Thanks to Dr. Anna-Lena Cremer for conducting the PET/CT scans that ended up being the basis for this project.

A special thank you goes to Julia Resch, our skilled technician, whose expertise has been essential in managing the practical parts of this project. I could not imagine having done the countless hours of lab work without her tips and tricks.

I am also deeply thankful to my family and friends, whose love and support have kept me going throughout this process. Their belief in me has been a constant source of strength, and their patience and understanding have been so valuable, especially during the more challenging times.

Finally, I would like to acknowledge all of my colleagues and the research community, in particular the consortium “CRC296/LocoTact”, whose discussions, feedback, and collaboration

have helped shape this thesis. Every bit of advice and constructive criticism has been important in bringing this work to completion.

To everyone who has played a role in this project, I offer my sincere thanks.